Determination of the largest clasts of tephra deposits for the characterization of explosive volcanic eruptions

FIELD-WORKSHOP REPORT

IAVCEI Commission on Tephra Hazard Modelling

(SALCEDO) Ecuador
January 16-18, 2006

Costanza Bonadonna[1], Simona Scollo[2], Raffaello Cioni[3,4], Laura Pioli[1], Marco Pistolesi[4]

[1]Earth and Environmental Sciences Section, University of Geneva, Switzerland,
[2]INGV sezione di Catania, Italy, [3]Universita' di Cagliari, Italy, [4]Universita' di Pisa, Italy

Data presented in this report result from the effort of all workshop participants (Appendix A)
All original data are available at: http://dbstr.ct.ingv.it/iavcei/report1.htm

Citation: Costanza Bonadonna; simona scollo; Raffaello Cioni; Laura Pioli; Marco Pistolesi (2011), "Determination of the largest clasts of tephra deposits for the characterization of explosive volcanic eruptions: report of the IAVCEI Commission on Tephra Hazard Modelling" https://vhub.org/resources/870.

Executive summary

This report summarizes the results of the field workshop of the IAVCEI Commission on Tephra Hazard Modelling that was carried out in Salcedo, Ecuador (January 16-18, 2006) with the main objective of assessing the best way to characterize the largest clasts of tephra deposits. Defining the largest clasts of a tephra deposit is necessary for the compilation of isopleths maps, which are important for two main reasons: i) determination of column height when no direct observations are available (e.g. Carey and Sparks 1986 and Pyle 1989) and ii) definition of eruptive style (e.g. Pyle 1989). In particular, the determination of the column height is extremely valuable because it represents a critical input of tephra models and because it is used to derive information on the mass discharge rate and the duration of eruptions (i.e., ratio between erupted mass and mass eruption rate). Nonetheless, our field exercise has shown the dependence of the results on different averaging and sampling techniques used, confirming the need of a standardized strategy, and that the characterization of the population of the largest clasts that fell at a given distance from the vent is more appropriate than the definition of a maximum clast.

Recommendations on the selection of sampling area, collection strategy, choice of clast typology and clast characterization (i.e., axis measurement and averaging technique) are given based on a thorough investigation of two outcrops at different distance from the vent. First, specified-area sections should be preferred to unspecified-area sections when possible (ideally $0.5m^2$ and a flat paleotopography). Second, in order to avoid large discrepancies from the assumptions of sphere considered in most empirical models (e.g. Carey and Sparks 1986), a clast should be characterized based on the geometric mean of its three axes taken perpendicularly between each other with the approximation of the minimum ellipsoid (lithics should also be preferred to pumices when present). Finally, the method of the 50th percentile of a population of 20 clasts was found as the best way to assess the largest clasts because it has the advantages of: i) eliminating the problem of outlier identification based on a rigorous statistical approach, ii) offering a more reliable reproducibility of the characterization of a given outcrop than the measurement of a small population of large clasts (e.g. 3 or 5), iii) reducing analysis time in the field by requiring the measurement of only one clast (i.e., the smallest of the 11 largest clasts). In addition, the underestimation of values is in the same order of magnitude of the differences due to the choice of the collection strategy, sampled volume and averaging technique and can also be corrected when compiling the isopleth map. Further investigations on the stability of the discrepancy between 50th percentile of a 20-clast population and the largest clasts found at a given outcrop should be carried out. Finally, the survivor-function data should also be calibrated with the method of Carey and Sparks (1986) in order to correct for the discrepancies with the 3- and 5-clast populations typically used.

Table of content

All original data are available at: http://dbstr.ct.ingv.it/iavcei/report1.htm

Determination of the largest clasts of tephra deposits for the characterization of explosive volcanic eruptions

FIELD-WORKSHOP REPORT
IAVCEI Commission on Tephra Hazard Modelling
(SALCEDO) Ecuador, January 16-18, 2006

1.0 INTRODUCTION

Field measurements of tephra deposits are used to characterize volcanic eruptions and their hazards. In particular, the distribution of tephra thickness and mass/area around the volcano (isopach and isomass maps) is necessary for the estimate of erupted volume (e.g. Bonadonna and Houghton 2005; Fierstein and Nathenson 1992; Froggatt 1982; Pyle 1989), whereas the distribution of maximum clasts around the vent (isopleth maps) is typically used for the estimate of column height and wind speed at the time of the eruption (Carey and Sparks 1986). The concept of maximum clast was firstly introduced by Walker and Croasdale (1971) to characterize and compare different tephra deposits, and then was adopted by Carey and Sparks (1986) to derive the maximum plume height based on the assumption that maximum plume height is associated with the deposition of the largest clasts found in the deposit. Both isopach/isomass maps and isopleth maps can also be used for the determination of the vent location and the classification of the eruptive style (Pyle 1989; Walker 1973; Walker 1980). The mass eruption rate and the duration of the sustained phase can be estimated from the combination of these parameters (e.g. Sparks 1986; Wilson and Walker 1987).

However, techniques used in making field measurements are not always straightforward or consistent among investigators. This leads to variability in estimation of eruption parameters (i.e. erupted volume, mass discharge rate, eruption duration, column height, wind speed) and makes it difficult to compare eruptions with confidence. One of the goals of the IAVCEI Commission on Modeling Tephra Hazards is to assess the limitations of current field techniques and to suggest standard methods for making field measurements.

During the 3rd meeting of this IAVCEI Commission (January 2006, Salcedo, Ecuador) we have focused on the field techniques for the determination of the maximum clast (lithic and juvenile clasts) in order to increase consistency in estimation of eruptive parameters based on these measurements (e.g. column height and wind speed).

During the first day of the meeting the participants (Appendix A) shared experiences and limits of the various techniques used for the determination of the maximum clast (summarized in the next section). During the second day the 32 participants (divided into 5 groups) worked directly on two

outcrops to assess the variability of measurements due to the application of different techniques and to the individual measurements. Data were partially processed during the meeting and discussed with the whole group.

2.0 PRELIMINARY DISCUSSION

Maps of the distribution of "maximum clasts" (isopleth maps) are typically used to determine: (i) vent location (Walker 1980), (ii) eruption style (Pyle 1989), (iii) column height (Carey and Sparks 1986) and (iv) wind speed and direction at the time of the eruption (Carey and Sparks 1986). In particular, the column height is used to compare eruptions and determine the mass eruption rate (Sparks 1986; Wilson and Walker 1987). As a result, it is very important to understand the assumptions and define the limitations of the concept of "maximum clast" introduced by (Walker and Croasdale 1971) and commonly used to apply the method of Carey and Sparks (1986).

Method of Carey and Sparks (1986):

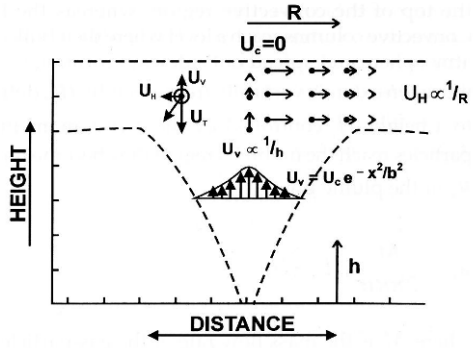

Fig. 1. Schematic representation of vertical and horizontal velocity components within a volcanic plume (from Carey and Sparks 1986).

Even though a buoyant eruptive column is characterized by fluctuating vertical velocities, plume studies have shown that the time-averaged vertical speed can be represented by a Gaussian function which is symmetrical with respect to the plume axis (Turner 1979) (Fig. 1). From the comparison between this Gaussian function and the settling velocities of volcanic particles, Carey and Sparks (1986) defined a series of theoretical "envelopes" that support the particles within the plumes (Fig. 2). Centerline velocities are typically sufficient to carry cm-sized clasts to the top of the eruption column, whereas larger clasts are deposited from the plume margins and can follow ballistic trajectories. When the particle settling velocity exceeds the plume upward velocity (characteristic of a given envelope), particles will leave the plume and eventually will deposit on the ground at a distance from the vent that depends on the column height and the wind speed and direction. As a result, the column height and the wind speed can be derived by plotting the maximum downwind range vs. the

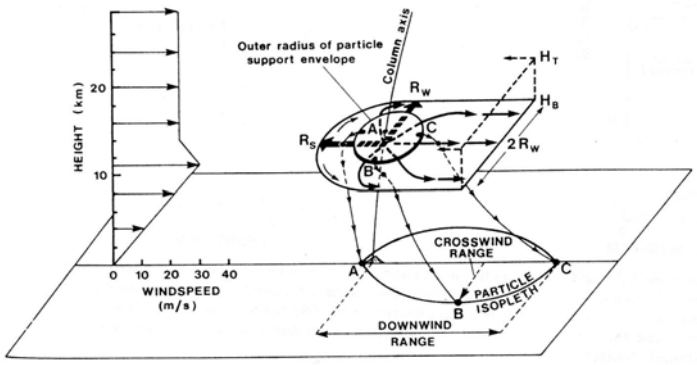

Fig. 2. Schematic representation of the influence of crosswind on clast fallout from an eruption column (from Carey and Sparks 1986).

crosswind range of any isoline describing the distribution maximum lithics and maximum pumices deposited on the ground (Figs 2 and 3).

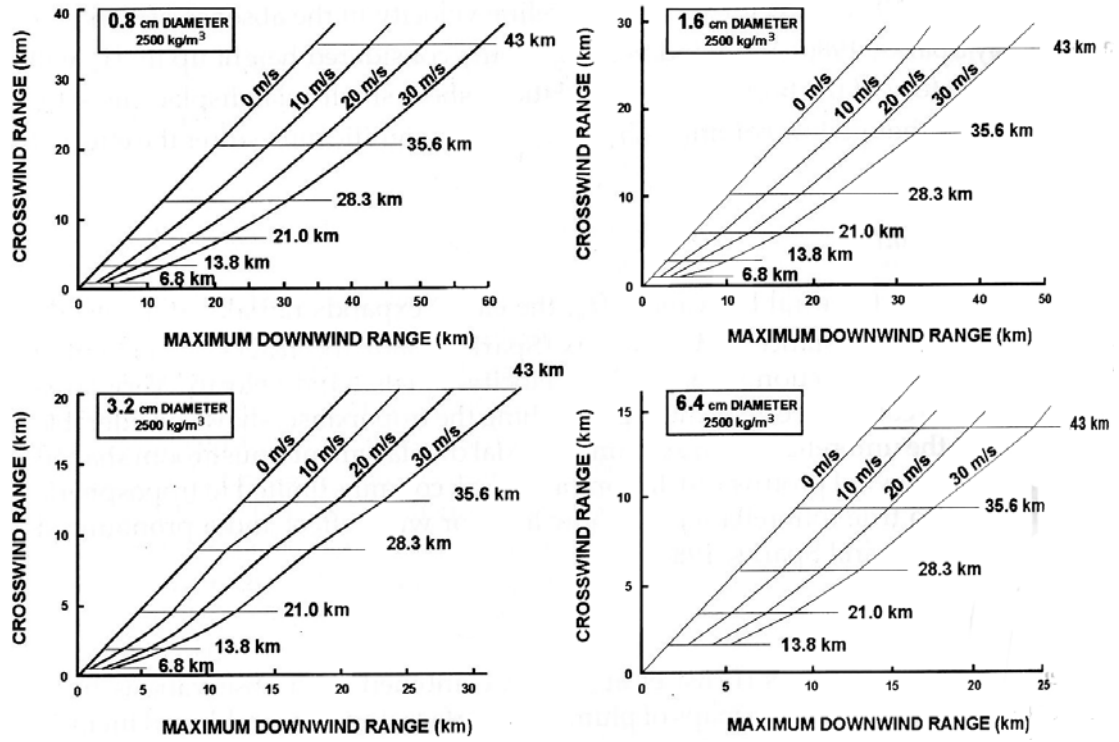

Fig. 3. Crosswind range vs. maximum downwind range for different clast sizes and a density of 2500 kg m^{-3}. A single clast isopleth defines a unique combination of column height (horizontal lines) and wind speed (from Carey and Sparks 1986).

Main assumptions and caveats of the method of Carey and Sparks (1986):

Vertical velocity: plume vertical velocity in the model of Carey and Sparks (1986) is determined for sustained plumes between about 7 and 43 km. As a result, such a model should only be applied to Plinian deposits. In addition, Woods (1988) has shown that large plumes might be characterized by superbuoyancy for which the vertical velocity profile is not monotone as assumed by Carey and Sparks (1986) (Fig.4). Such effect could support higher plumes than predicted by Carey and Sparks (1986).

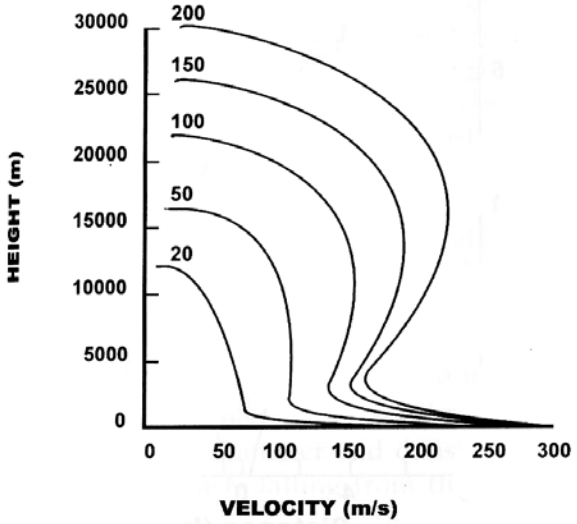

Fig. 4. Variation of the vertical velocity of volcanic plumes from a central vent with radii ranging between 20 and 200 m. For all profiles the initial conditions were an eruption velocity of 300 m/s and a magma temperature of 1000K (727° C) (Woods 1988).

Wind profile: the vertical wind profile considered in Carey and Sparks (1986) is from Shaw (1974) that assumes a maximum velocity (5-30 m/s) at the tropopause level (considered fixed at 11 km for all latitudes). The wind

velocity then decays linearly to zero at ground level and is 0.75 the maximum value above the tropopause (Figs 2 and 5). However, wind profiles are typically very variable. As an example, Carey and Sigurdsson (1986) modified the wind profile used in Carey and Sparks (1986) in order to account for a direction inversion above the tropopause occurred during the 1982 eruption of El Chichon (Fig. 5).

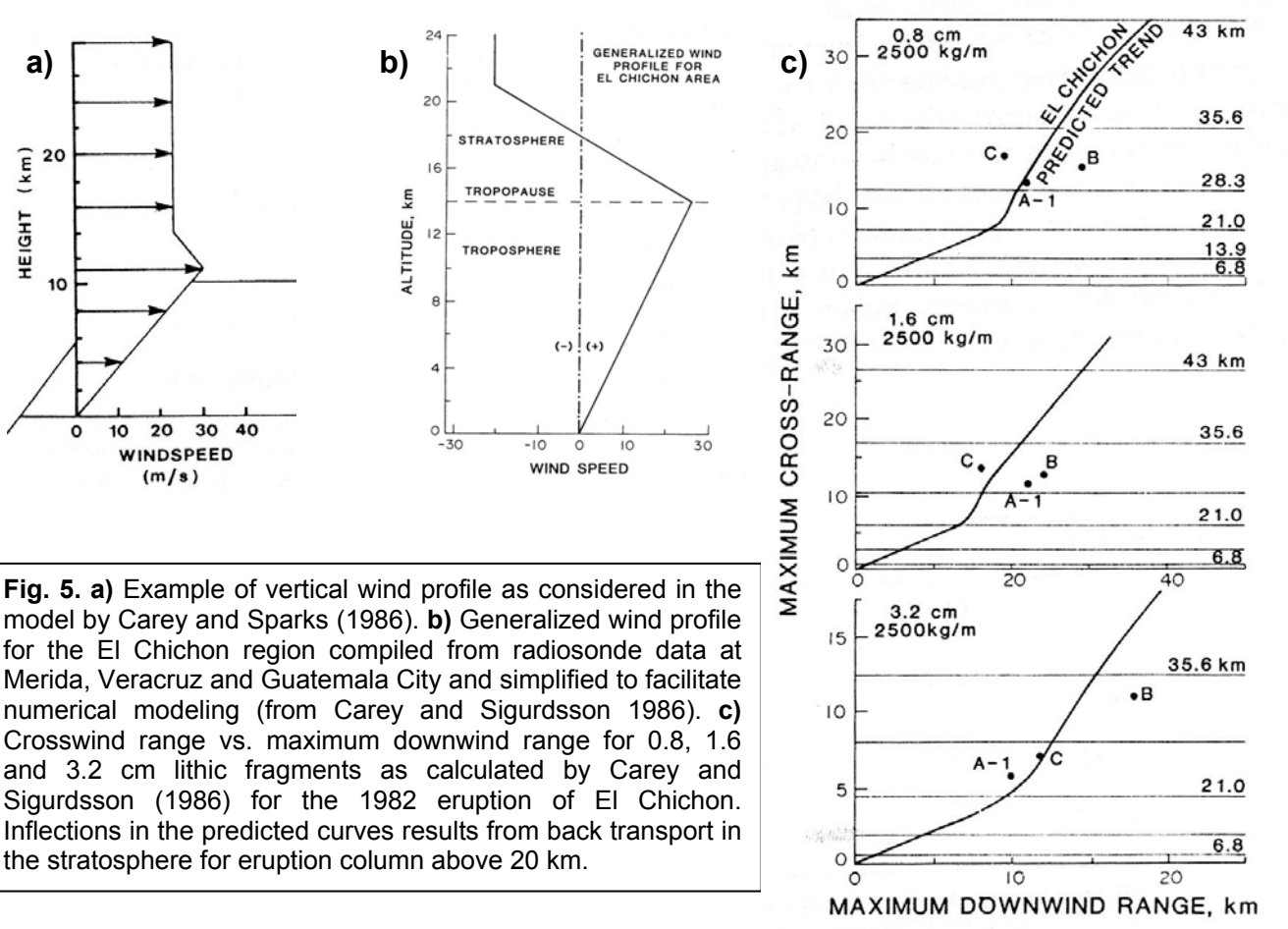

Fig. 5. a) Example of vertical wind profile as considered in the model by Carey and Sparks (1986). **b)** Generalized wind profile for the El Chichon region compiled from radiosonde data at Merida, Veracruz and Guatemala City and simplified to facilitate numerical modeling (from Carey and Sigurdsson 1986). **c)** Crosswind range vs. maximum downwind range for 0.8, 1.6 and 3.2 cm lithic fragments as calculated by Carey and Sigurdsson (1986) for the 1982 eruption of El Chichon. Inflections in the predicted curves results from back transport in the stratosphere for eruption column above 20 km.

Main issues related to the interpretation of the maximum clast:

Column height and mass eruption rate:

The plume height derived using the method of Carey and Sparks (1986) represents the maximum height reached during a given eruption because it is based on the distribution of the largest clasts found in the deposit. As a result, also the mass eruption rate determined using a column height derived with the method of Carey and Sparks (1986) represents a maximum value. In order to assess the fluctuation of plume height and mass eruption rate at different times, isopleth maps should be compiled for different stratigraphic levels (e.g. Vesuvius 79 DC eruption; Fig. 6) (Carey and Sigurdsson 1987).

PROBLEM: stratigraphic levels are normally difficult to distinguish in distal areas, being traceable with distance from vent only when the tephra deposit is characterized by distinct markers.

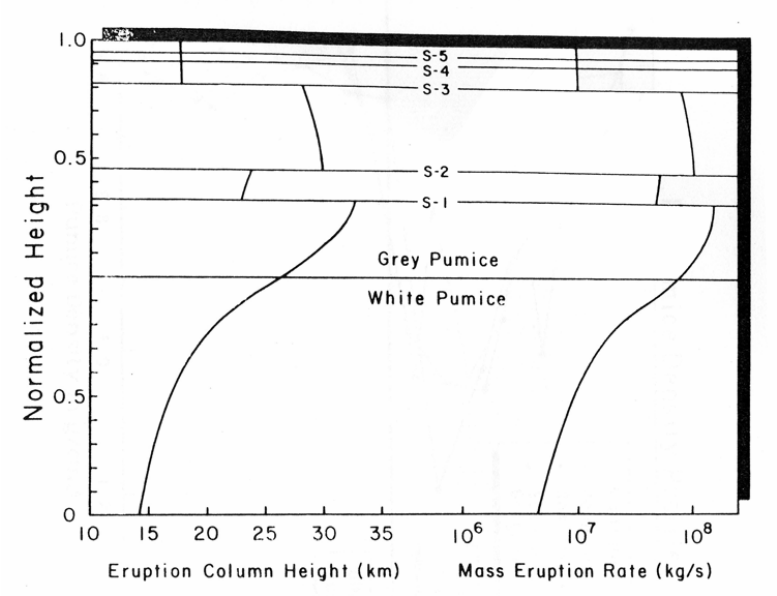

Fig. 6. Variation of column height and mass eruption rate with respect to the stratigraphic height of the associated tephra deposit (from Carey and Sigurdsson 1987)

Eruption classification and bt/bc value:

Pyle (1989) has introduced a plot to classify volcanic eruptions (Fig. 7), alternative to the classification of Walker (1973).

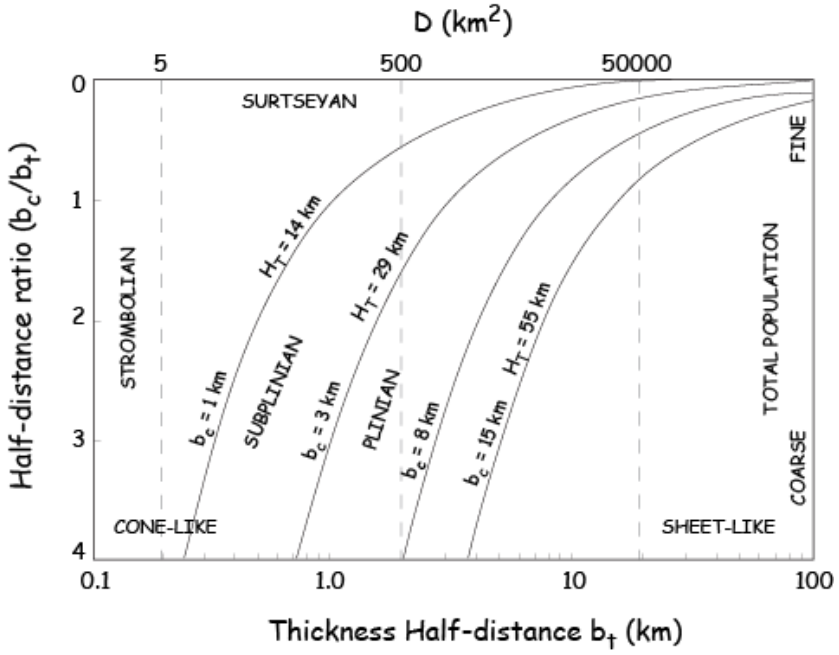

Fig. 7. Classification scheme from Pyle (1989). bt represents a proxy for dispersal and the half-distance ratio represents the total grainsize population. Walker's dispersal index (D) is shown for comparison.

Such a plot is based on the concept of the thickness half distance (bt) and the half distance ratio (bc/bt) introduced by Pyle (1989), where bc is the maximum clast size half-distance. Such a diagram is, in theory, easier to apply than the classic diagram of Walker (1973) because it does not require any grainsize analyses.

PROBLEM: tephra deposits often show one or more breaks-in-slope on semilog plots of thickness and maximum clasts vs square root of the areas, making the diagram of Fig. 7 more difficult to apply. However, data show that often tephra deposits characterized by breaks-in-slopes on thickness plots also show breaks-in-slopes on maximum-clasts plot and these breaks-in-slopes typically occur at similar distances. In addition, the bc/bt ratio for these deposits is typically constant (Table 1).

Deposit	Ht	$\sqrt{\pi}\, X_o$	BSth (km)	BSML (km)	ML (cm)	bc/bt 0	bc/bt 1	bc/bt 2
El Chichon A1	27	10	12,48	13,49	3,0.1	0.9	1.0	1.2
Fogo A	30	11	6	6	20	0.5	0.6	-
Fogo 1563	18	6	4	4	9	0.8	0.8	-
Quizapu	30	11	11	5	7	0.4	0.5	-
Vesuvius (g.p.)	33	12	10	25	20	0.7	0.7	

Table 1. Values of bc and bt derived from isopach and isopleth maps of the following eruptions: El Chicon 1982, Mexico (Carey and Sigurdsson 1986); Fogo A, Azores (Bursik et al. 1992); Fogo 1563, Azores (Walker and Croasdale 1971); Quizapu 1932, Chile (Hildreth and Drake 1992); Vesuvius 79 a.d. (Sigurdsson et al. 1985). X_o is the position of the plume corner, whereas $\sqrt{\pi}\, X_o$ should correspond to the first break in slope on semi-log plots of thickness vs. square root of isopach area (Bonadonna et al. 1998; Bursik et al. 1992).

Lithics or juveniles?

At a same location the size of pumice clasts is typically two to five times of that of associated lithics due to their lower density (Carey and Sparks 1986), with the ratio of pumice diameter over lithic diameter becoming progressively smaller as the vent is approached (Sparks et al. 1981). In fact, often juvenile clasts (both pumices and scorias) tend to be smaller than their originally size because they are likely to break with impact with the ground, and breakage is more efficient for coarse grains (Sparks et al. 1981). On the other hand, lithics are typically less breakable (unless strongly altered) and therefore lithic isopleth maps should be preferred when applying the method of Carey and Sparks (1986).

PROBLEM: some tephra deposits do not contain many lithics and/or the lithics are difficult to distinguish from the juvenile clasts. This is common in basaltic explosive deposits (e.g. Etna 122 BC Plinian eruption; (Coltelli et al. 1998)).

Assessment and meaning of the maximum clast:

The choice of the averaging technique for the assessment of the maximum clast is probably the most controversial issue of the application of the method of Carey and Sparks (1986). In fact, scientists calculate "maximum clasts" in different ways and have also applied different techniques to different deposits. Suzuki et al. (1973) have shown how the average of the maximum axis of the 10 largest clasts is comparable to the 1% coarsest percentile of the grainsize of a given outcrop, whereas Sparks et al. (1981) have shown that the geometric mean of the three axes of the 5 largest clasts is 1.5 times larger than the 1%. In Table 2 we present a list of the most used methods for the calculation of the maximum clast. In Table 3 we present a statistics of the most common number of axes, number of clasts and sampled area considered in 44 papers. Table 4 shows that the most common methods used are: (i) the average of maximum axis of the 3 largest clasts, (ii) the average of maximum axis of the 5 largest clasts, and (iii) the average of 3 axes of the 5 largest clasts (Table 4) (statistic still based on the same 44 papers as in Table 3).

Technique	Sampled area	Authors
Average of max axis of 3 largest clasts	unspecified	Fogo A, 1563 (Walker and Croasdale 1971); Taupo; Hatepe; Tarawera (Walker 1980; Walker 1981; Walker et al. 1984); Sta Maria (Williams and Self 1983)
Average of max axis of 10 largest clasts	1 m^2	Tarumai (Suzuki et al. 1973)
Geometric mean of 5 largest clasts	unspecified	Askja D 1875 (Sparks et al. 1981)
Average of 3 axes of 10 largest clasts	0.5 m^2	El Chichon 1982 (Sigurdsson et al. 1984)
Average of max axis of 5 largest clasts	1 m^2	Vesuvius 79AD (Sigurdsson et al. 1985); Mt St Helens (Carey et al. 1990)?
Average of 3 axes of 5 largest clasts	0.5 m^2	El Chichon 1982 (Carey and Sigurdsson 1986); Pululagua (Papale and Rosi 1993)
Average of 3 axes of 3-5 largest clasts	unspecified	Quizapu 1932 (Hildreth and Drake 1992); Novarupta 1912 (Fierstein and Hildreth 1992)
Average of max axis of 5 largest clasts	0.5 m^2	Cotopaxi, last 5000 yrs (Barberi et al. 1995)

Table 2. Techniques for the assessment of the maximum clasts reported in the literature

Number of axes	1	3	N.S.		
Number of papers	28	11	5		
Number of clasts	3	3-5	5	10	
Number of papers	12	6	22	4	
Sampled area (m^2)	0.25	0.50	1.0	vary	N.S.
Number of papers	1	8	2	4	28

Table 3. Statistics of the techniques for the assessment of the maximum clasts reported in the literature. References: (Ablay et al. 1995; Adams et al. 2001; Andronico and Cioni 2002; Barberi et al. 1995; Bryan et al. 2000; Carey and Sigurdsson 1987; Carey et al. 1990; Carey and Sigurdsson 1986; Fierstein and Hildreth 1992; Gardner and Tait 2000; Giannetti and De Casa 2000; Hildreth and Drake 1992; Jurado-Chichay and Walker 2000; Jurado-Chichay and Walker 2001; Kanisawa and Yoshida 1989; Limburg and Varekamp 1991; Lirer et al. 1973; Luhr 2000; McPhie et al. 1990; Milner et al. 2002; Papale and Rosi 1993; Pyle 1989; Rolandi et al. 2004; Sigurdsson and Carey 1989; Sigurdsson et al. 1985; Sigurdsson et al. 1984; Smith and Houghton 1995; Smith and Houghton 1995; Sottili et al. 2004; Sparks et al. 1981; Suzuki et al. 1973; Suzukikamata and Kamata 1990; Thouret et al. 2002; Walker 1980; Walker 1981; Walker and Croasdale 1971; Walker et al. 1981; Walker et al. 1984; Walker et al. 1981; Williams and Self 1983). NS: not specified.

Axes	clasts	Number of papers
1	3	12
1	3-5	4
1	5	11
1	10	2
1	NS	0
3	3	0
3	3-5	3
3	5	4
3	10	1
3	NS	0
NS	3	1
NS	3-5	0
NS	5	2
NS	10	1
NS	NS	3

Table 4. Statistics of the number of axis and clasts reported in literature (references as in Table 3).

The application of different techniques generates different isopleth maps and therefore can significantly affect the determination of column height and wind speed using the method of Carey and Sparks (1986). As an example, Barberi et al. (1995) have shown how the average of the maximum axis of the 3 largest clasts collected from a 2-m length exposure and excavating 5 cm of the deposit underestimates the crosswind range by 20-40% with respect to an isopleth map compiled averaging of the maximum axis of the 5 largest clasts sampled over 0.5 m^2 area (i.e. larger sampled volume) (Fig. 8).

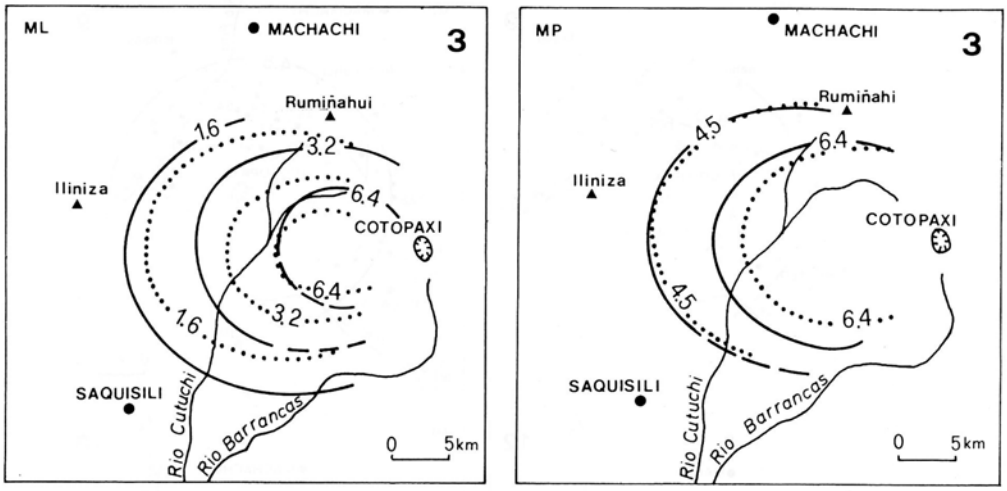

Fig. 8. Comparison between lithic and pumice isopleths (in cm) of tephra layers 3 measured averaging the three largest clasts (dotted lines) and the five largest clasts (solid lines). Three-clast isopleths are underestimated of about 20-40% (Barberi et al. 1995).

PROBLEM: sometimes tephra deposits do not show large exposures and can often be reachable only by digging deep holes (e.g. Unit 6 of Keananakakoi formation; D. Swanson unpublished data). As a result, some authors have suggested standardizing the time instead of the size of sampled area. In particular, D. Swanson has shown results for a sampling over 18 and 90 minutes respectively for the scoria on unit 6 of the Keanakakoi formation (Kilauea; Fig. 9).

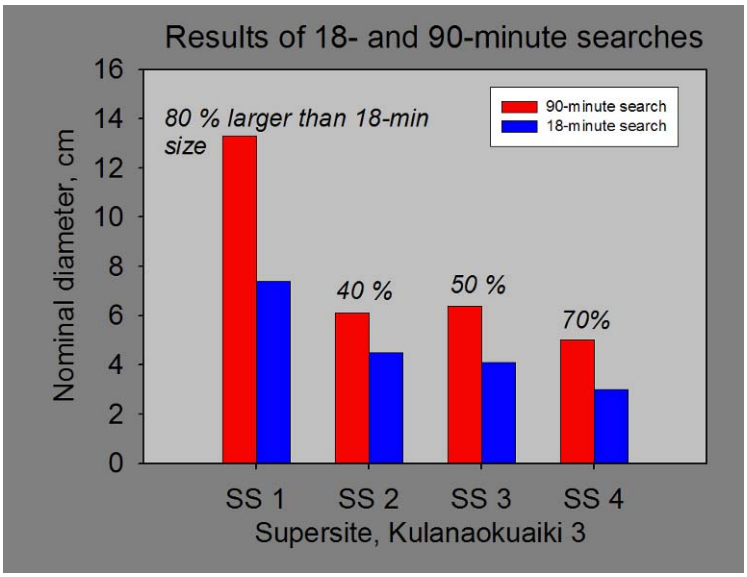

Fig. 9. Results from "time-sampling" at an outcrop of the Keanakakoi formation (Unit 6), Kilauea, Hawaii (Don Swanson unpublished data)

Oversize clasts:

When collecting the largest clast at a given outcrop, it is common to find a clast that is much larger in size than the rest of the population.

PROBLEM: do we disregard such a clast? Or is this clast part of the population? Several statistical methods are available to determine whether a given clast belongs to a given population. Two of the most common methods are the method of Dixon (1950) (typically used to determine outliers in small samples) and the boxplot method (Tukey 1977). Advantages and limits of these methods are discussed in the Data processing section (section 3.2).

Isopleth contouring:

Another, often underestimated, issue in the application of the method of Carey and Sparks (1986) is the contouring of the isopleth lines. Carey and Sparks (1986) have shown how even using the same techniques for the determination of the maximum clast of the Fogo A deposit (average of maximum axis of the 3 largest clasts), the resulting column height can differ significantly if different contouring assumptions are made. In particular, the derived column height is 35 km when contours were made based on the maximum value in concentric zones around the vent (Walker and Croasdale 1971), whereas a column height of 30 km was obtained when contours were based on the average value in concentric zones around the vent (Carey and Sparks 1986).

3.0 WORKSHOP EXERCISE

3.1. Methods

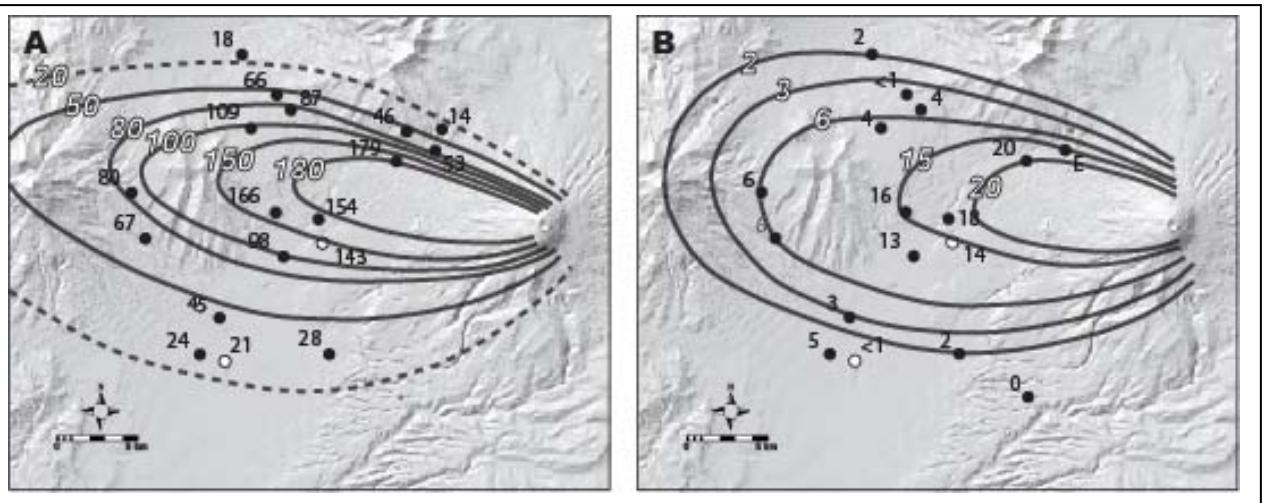

Fig. 10. a) Isopach map (cm) of Layer 3 (Biass and Bonadonna 2011). **b)** Isopach map (cm) of yellow top of Layer 3. The location of outcrops 1 and 2 is indicated with white circles.

In this exercise of the 3rd Meeting of the IAVCEI Tephra Commission we have assessed the effects of the following parameters on the evaluation of the maximum clast: (i) measurement of clast axes, (ii) collecting strategies (i.e. unspecified area vs fixed outcrop area), (iii) size of sampling area, (iv)

number of clasts considered in the calculation, and (v) different averaging techniques. In addition, we have also tested the reproducibility of grainsize analyses with respect to sample volume and data processing.

The assessment of these different parameters was tested on two outcrops of a massive andesitic pumice layer produced by a Cotopaxi eruption around 800 years ago (i.e., top unit of Layer 3 in Barberi et al. (1995) defined here as "yellow top") (Fig. 10). Layer 3 is the largest Cotopaxi eruption of the last 2000 years and is dispersed to the west of the volcano (Barberi et al. 1995), whereas the "yellow top" is dispersed to the northwest and separated from the rest of Layer 3 by a characteristic lithic-rich layer (Figs 10 and 11). Major element analyses of the juvenile fraction indicates a silica content of Layer 3 around 61.86 wt% and the associated erupted volume was estimated around 0.65 km^3 with a column height of about 28 km and a mass discharge rate of 1.1 x 10^8 k/s (Barberi et al. 1995). The "yellow top" is moderately sorted with abundant dark lithics (typically grey lava) and pumice clasts characterized by a more pronounced yellow color compared to the rest of the Layer.

The two outcrops of the "yellow top" were carefully selected at different distance from the vent (13 km and 22 km from the vent respectively; Fig. 10) in order to investigate the effect of grainsize variations on the determination of the maximum clast. The 32 participants of this workshop (Appendix A) were divided into 5 groups and different strategies for collecting clasts were applied.

OUTCROP 1 (UTM 17; 0772194, 9923567; Prov. Am. 56)

Distance from vent: 13 km

Thickness: 14 cm

Lithic content: 10-20 wt%

Stratigraphic description: massive, moderately sorted tephra layer with grainsize ranging from coarse ash up to 3 cm particles and an average size of about 1.5 cm (Figs 11 and 12).

Fig. 11. Outcrop 1

Exercise: On outcrop 1 the following sampling depositional areas were investigated: 0.1 m^2 (50x20 cm; adjacent areas α to ε; Fig. 13), 0.5 m^2 (250x20 cm; adjacent areas A to H) and unspecified-area sections (A to E; section length: 2, 2, 4, 4, 4 m) (Fig. 14). The unspecified-area collection consists in collecting the largest clasts along fixed-length sections without excavating a fixed outcrop area

(i.e. investigation of an unknown volume of material). We have also carried out the collection of the largest clasts at all unspecified-area sections varying the sampling time between 2, 4, 6, 8 and 15 minutes (Fig. 14).

Fig 12. Workshop participants working on the 0.5 m^2 areas at outcrop 1.

Various samples for the analyses of the outcrop grainsize were also collected: two samples of outcrop areas A and F and samples from two sections of approximately 0.1 m^2 areas that we sieved in the field down to 8mm (samples 1 and 2) (Table 5).

	SAMPLE 1	SAMPLE 2	Area A	Area F
Dimensions (cm)	47x 28.5 x 9.5	50 x 24 x 12.5	-	-
Volume (cm^3)	12725	15000	-	-
Weight in the field (g)	15533	13682	1253 (dry)	889 (dry)
Bulk density (kg m^{-3})	911±36	931±38	-	-
A, Hawaii lab (weight, g)	514	474	-	-
B, Pisa (weight, g)	557	437	-	-
C, Tampa (weight, g)	417	450	-	-
D, Catania (weight, g)	475	508	-	-

Table 5. Characteristics of samples collected at outcrop 1 for grainsize analysis.

During the workshop we sieved all the samples down to 8mm and we also counted and weighted individual clasts in the size fraction 8-16 mm of the two 0.1-m^2-area samples (i.e. samples 1 and 2; Tables 6 and 7). Finally, four splits of material below 8 mm for the two samples were given to four different labs for grainsize analyses (University of Hawaii at Manoa, University of Pisa, University of South Florida-Tampa and INGV- Section of Catania) (Table 5).

SAMPLE 1	*Volume:* *0.013 m^3*					
	Pumices		Lithics		TOT	
	Wt (g)	Number	Wt (g)	Number	Wt (g)	Number
32 mm	31.4	2	31.9	1	63.3	3
16 mm	2094.3	480	82.9	12	2177.2	492
8 mm	4433	4362	535	401	4968	4763
TOT	**6558.7**	**4844**	**649.8**	**414**	**7208.5**	**5258**

Table 6. Number of clasts in 8-16 mm size category of sample 1

SAMPLE 2	*Volume:* *0.015 m^3*					
	Pumices		Lithics		TOT	
	Wt (g)	Number	Wt (g)	Number	Wt (g)	Number
32 mm	0	0	0	0	0	0
16 mm	1764.7	397	95	16	1859.7	413
8 mm	2788	ND	1708	ND	4496	ND
TOT	**4552.7**	ND	**1803**	ND	**6355.7**	ND

Table 7. Number of clasts in 8-16 mm size category of sample 2. ND: not determined

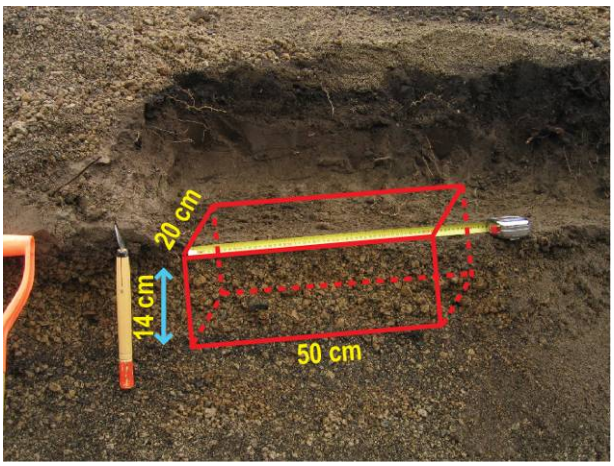

Fig. 13. Example of sampling a specified-area section (i.e. 50 x 20 cm = 0.1 m^2). Outcrop thickness: 14 cm.

Fig. 14. Example of sampling an unspecified area of section C in different time steps: 2, 4, 8 and 15 minutes (from right to left).

OUTCROP 2 (UTM 17; 0764716, 9916814; Prov. Am. 56)

Distance from vent: 22 km

Thickness: 5 cm

Lithic content: 20 wt%

Stratigraphic description: massive, moderately sorted tephra layer with grainisize ranging from 1 mm up to 1.5 cm and an average size of about 0.5 cm (Fig. 15).

Fig. 15. Outcrop 2

Exercise: On outcrop 2 the following sampling depositional areas were investigated: 0.1 m^2 (50x20 cm; adjacent areas A to J) and unspecified-area sections (A to E; section length: 0.5, 0.5, 1, 1, 1 m) (Fig. 16). Finally, a sample was also collected for grainsize analyses of the whole outcrop (dry weight: 430 g).

Fig. 16. Workshop participants working on the 0.1 m^2 areas at outcrop 2.

3.2 Data processing

As part of the exercise we have investigated: effects of sample volume and analyses techniques on grainsize distribution (section 3.2.1); measurement of clast axis (section 3.2.2); variability of clast shape (section 3.2.3); detection of outliers (section 3.2.4); comparison amongst different averaging techniques and different collection strategies (section 3.2.5); variability of measurement within a given outcrop (section 3.2.6); comparison of different strategies of clast collection (section 3.2.7); effects of the size of sampling area (section 3.2.8); effects of the size of sampling area with respect to different averaging techniques (section 3.2.9); combined effects of the size of sampling area and collection strategy (section 3.2.10). A larger selection of data and plots is reported in Appendices B to J.

3.2.1. Grainsize distribution

Grainsize analysis carried out using the sieving technique by three different labs has given very similar results on two samples of the same outcrop (samples 1 and 2 in Table 5) with an average standard deviation of 0.2 and 0.4 wt% respectively (Fig. 17).

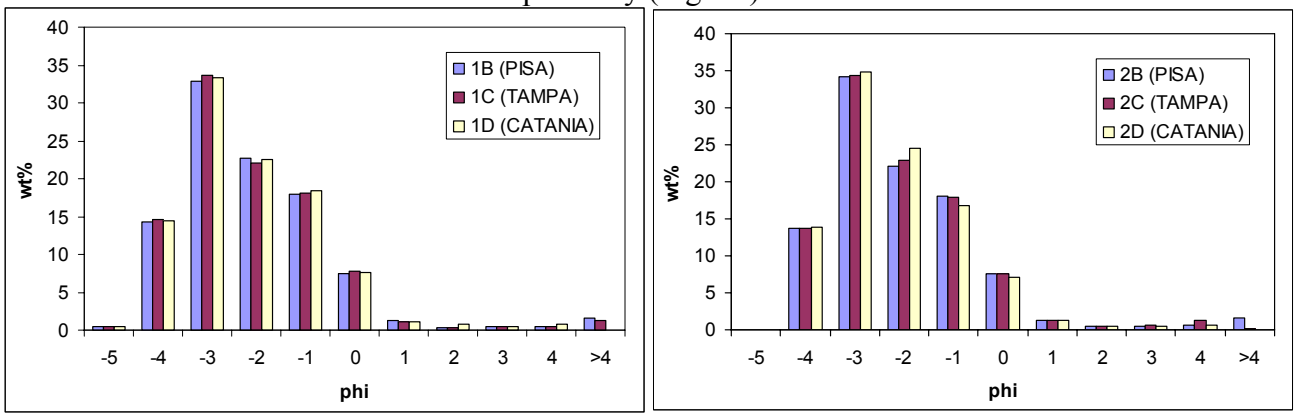

Fig. 17 Sieving grainsize analyses carried out by three labs (Pisa, Tampa and Catania) on two samples collected at outcrop 1 (sample 1 and 2; Table 5). STDV of each size class ranges between 0.0 and 0.9wt% for both samples (average STDV is 0.2wt% and 0.4 wt% for sample 1 and 2 respectively).

The comparison between different analyses techniques, Pharmavision 830 (www.malvern.co.uk) (USF-Tampa) and Camsizer (http://www.horibalab.com/) (INGV-Catania), has also given a reasonable agreement (Figs 18 and 19) with an average standard deviation with respect to sieving of 0.2 and 0.9 wt% respectively.

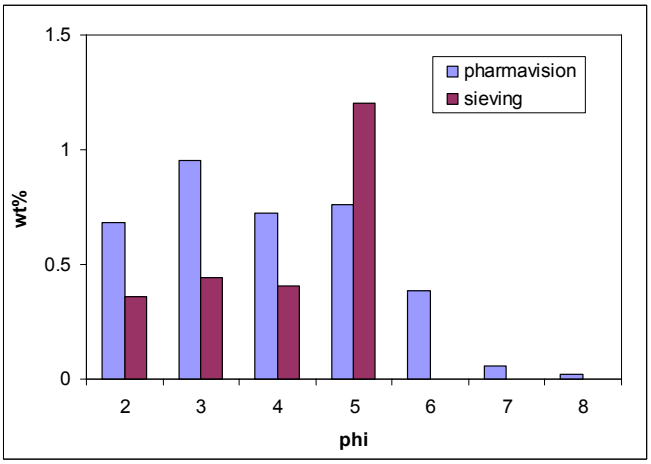

Fig. 18 Grainsize distribution of sample 1C carried out using both only sieving and sieving down to 1mm (0 phi) and Pharmavision for particle <1mm. STDV of each size class is between 0.0 and 0.8wt% (average STDV=0.2wt%). Analyses carried out in Tampa.

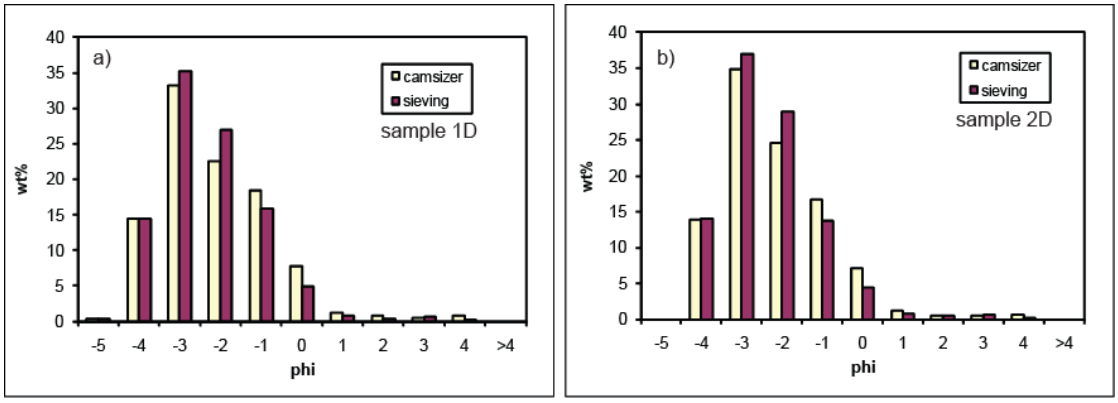

Fig. 19 Grainsize distribution of samples 1D and 2D carried out using both sieving and Camsizer analyser. Standard deviation of each size class is between 0.0 and 3.1wt% for sample 1D and between 0.0wt% (average standard deviation=0.9wt%) and 2.2wt% for sample 2D (average standard deviation=0.9wt%). Analyses carried out in Catania.

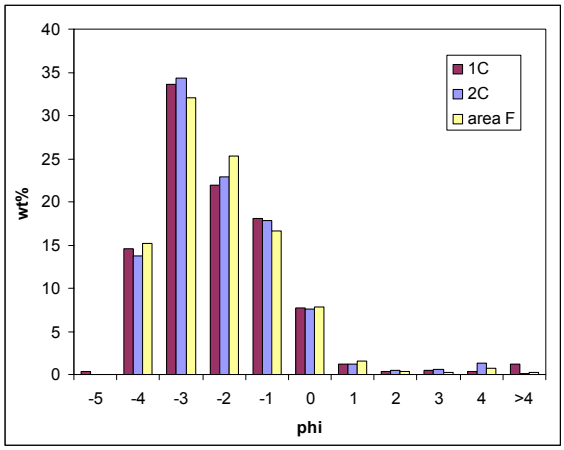

Fig. 20 a) Grainsize distribution of three samples of the same outcrop (1C, 2C and area F; Table 5) carried out using hand sieving. Samples 1C and 2C are of similar volume (0.01 m^3), whereas the sample of area F was collected of unspecified area. Standard deviation of each size class is between 0.0% and 1.7wt% (average standard deviation=0.6wt%).

In addition, samples of the same outcrop (i.e. sample 1, sample 2 and a sample form area F in table 5) also gave very similar results, with an average standard deviation of 0.6 and 0.5 wt% (Fig. 20). Values of Md_ϕ and σ_ϕ are summarized in Table 8 showing consistent results for all techniques used and sampled analyzed. All data of these grainsize analyses are given in Appendix B.

	Mdϕ	σϕ
1B (sieving)	-2.9	1.4
2B (sieving)	-2.9	1.3
1C (sieving +parmavision830)	-2.9	1.4
1C (sieving)	-2.9	1.4
2C (sieving)	-2.9	1.3
1D (sieving)	-2.9	1.3
2D (sieving)	-2.9	1.3
1D (camsizer)	-3.0	1.2
2D (camsizer)	-3.0	1.1
Area A (sieving +parmavision830)	-2.8	1.3
Area F (sieving)	-2.9	1.3
Outcrop 2 (sieving +parmavision830)	-1.5	1.4

Table 8 Parameters of Inmann (1952) derived for all sampled analyzed.

3.2.2. Measurement of clast axis

Any particle size and shape analysis starts from the measurements of the associated axes. Typically, the determination of the largest clast is based on the measurement of one or three axes out of the longest (a-axis), the intermediate (b-axis), and the shortest (c-axis) axis. However, the determination of such axes is not unique. Therefore, we have investigated the variation of clast characterization by having 7 people measuring 3 axes of the same 10 lithic clasts (Appendix C). Fig. 21a shows the scatter of these measurements with respect to the actual diameter of the equivalent sphere (calculated from the clast volume). Fig. 21b shows the associated arithmetic mean and standard deviation.

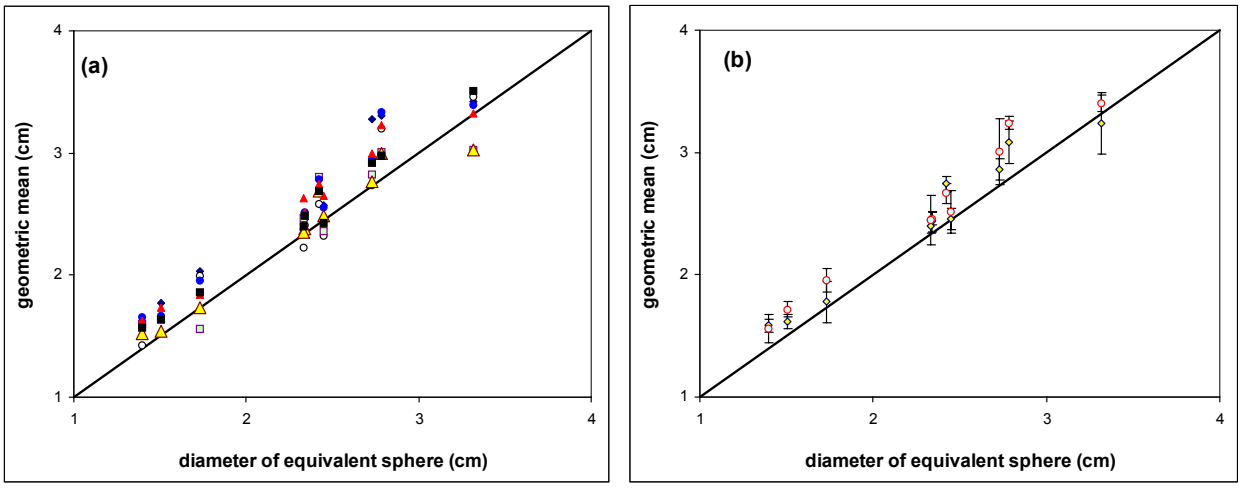

Fig. 21 a) Variation of clast measurements with respect to the diameter of the equivalent sphere determined from the volume derived using the Archimede's principle; **b)** mean and standard deviation of two sets of data based on the assumption of minimum (yellow triangles) and maximum ellipsoid (blue circles) respectively. The straight line indicates the 1:1 relation.

The percentage difference between the geometric mean (determined from the measured axes) and the diameter of the equivalent sphere (determined from the real volume of the particle) varies between 0.2 and 18.5% with an average percentage difference per person that varies between 2 and 12% (Appendix C). The lowest percentage difference was obtained by the investigators that approximated the clast considering the smallest ellipsoid (i.e. solid lines in Fig. 22 and yellow triangle in Fig. 21a).

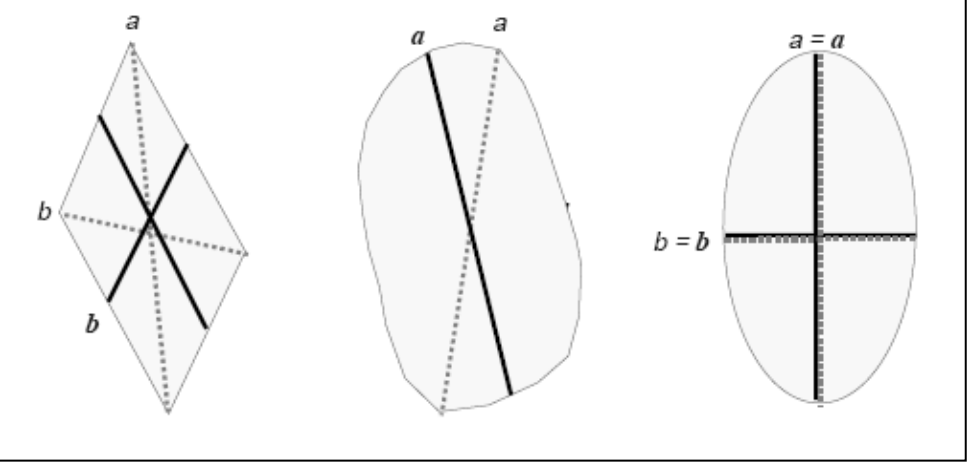

Fig. 22 Discrepancy in b- and a-axes definitions for rhombic, irregular ellipsoidal, and ellipsoidal particle shape. Dashed and solid lines consider the approximation for the maximum and minimum ellipsoid respectively (Bunte and Abt 2001).

3.2.3. Clast shape

Given that the measurements of the largest clast are used for application in models that are based on the assumption of spherical particles (e.g. Carey and Sparks 1986), it is important to assess the equidimensionality of clasts to avoid large discrepancies with the model assumptions. Fig. 23 shows the scatter of shape factors (defined as in Wilson and Huang (1979): F=(b+c)/2a with a>b>c) with respect to the geometric mean, which represents the diameter of a sphere with the same volume of an ellipsoid with the same axes of the measured clast. Shape factors vary equally for lithic and pumice clasts between 0.3 and 0.95.

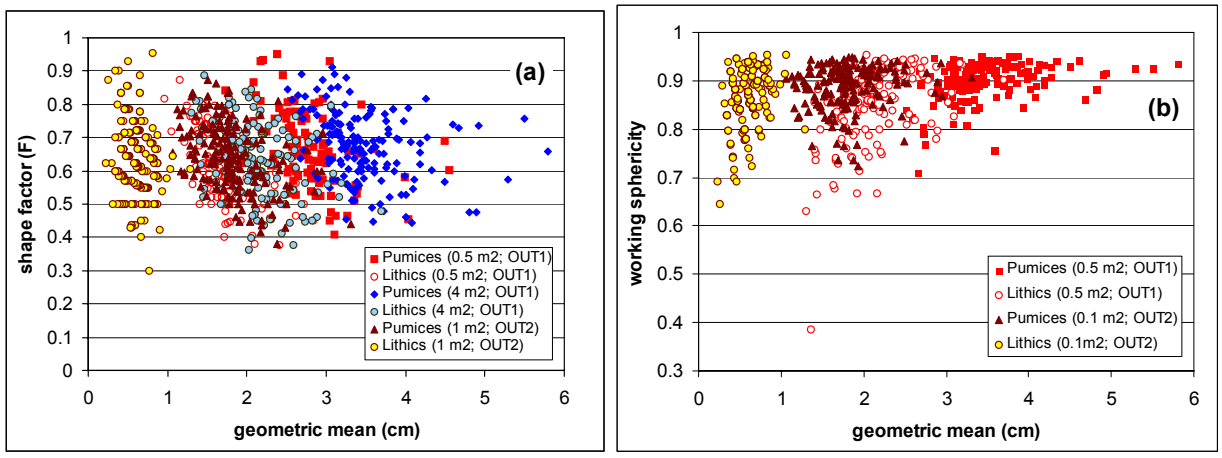

Fig. 23 Plots showing the variation of: **a)** the particle shape factor, F (Wilson and Huang 1979), and **b)** the working sphericity (Aschenbrenner 1956) with the particle geometric mean for pumice and lithic clasts collected in the largest areas in both outcrop 1 and 2, i.e. α+β+γ+δ+ε outcrop 1 (total of 0.5 m^2); A+B+C+D+E+F+G+H outcrop 1 (total of 4 m^2); A+B+C+D+E+F+G+H outcrop 2 (total of 1 m^2)

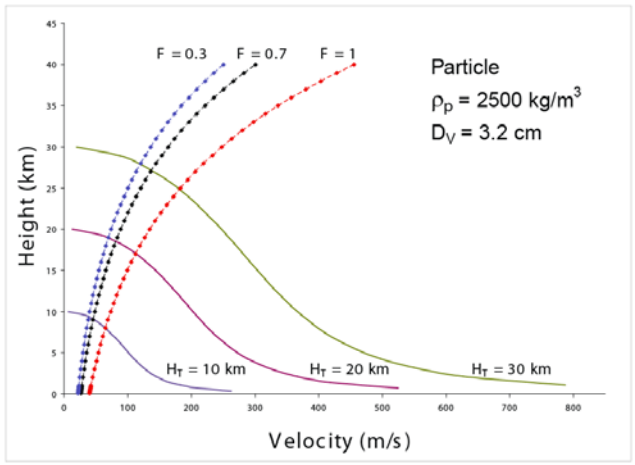

Fig. 24 Comparison between plume vertical velocities and settling velocities of a clast with diameter of 3.2 cm (i.e. diameter of equivalent sphere) and a density of 2500 kg m^{-3}. Plume velocities are calculated using the model of Sparks (1986) for a 10, 20 and 30 km plume respectively and clast terminal velocities are calculated using the model of Wilson and Huang (1979).

Independent calculations show that the height at which clasts with F=0.3 are supported by the plume velocity is about 10% and 20% larger (for a 30 and 10 km high plume respectively) than for a sphere of equivalent diameter (i.e. F=1) (Fig. 24). Larger discrepancies would exceed the error of this technique (20%; Carey and Sparks 1986).

3.2.4. Outliers

The presence of "oversize" clasts, i.e. size outliers, is a delicate issue in the assessment of the largest clasts. Several methods for treating outliers exist in the statistic literature (see Barnett and Lewis 1998 for a review) but no standard method is currently used in tephra studies. Data outliers can be due to inherent variability, measurement error or execution error (Barnett and Lewis 1998). Given that clast measurements are typically done in the field, we exclude the possibility of measurement error (assuming that the detection of outliers is firstly done visually). In contrast, execution error (imperfect collection of the data) and inherent variability (natural variation of the population) are two possible causes of the presence of outliers that need to be carefully analyzed. In addition, even when the outlier values are perfectly legitimate, if they lie outside the range of most of the data, they can cause calculation anomalies. As a result, different strategies have been proposed to deal with outliers, mainly accommodation (not requiring outlier identification) or rejection of outliers (requring the application of detection tests). There are several ways to accommodate outliers to mitigate their harmful effects (e.g. non parametric analysis, data transformation). Deletion can be considered only as a last resort should outliers be detected and only if they significantly affect the final results. Below we have discussed the application of two methods commonly used to detect outliers: boxplot (Tukey 1977) and Dixons test (Dixon 1950).

geometric mean (cm)
4.55
4.49
3.38
3.07
2.96
2.85
2.76
2.73
2.67
2.63
2.59
2.57
2.56
2.52
2.46
2.38
2.24
2.23
2.13
2.11

Table 9. Geometric mean (cm) of ten pumices collected at the 0.1-m^2 area α of outcrop 1

Population= 5 clasts		
first quartile	third quartile	interquartile range
3.07	4.49	1.43
potential outliers:	<0.92	>6.64
problematic outliers:	<-1.22	>8.78

Population= 10 clasts		
first quartile	third quartile	interquartile range
2.74	3.30	0.57
potential outliers:	<1.89	>4.15
problematic outliers:	<1.04	>5.00

Population= 20 clasts		
first quartile	third quartile	interquartile range
2.44	2.87	0.43
potential outliers:	<1.79	>3.53
problematic outliers:	<.14	>4.18

Table 10. Results (in cm) of the boxplot method considering different population sizes, i.e. first 5 clasts, first 10 clasts and all 20 clasts.

The boxplot method is a convenient way to describe a population of values and identifies potential and problematic outliers. However, the boxplot is typically more appropriate for large datasets,

whereas the Dixons test is more appropriate for small datasets. A sensitivity analysis was carried out on a population of pumice clasts collected at the 0.1-m^2 area α of outcrop 1 (Table 10). Results show how both the boxplot and the Dixon's test are affected by the size of the population. In fact, when applying the boxplot method to populations of different sizes, the first two clasts (geometric mean of 4.55 and 4.49 cm) are not outliers in the 5-clast population, are potential outliers in the 10-clast population and are problematic outliers in the 20-clast population (Table 11). In contrast, according to the Dixon's test, the first clast (geometric mean of 4.55 cm) is an outlier when considered in a population of 20 clasts (given a critical value of 10%) and for populations of 10 and 5 clasts when the second clast is removed (geometric mean of 4.49 cm) (see Appendix D for the application of the Dixons test). However, if we include the second clast in the calculation, the first clast is not an outlier anymore for populations of 10 and 5 clasts (Table 11).

	Outlier	R	Rcrit (10%)
Population 5	NO	0.038	0.557
Population 5*	YES	0.686	0.557
Population 10	NO	0.032	0.409
Population 10*	YES	0.610	0.409
Population 20	YES	0.504	0.401

Table 11. Application of the Dixons test to populations of 5, 10 and 20 clasts from Table 10. 5* and 10* represent populations without the second clast (geometric mean of 4.49 cm). R and Rcrit are derived from Table D1 (Appendix D).

The use of the median of a population (i.e. middle value when all values are listed in ascending order) instead of the arithmetic mean represents an alternative to "rejection tests" used to deal with outliers, because the median is less affected by the presence of extreme values (example of accommodation strategies using a robust parameter). Table 12 shows the mean and median associated with different populations considered in Table 10.

	mean	median
population 5	3.69	3.38
population 5*	3.36	3.07
population 5**	3.00	2.96
population 10	3.21	2.90
population 10*	3.02	2.80
population 10**	2.82	2.75
population 20	2.79	2.61

Table 12. Mean and median of the different populations considered in the sensitivity analysis. Populations 5, 10 and 20 refer to the populations of first 5, 10 and 20 clasts in Table 10. Populations 5* and 10* refer to the population of the first 5 and 10 clasts ignoring the clast with geometric mean of 4.49 cm (second clast). Populations 5** and 10** refer to the population of the first 5 and 10 clasts ignoring the clasts with geometric mean of 4.55 and 4.49 cm (first and second clast).

The median seems to be more stable than the mean, with an associated standard deviation of 0.25 cm and 0.32 cm respectively. However, the variation of the mean and the median between population 5 and population 20 are of similar scale (0.90 and 0.77 cm respectively). In addition, Fig. 25 shows how values of mean and median follow a similar trend for the maximum axis of three clasts (1/3), the arithmetic mean of the three axes of 5 clasts (A3/5) and the arithmetic mean of the three axes of 20 clasts (A3/20). The differences between the median values of 1/3, A3/5, A3/20 are comparable with the differences between the mean values of 1/3, A3/5 and A3/20. As a result, the

use of the median for this kind of populations does not seem to provide a better solution to the stability of the data.

Finally, volcanologists are traditionally mostly concerned with size outliers, but also large differences in density and shape could affect the final results. However, density outliers are difficult to determine in the field because of the variable humidity of the deposit affecting clast density. Fig. 26 shows a 42% and 6% difference between wet (as measured in the field) and dry weight (as measured in the lab) for pumices and lithics respectively. Nonetheless, lithics are typically characterized by smaller variability. As an example, the relative standard deviation (%RSD) for 20 clasts of Layer 3 is only about 7% for lithics and 29% for pumices.

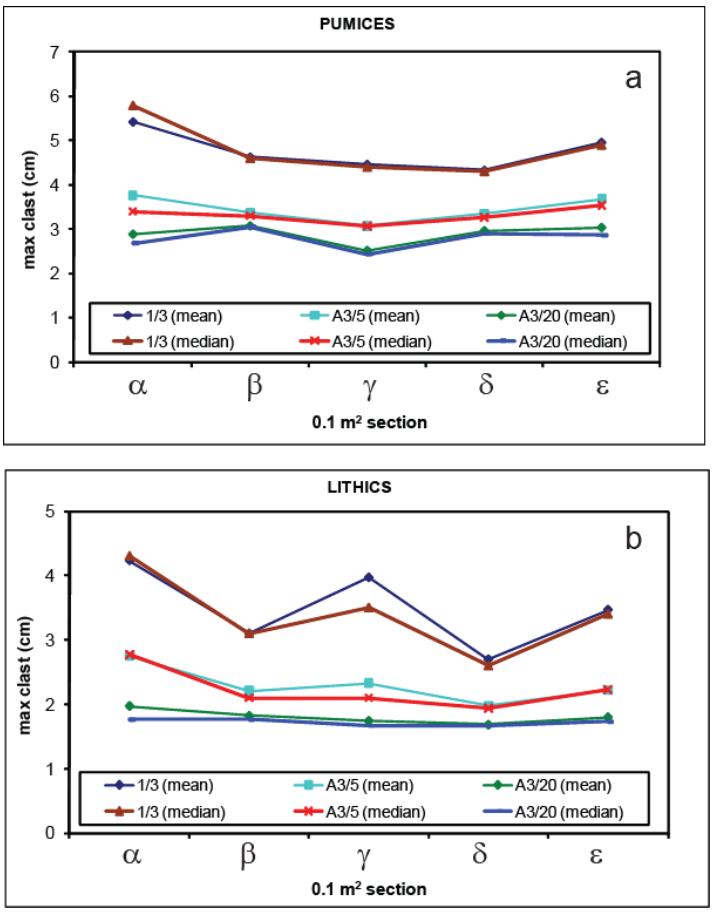

Fig. 25. Comparison amongst arithmetic mean and median of three different data population for pumices (a) and lithics (b): 1/3 (maximum axis of 3 clasts), A3/5 (arithmetic mean of three axes of 5 clasts) and A3/20 (arithmetic mean of three axis of 20 clasts).

In addition, shape analysis carried out to identify discrepancies from sphericity (e.g., section (3.2.3)) could be more valuable than the determination of shape outliers. As a result, both density and shape outliers are not useful information that can be determined in the field.

Given the dependence of the determination of outliers on the detection method used and on the size of the population considered, and assuming that the most likely cause of outliers in our analysis is the inherent variability of the system, we have decided not to exclude any clasts in our data processing.

	Lithics	Pumices
Density range (g cm^{-3})	2.6 – 3.1	0.3 – 1.2
Density mean (g cm^{-3})	2.7	0.7
Standard deviation (g cm^{-3})	0.2	0.2
Relative standard deviation %	7.4	28.6

Table 13. Density values of 20 lithics and pumices of Layer 3

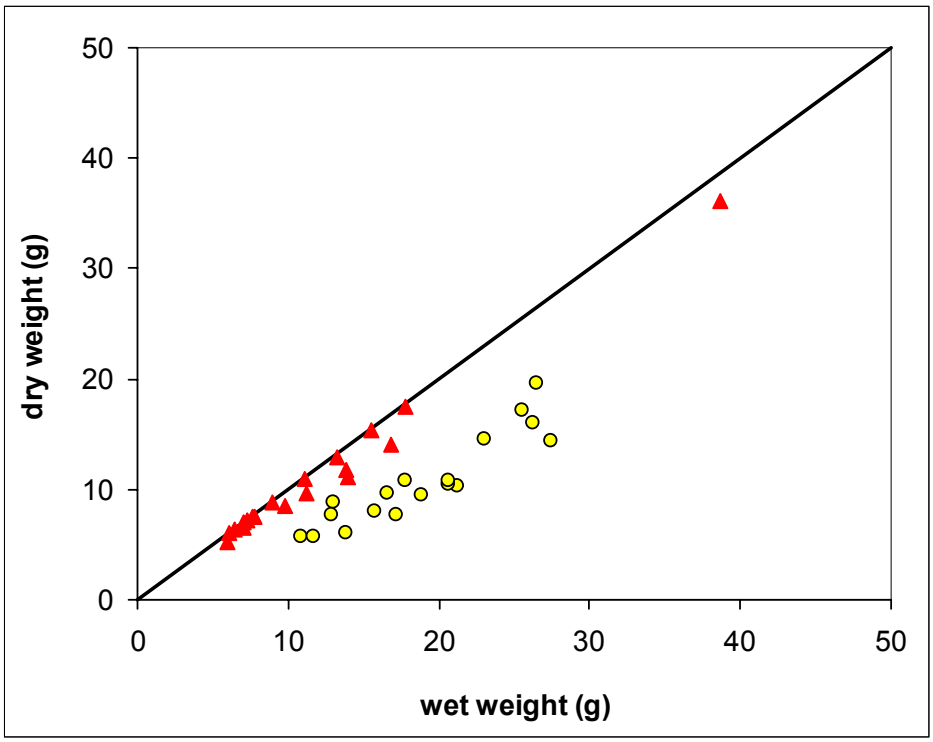

Fig. 26. Discrepancy between dry (measured in the lab) and wet (measured in the field) weight (grams) for 20 pumices and 20 lithics collected in the 0.5 m^2 section of outcrop 1 (section C).

3.2.5. Comparison amongst different averaging techniques and different collection strategies

In this section we report the results of the evaluation of the largest pumice and lithic clasts at outcrop 1 and 2, for different sampling areas, using both the specified- and unspecified-area collecting strategies and applying different averaging techniques (Table 14).

Averaging technique	Description
1/3	arithmetic average of maximum axis of 3 clasts
1/5	arithmetic average of maximum axis of 5 clasts
A3/3	arithmetic average of arithmetic mean of the 3 axes of 3 clasts
A3/5	arithmetic average of arithmetic mean of the 3 axes of 5 clasts
G3/5	arithmetic average of geometric mean of the 3 axes of 5 clasts
A3/10	arithmetic average of arithmetic mean of the 3 axes of 10 clasts
A3/12	arithmetic average of arithmetic mean of the 3 axes of 12 clasts

Table 14. Description of all averaging techniques used to determine the largest clasts in all areas and all outcrops

OUTCROP 1

Collection strategy: specified-area sections (0.1 and 0.5 m^2)

As described in section 3.1, 20 pumices and 20 lithics were collected at outcrop 1 in 5 areas of 0.1 m^2 each (α to ε) and 8 areas of 0.5 m^2 each (A to H). First of all, Fig. 27 shows how the technique of averaging the largest axis of 3 and 5 clasts gives very different results compared to the

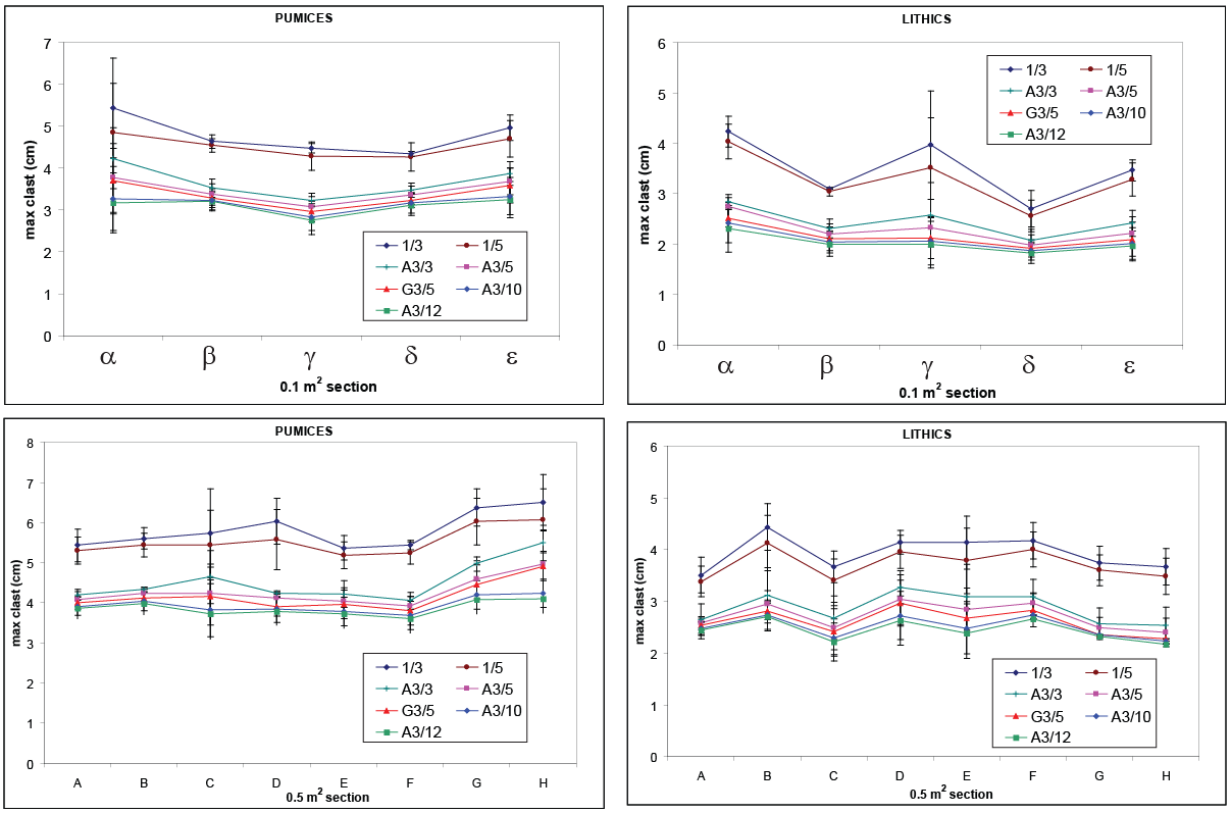

Fig. 27. Variation of the values of the largest pumices and the largest lithics determined using different averaging techniques and different sampling areas (0.1 and 0.5 m^2 respectively). Standard deviations for each clast population are also shown.

techniques that consider the arithmetic and geometric mean of the three axes. In fact, a population of values resulting from the average of the maximum axes (1/3 and 1/5) and a population of values that average the arithmetic and geometric mean of the three axis (A3/3, A3/5, G3/5, A3/10, A3/12) can be identified.

Collection strategy: unspecified area (section length: 2 and 4 m)

Section length shows a strong influence on the application of the unspecified-area collection, with the lowest values given by clasts collected in the smallest sections (i.e. A and B; 2 m) (Fig. 28).

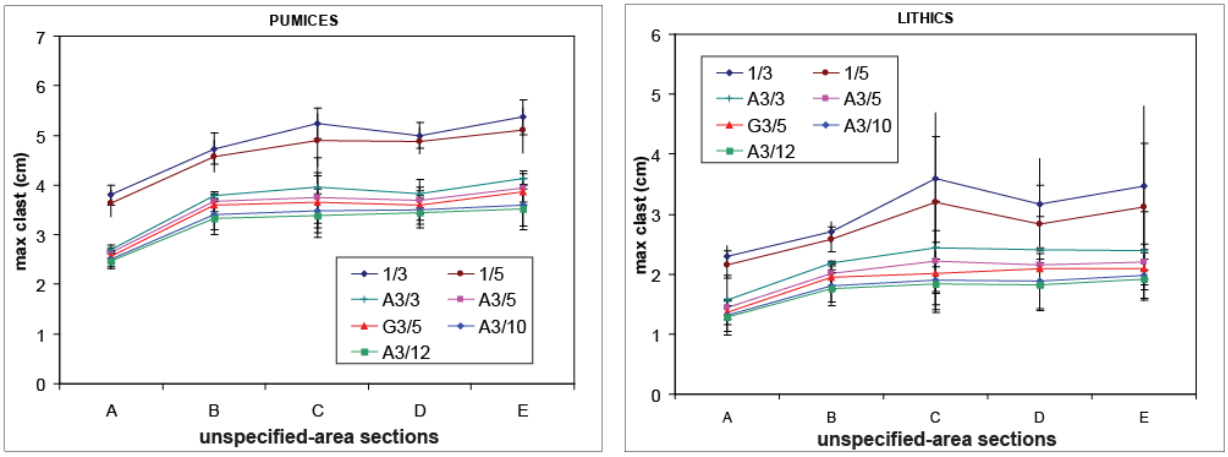

Fig. 28. Variation of the values of the largest pumices and the largest lithics determined using different averaging techniques and different unspecified-area sections of 2 m (A and B) and 4 m (C, D and E). Standard deviations for each clast populations are also shown.

Collection strategy: unspecified area (fixed time on different section lengths: 2 and 4 m)

Clast collection carried out at the area A (section length: 2m; Fig. 29) results in lower values compared to the clast collection carried out at area E (section length: 4m; Fig. 30) regardless the sampling time. However, a small increase in values is mostly recorded after 8 minutes (see also Appendix E for plots of areas B, C and D).

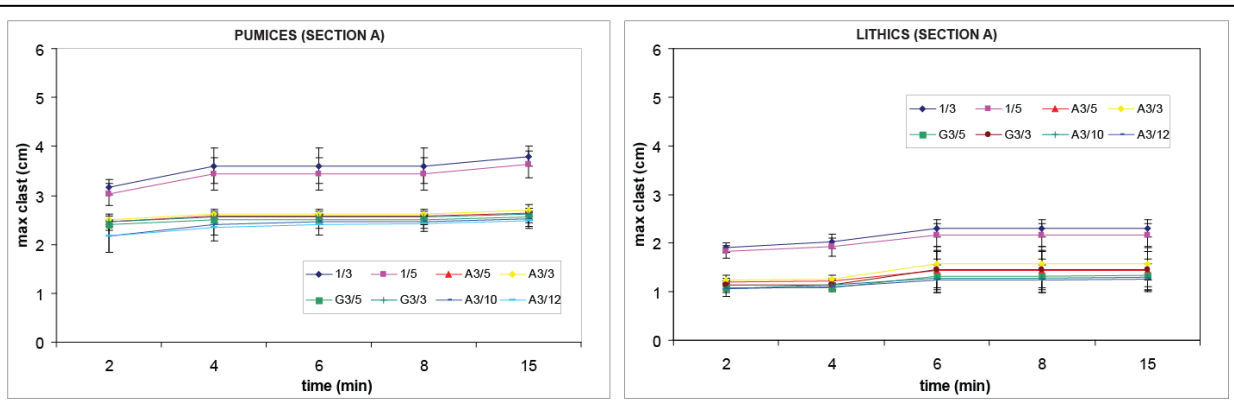

Fig. 29. Example of variation of large-clast values for pumices and lithics collected over an unspecified-area section of 2-m length at increasing times from 2 to 15 minutes (section length= 2m; A).

Finally, clasts collected over the 5 different sections (A to E) for 15 minutes give a significant variability, with 2-m sections significantly underestimating the values of largest clasts regardless the averaging technique (maximum axis and geometric mean respectively) (Fig. 31). Variability is illustrated through the application of a survivor function (i.e., reliability function) which describes the probability that clast size takes on a value greater than a certain value x (Evans et al. 2000). As a result, both section length and collection time seem to have a strong influence on the evaluation of the largest clasts.

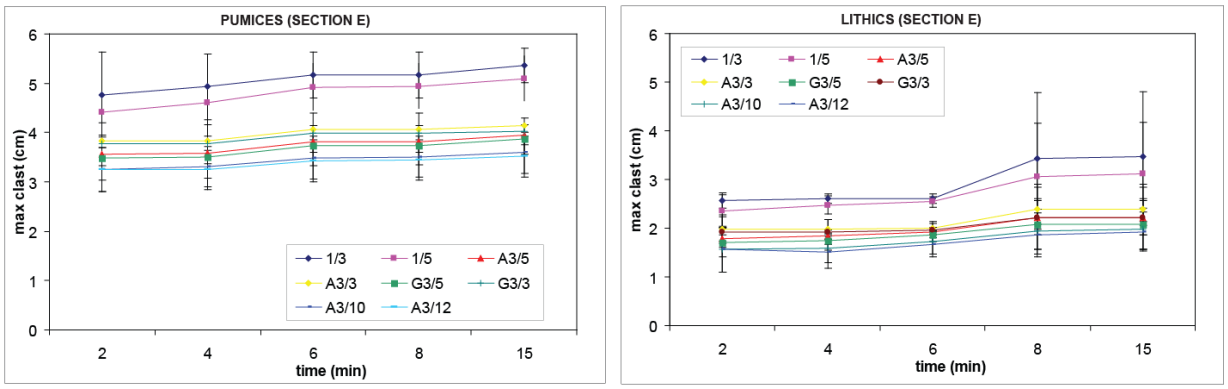

Fig. 30. Example of variation of large-clast values for pumices and lithics collected over an unspecified area section of 4-m length at increasing times from 2 to 15 minutes (section length= 4m; E).

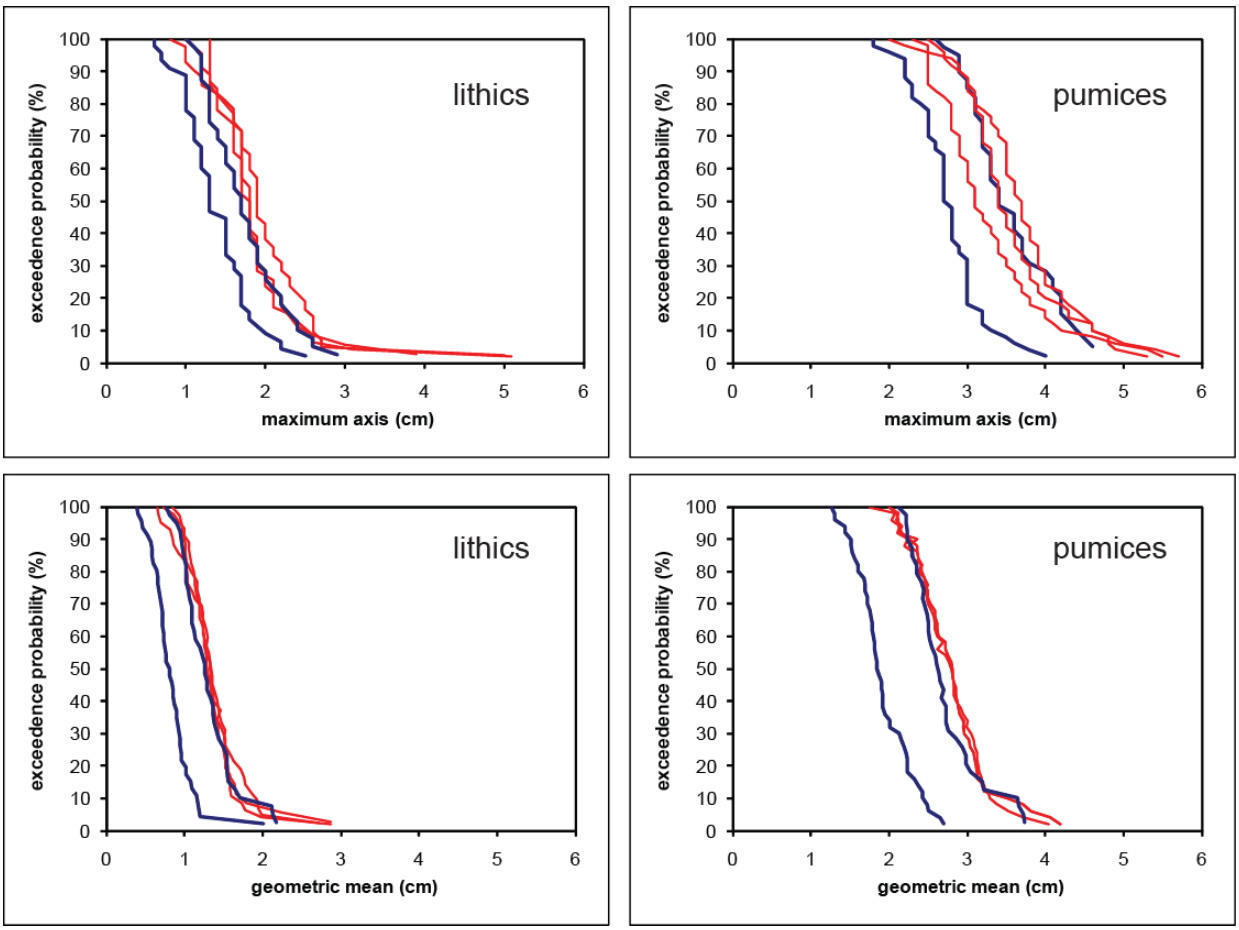

Fig. 31 Survivor functions showing the variability of values associated to the sampling of clasts over 15 minutes at the unspecified-area sections A to E (averaging technique: 1/5 and G3/5; clast number: 35 to 50). Thick blue lines indicate areas A and B (2m sections), whereas red thin lines indicate areas C, D and E (4m sections).

OUTCROP 2

Collection strategy: fixed area (0.1 m^2)

As described in section 3.1, 20 pumices and 20 lithics were collected at outcrop 2 in ten areas of 0.1 m^2 each (A to J). The effect of the size of sampling area was investigated by coupling the results of sequential areas of 0.1 m^2 to obtain nine areas of 0.2 m^2 each (Table 8). For outcrop 2, which is characterized by a lower grainsize than outcrop 1 (Fig. 21), values collected over an area of 0.2 m^2 seem to be more stable than values resulting from the collection over 0.1-m^2 areas (Fig. 32). However, an accurate analysis of all possible combinations of the 0.1 m^2 areas show a significant fluctuation of values (Appendix F).

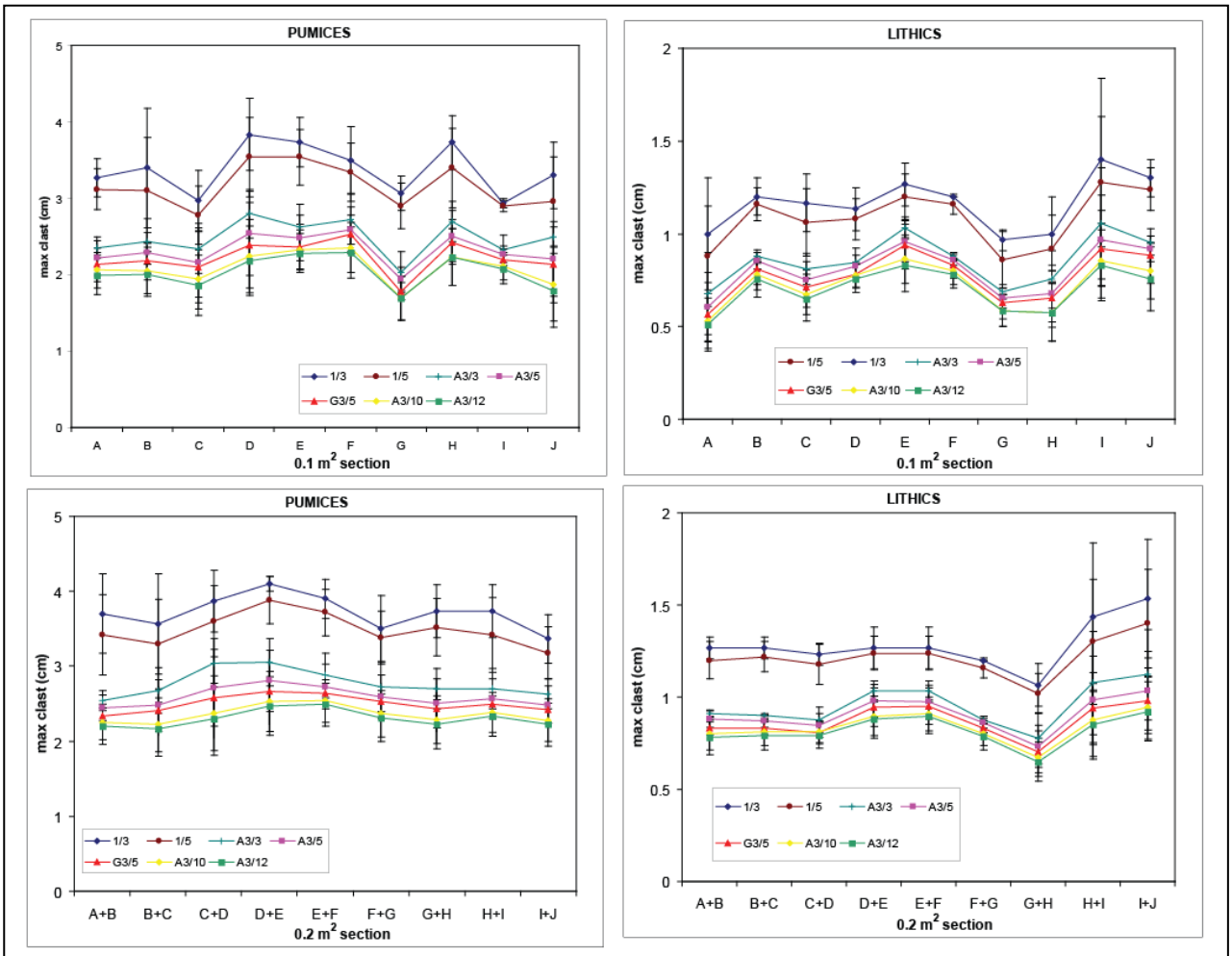

Fig. 32. Variation of the values of the largest pumices and the largest lithics determined using different averaging techniques and different sampling areas (0.1 and 0.2 m^2 respectively). Standard deviations for each clast population are also shown.

Collection strategy: unspecified area (section length: 0.5 and 1 m)

Clast collection over an unspecified area of tephra was carried out also at outcrop 2 considering section lengths of 0.5 m (A and B) and 1 m (C, D and E). Fig. 33 shows the large variability of values with unsuccessful lithic collection associated with areas A and B where no lithics were found.

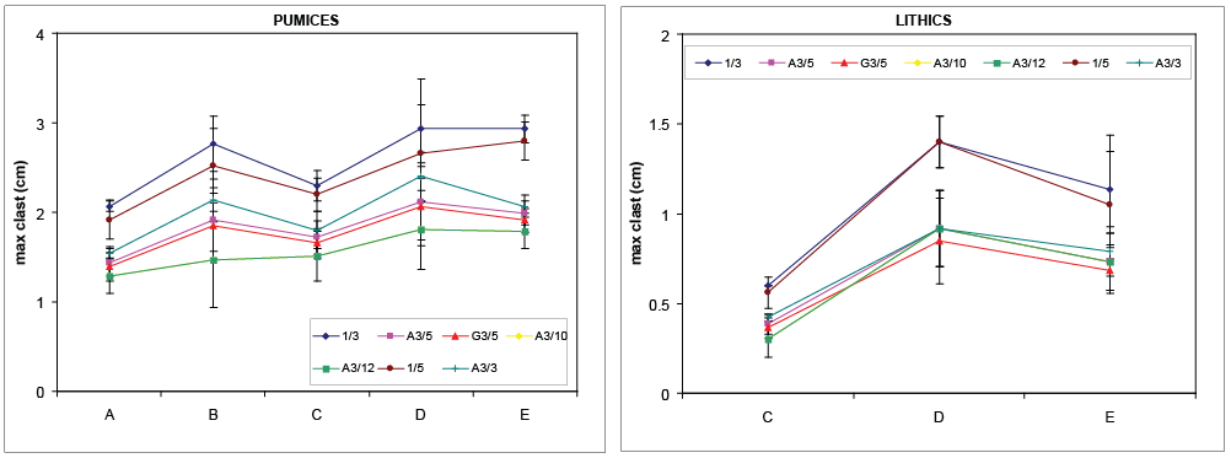

Fig. 33 Variation of the values of the largest pumices and the largest lithics determined using different averaging techniques and different unspecified-area sections of 0.5 m (A and B) and 1 m (C, D and E). Standard deviations for each clast populations are also shown. Lithics for areas A and B are missing from the plot because none was found during the collection.

3.2.6. Variability of measurement within a given outcrop

An important aspect of any data collection is the reproducibility of measurements. As a result, we have investigated the reproducibility of the evaluation of the largest clast within a same outcrop for: (i) outcrop 1 and 2; (ii) pumices and lithics; (iii) different averaging techniques (Fig. 34 and Appendix G). The large variability of the values of the largest clasts is obvious in most plots, and in particular for the pumice plots. Lithic measurements are affected by smaller variations than pumices, and variability seems to increase below the 50th percentile (Fig. 34, Table 15 and Appendix G). Percentage differences with respect to the 5th percentile vary between 27 and 41% for the maximum axis technique and 29 and 37% for the geometric mean technique for both outcrops.

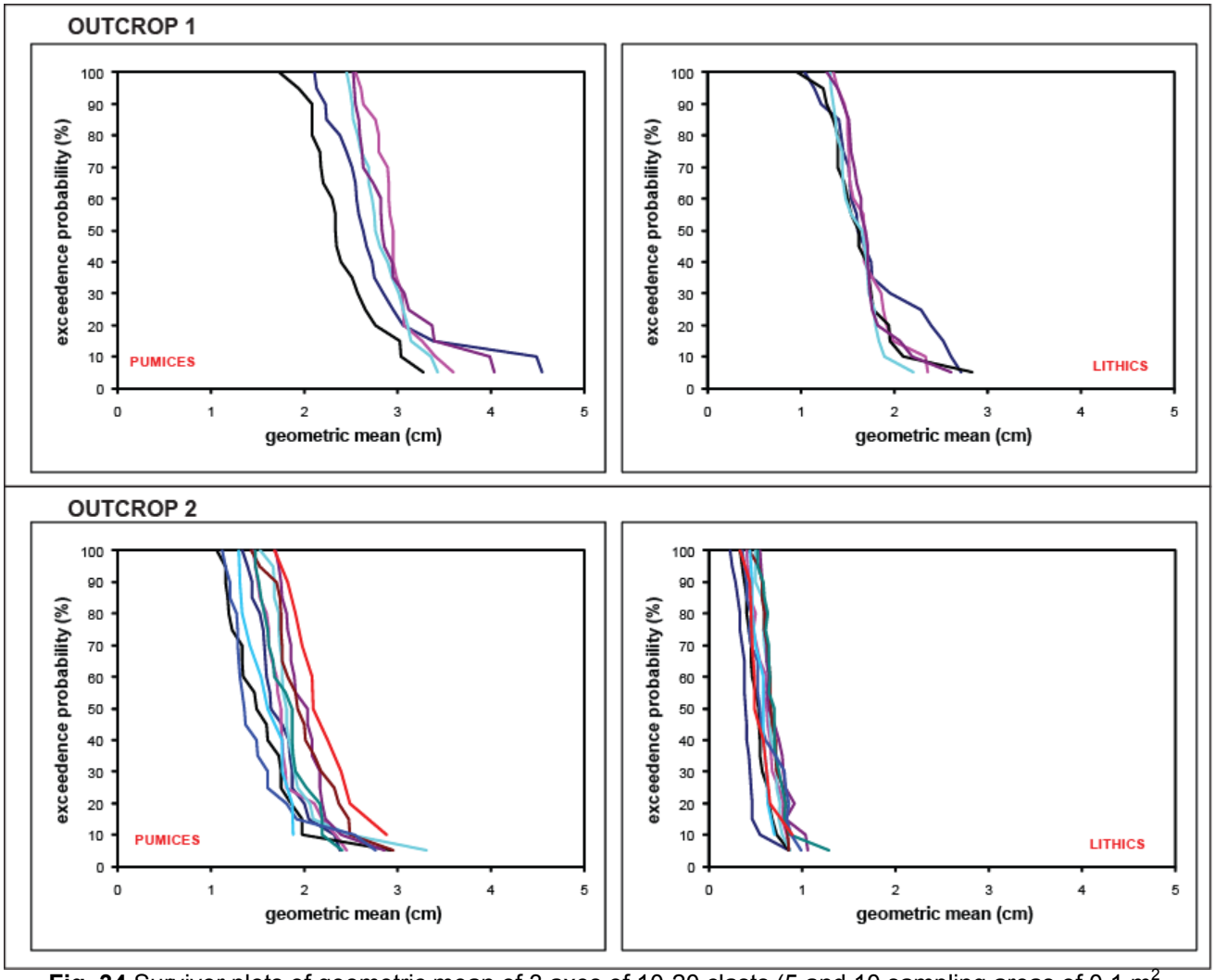

Fig. 34 Survivor plots of geometric mean of 3 axes of 10-20 clasts (5 and 10 sampling areas of 0.1 m^2 at outcrop 1 and 2 respectively)

		OUT 1		OUT 2	
		pumices	***lithics***	***pumices***	***lithics***
Max axis	***50th perc.***	3.7± 0.3	2.3± 0.2	2.4± 0.4	0.8± 0.2
	5th perc.	5.1± 0.8	3.9± 0.9	3.7± 0.5	1.3± 0.2
Geom. mean	***50th perc.***	2.7± 0.2	1.7± 0.0	1.7± 0.2	0.6± 0.1
	5th perc.	3.8± 0.5	2.6± 0.3	2.7± 0.4	0.9± 0.2

Table 15. Comparison of values of the largest clast for the 50% and 5% for both outcrops. Values are indicated as arithmetic mean ± standard deviation (all data are in Appendix G).

3.2.7. Comparison of different strategies of clast collection

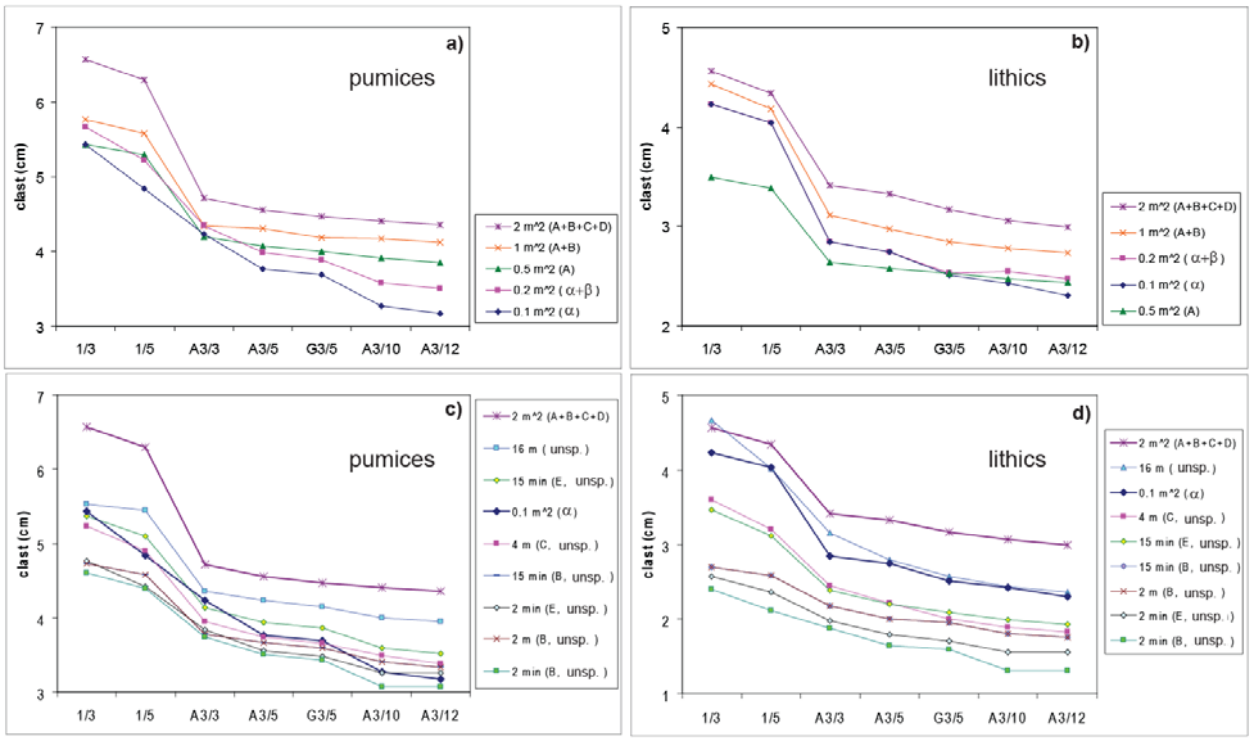

Fig. 35 Comparison amongst different collection techniques at outcrop 1: **a)** and **b)** show the pumice and lithic comparison amongst areas α (0.1 m^2), α+β (0.2 m^2), A (0.5 m^2), A+B (1 m^2), A+B+C+D (2 m^2). **c)** and **d)** show the pumice and lithic comparison amongst unspecified-area sections B (2 m) and C (4 m) and unspecified-area sections sampled for 2 and 15 minutes (B: 2m; E: 4 m). Specified-area sections values for A+B+C+D (2 m^2) and α (0.1 m^2) area also shown for reference (as max and min values of specified areas; thick lines).

The increase of "maximum-clast" value with the volume of sampled material in the specified-area collections is evident for both outcrops (Figs 35a,b and 36). In particular, the largest areas resulted from the combination of 0.1 and 0.5 m^2 sections show the highest values (i.e. 2 and 1 m^2 for outcrop 1 and 2 respectively). In contrast, unspecified-area collections display a larger variability, with values always below the results from the specified-area collections, with the exception of the 15-minute sampling of section E in outcrop 1 and the 16-m and 4-m sections of outcrop 1 and 2 respectively (Figs. 35c,d and 36). In particular, data show how the collection time has a stronger

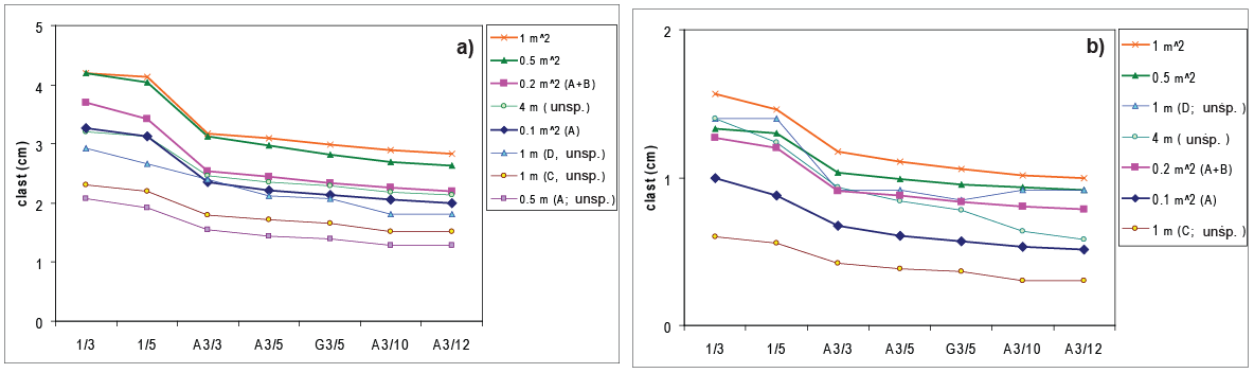

Fig. 36 Comparison amongst different collection techniques at outcrop 2: **a)** and **b)** show the pumice and lithic comparison amongst areas A (0.1 m^2), A+B (0.2 m^2), A+B+C+D+E (0.5 m^2), A+B+C+D+E+F+G+H+I+J (1 m^2), unspecified-area sections A (0.5 m) and C and D (1 m). Specified-area trends are indicated with thick lines.

influence than the section length on the unspecified-area collection, with the lowest values always resulting from the 2-minute collections regardless the section length (2 or 4 m). Values from the 1-m and 4-m unspecified-area collections of outcrop 2 are close to the values resulting from the specified-area collection (Fig. 36). However, it is important to bear on mind that no lithics were found in the 0.5-m unspecified-area collection of outcrop 2 and that the variability of the 1-m collection is also large. In fact, values from the C and D sections (both 1 m) show very different results (Fig. 36).

3.2.8. Effects of the size of sampling areas

The effect of sampling area and volume on the evaluation of the maximum clast was tested by investigating the stabilization of data for the two outcrops for different collection strategies.

Collection strategy: specified-area sections

Values for the largest lithics of outcrop 1 seem to stabilize around the 2-m^2 section, whereas values for pumices of the same outcrop do not show a clear plateau (Fig. 37). This is confirmed by Fig. 38 where the percentage differences of values for pumices at the 2 and 4 m^2 sections are between 5 and 15%, whereas values for lithics are below 5%. However, values for both largest pumices and largest lithics of outcrop 2 stabilize around the 0.5 m^2 section (percentage differences < 10%), even though lithic values of the 0.9 and 1m^2 section are affected by an abrupt increase (Figs 39 and 40).

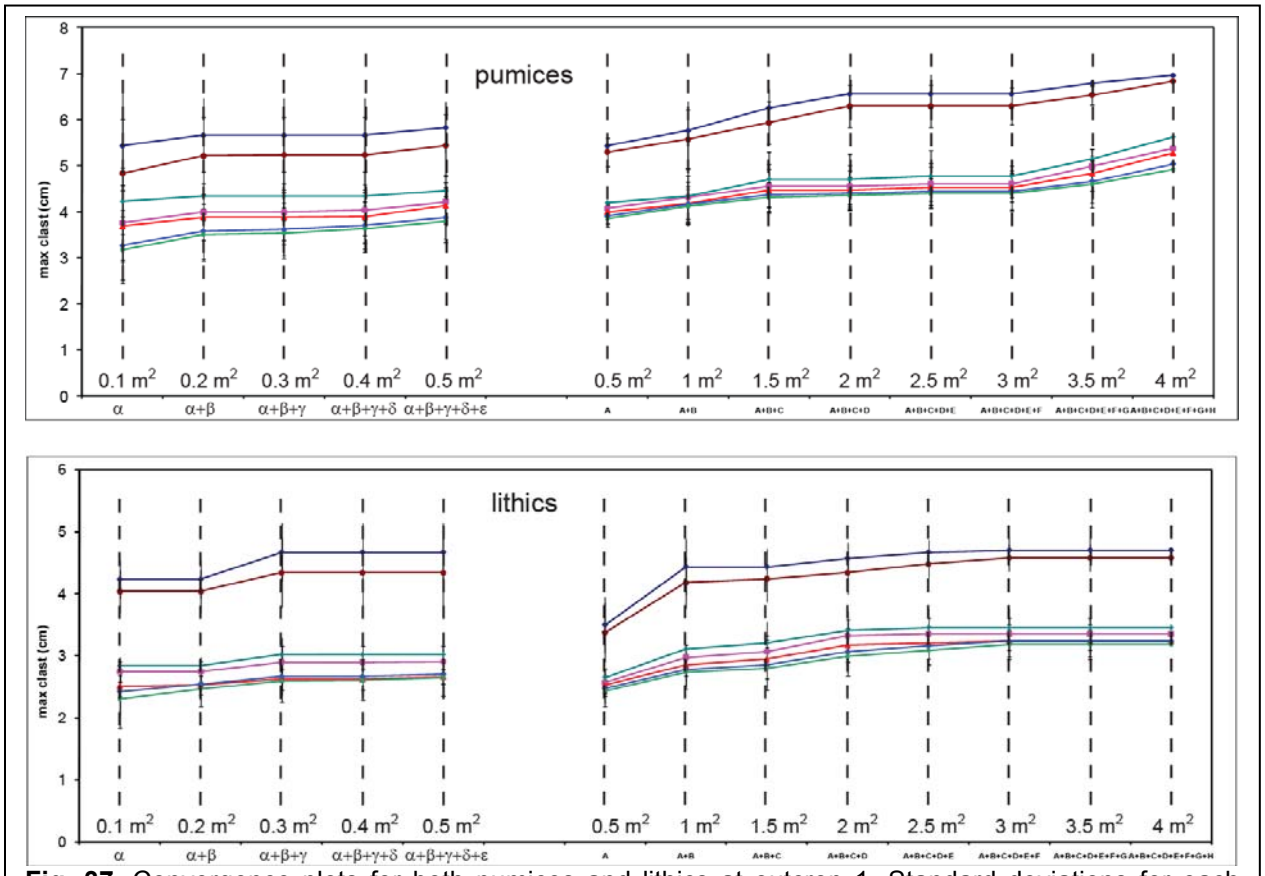

Fig. 37. Convergence plots for both pumices and lithics at outcrop 1. Standard deviations for each technique are also shown. Areas α to ε are of 0.1 m^2, whereas areas A to H are areas of 0.5 m^2 each. As a result, both α+β+γ+δ+ε and A are areas of 0.5 m^2. A+B+C+D+E+F+G+H represents a continuous area of 4 m^2.

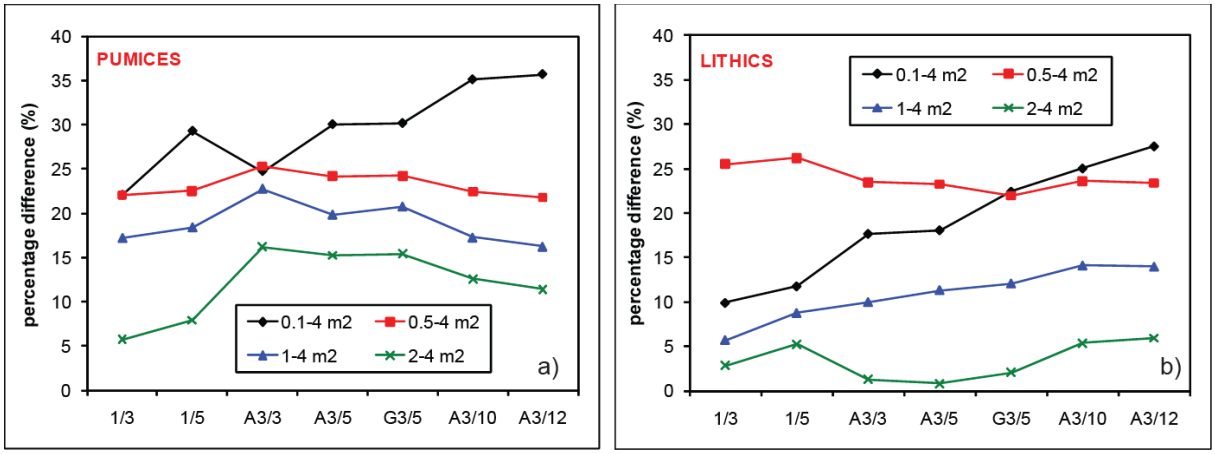

Fig. 38. a) Percentage difference between values of the largest pumices and **b)** largest lithics calculated over different areas (α: 0.1 m^2; A: 0.5 m^2; A+B: 1 m^2; A+B+C+D+E+F+H+G: 4 m^2) for different averaging techniques. (outcrop 1)

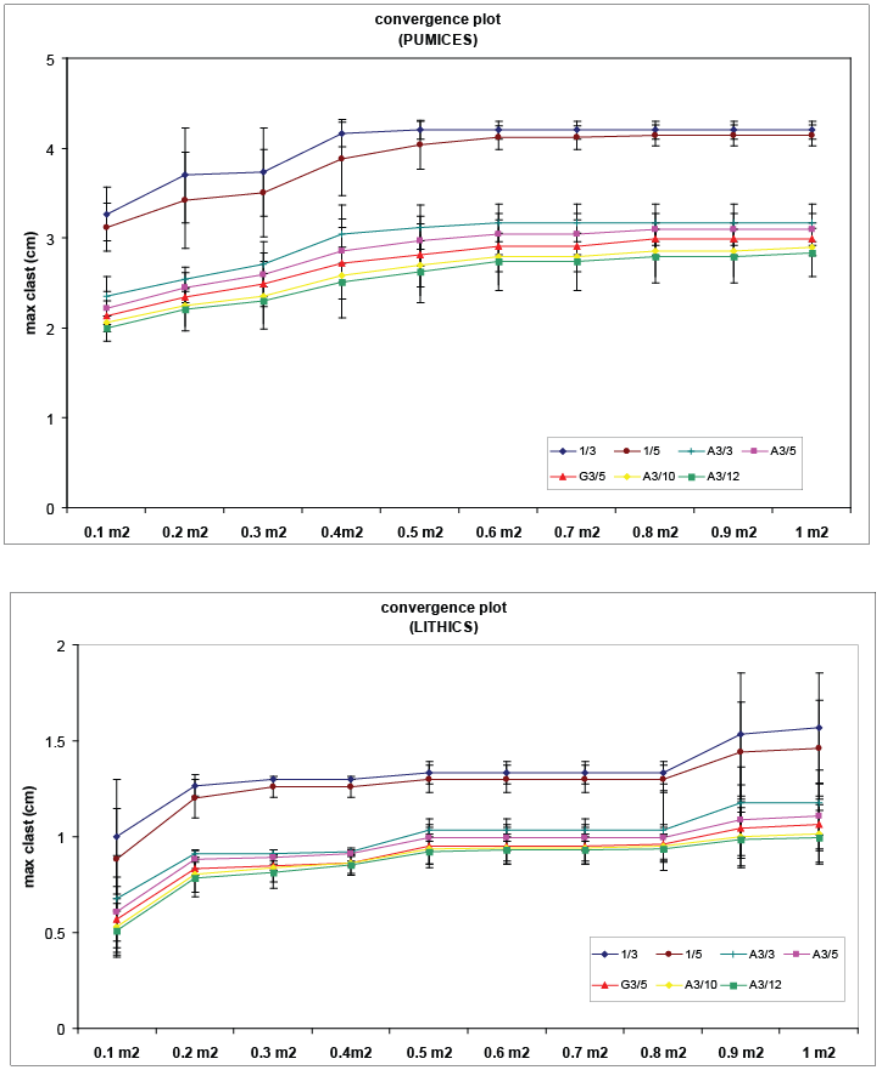

Fig. 39 Convergence plot for sampling areas of 0.1 m^2 (A to J) (outcrop 2).

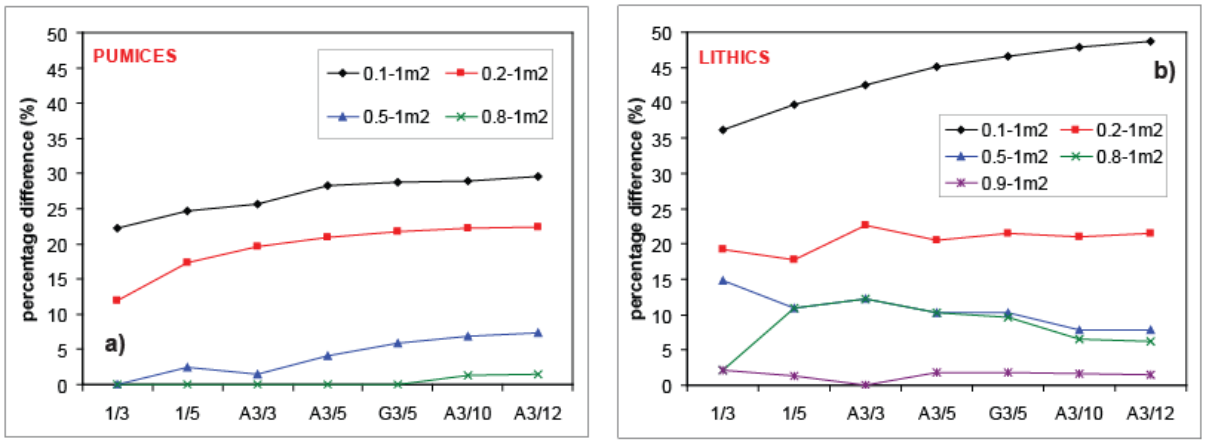

Fig. 40. Percentage differences between values of the **a)** largest pumices and **b)** largest lithics calculated over different areas (0.1 vs 1 m^2; 0.2 vs 1 m^2; 0.5 vs 1 m^2; 0.8 vs 4 m^2) for different averaging techniques. The percentage difference "0.9 vs 4 m^{2}" for is also shown for the lithics given the large values shown by the "0.8 vs 4 m^{2}" comparison.

Collection strategy: unspecified-area sections

Values of largest clasts collected over an unspecified area of fixed section length seem to stabilize only for pumices of the first outcrop (Figs 41 and 42). In fact, values of the largest pumices reach a plateau around the 8-m section, with percentage differences with clasts collected at the largest section (16-m) below 10%. However, percentage differences for both pumices and lithics of outcrop 2 are all mostly above 10%, with lithics showing the largest discrepancies. This could be due to the size of clasts. In fact, clast collection carried out over a unspecified area at outcrop 2 was sometimes unsuccessful because of the small number of lithic clasts found.

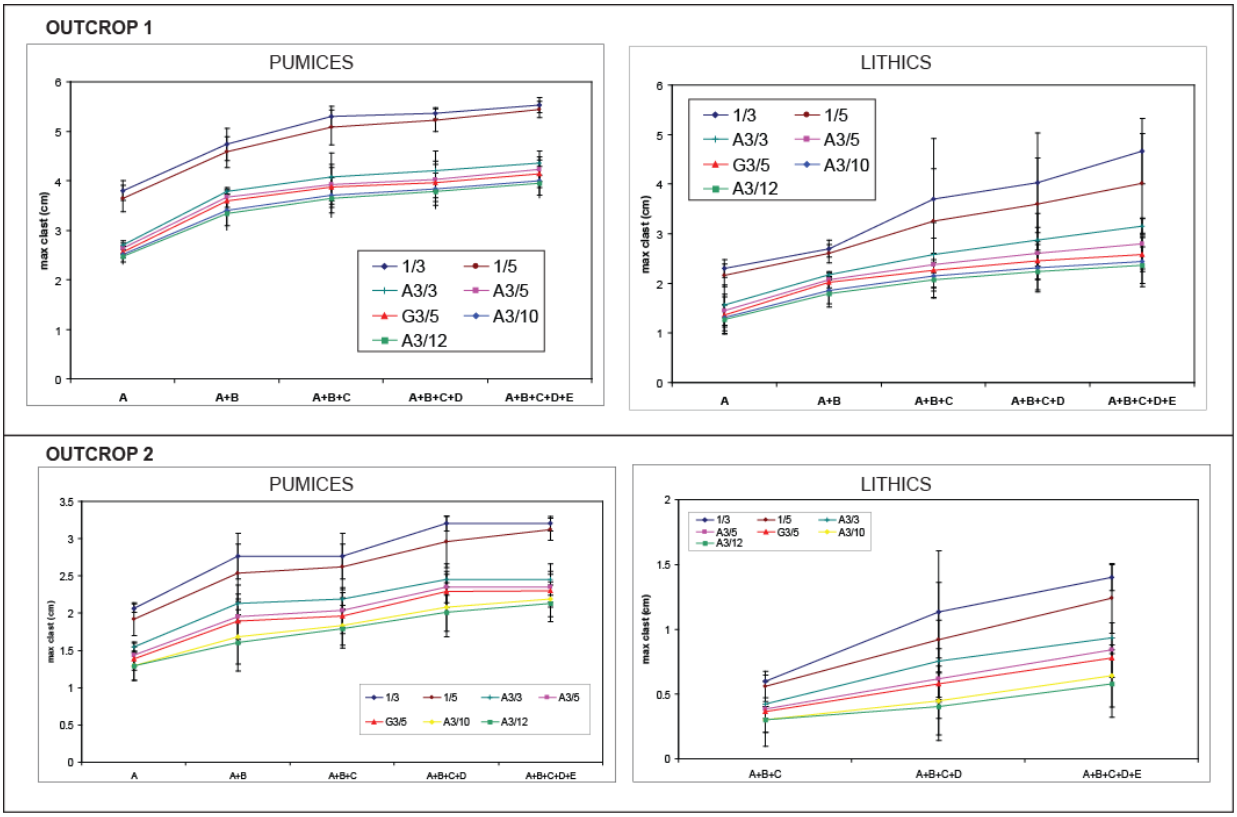

Fig. 41. Convergence plot for unspecified-area sections at both outcrop 1 and 2.

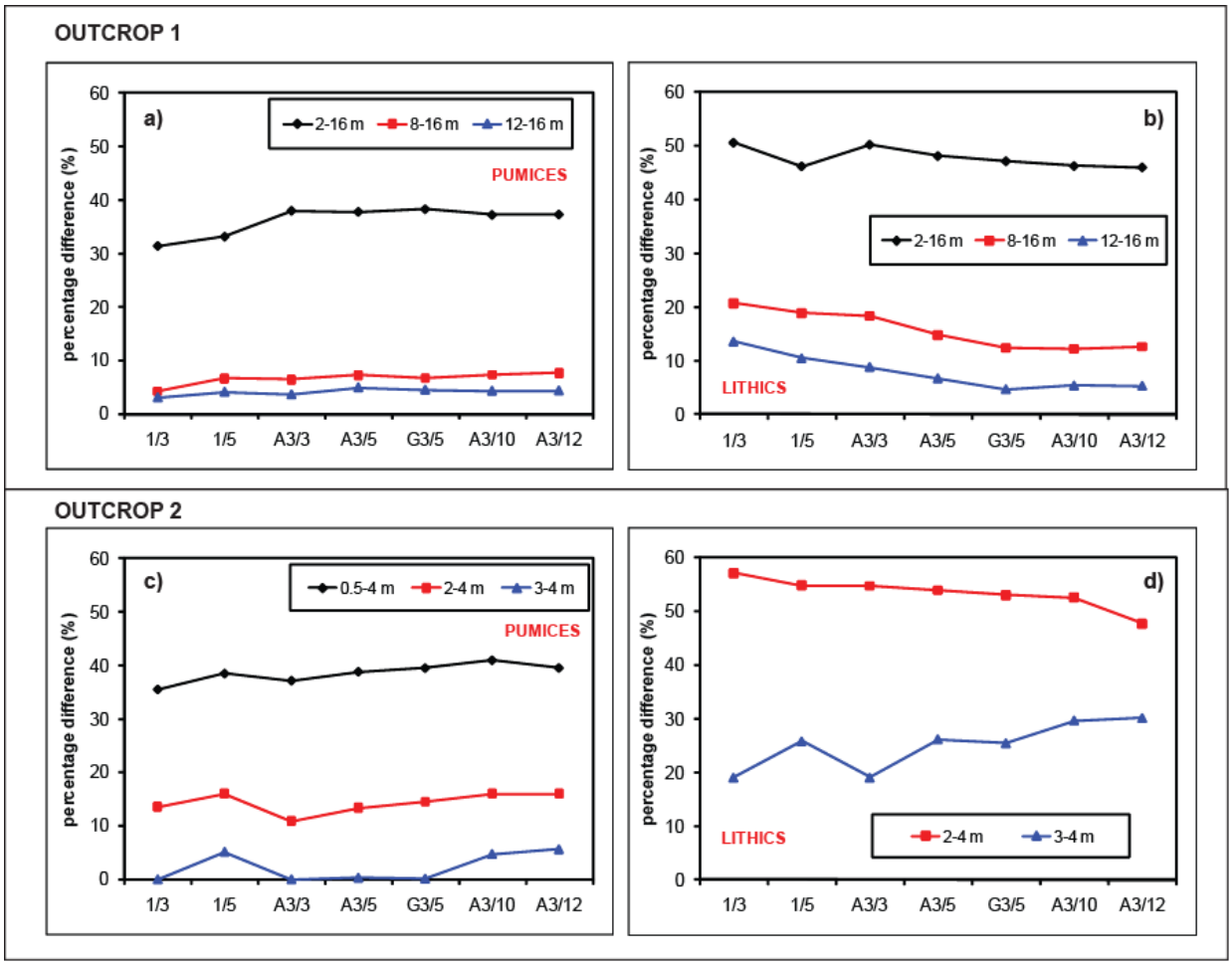

Fig. 42 Percentage differences for both pumices **(a)** and lithics **(b)** determined for unspecified-area sections of different length (A: 2 m; A+B+C: 8 m; A+B+C+D: 12 m; A+B+C+D+E: 16m) for different averaging techniques (from Fig. 41 a and b; Outcrop 1); and both pumices **(c)** and lithics **(c)** determined for unspecified-area sections of different length (A: 0.5 m; A+B+C: 2 m; A+B+C+D: 3 m; A+B+C+D+E: 4 m) for different averaging techniques (from Fig. 41c and d; Outcrop 2). Comparison 0.5-4m is missing for the lithic calculation because no lithics were found at area A and B.

3.2.9. Effects of the size of sampling areas with respect to different averaging techniques

The difference between different averaging techniques is mostly unaffected by the sampling area (Fig. 43). Nonetheless, results from different averaging techniques show large discrepancies when the number of clasts considered is not statistically representative of the outcrop (e.g., lithics of outcrop 2), with the technique 1/3 showing the largest discrepancies (Fig. 43d). In addition, the 1/3 technique gives values around 40% higher than the G3/5 technique for both pumices and lithics at both outcrops. Data and remaining plots comparing different averaging technique and different sampling areas for both outcrops are summarized in Appendices H and I.

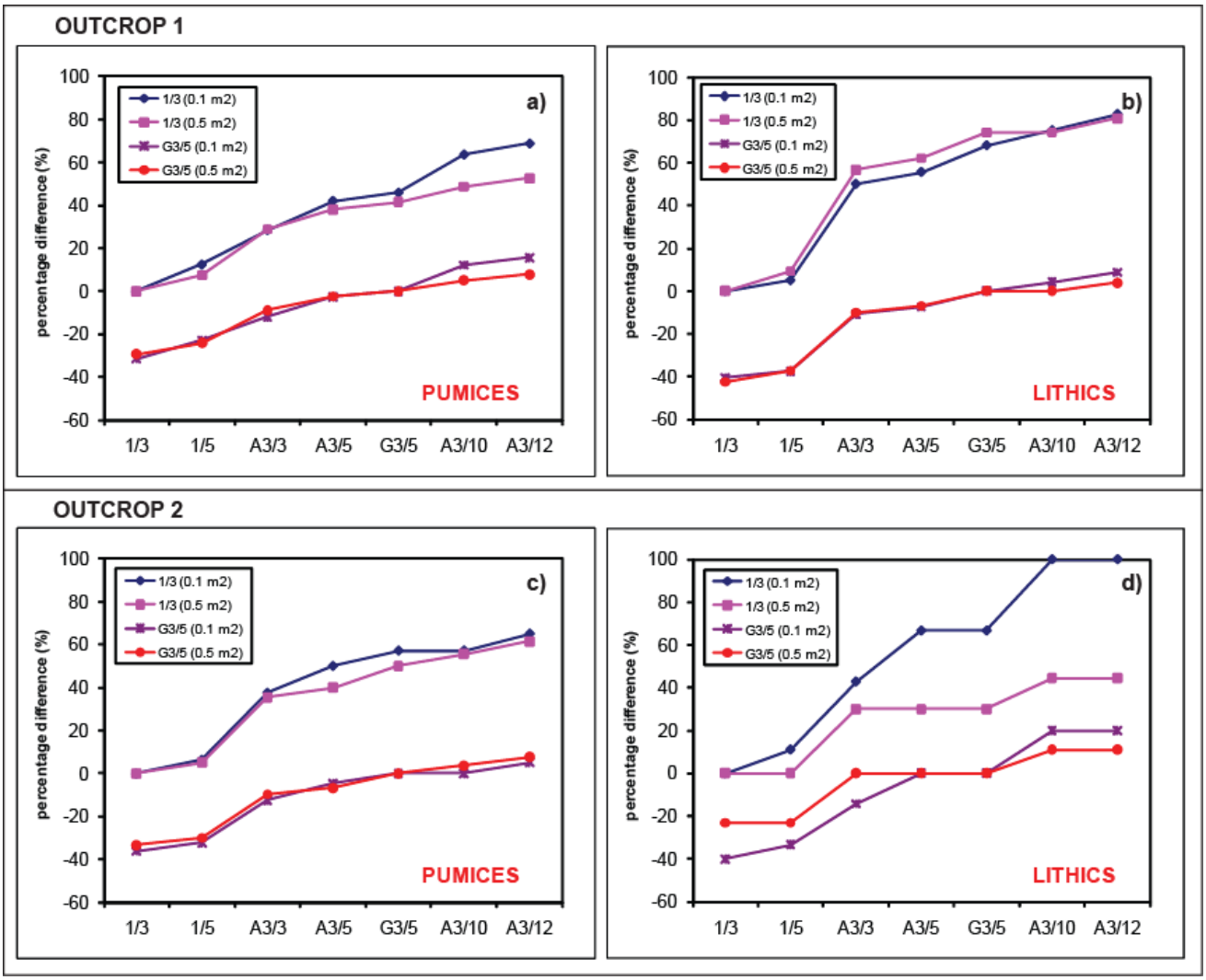

Fig. 43 Percentage difference amongst different averaging techniques (1/3 and G3/5) for both outcrop 1 and 2 and for two different sampling areas: A=0.1 m^2 and AE= 0.5 m^2 for both outcrops.

3.2.10. Combined effects of the size of sampling area and collection strategy

Figure 44 shows how the assessment of the maximum clast never stabilizes for both outcrops, in particular for pumices, and how the values resulting from the unspecified-area technique are typically lower than the values derived from the fixed-area collection. Only unspecified-area collections carried out on long sections for a long time result in measurements similar to fixed-area measurement (i.e. 15 minute collection of section E for outcrop 1 and 4 m sections for outcrop 2).

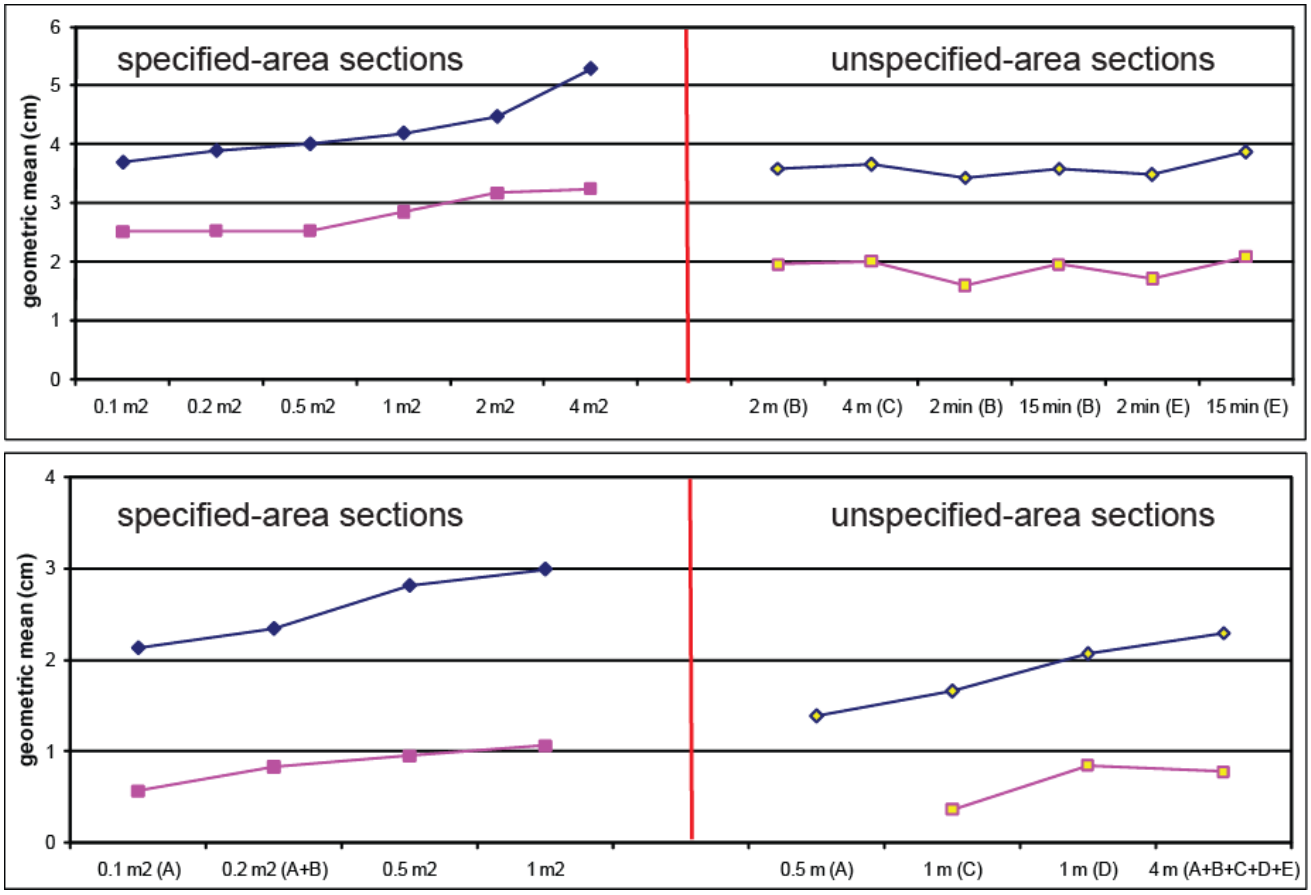

Fig. 44 Assessment of the maximum pumice and lithic for sampling areas of different size and different collection strategies (specified- and unspecified-area sections) for **a)** outcrop 1 and **b)** outcrop 2.

4.0 DISCUSSION

Grainsize measurements

Results have shown that sieving techniques are stable for the range of particle size analyzed (i.e. outcrop 1: Md$\phi \approx -3$), and also that different samples of different volumes collected at the same outcrop gave very similar results (Figs 17 to 20). In addition, analyses of different samples from the same outcrop obtained from different labs and using different techniques are in good agreement both in terms of Mdϕ and sorting (Table 8). This result strongly accounts for representativeness of samples and reproducibility of measurements done with classical techniques used for grainsize analyses.

Axes measurement

Investigations on the characterization of clasts size, have shown that the best agreement with an idealized ellipsoid are given by approximating each clast to the minimum ellipsoid (e.g. Fig. 22). In fact, investigators using this technique obtained the best agreement with the diameter of the equivalent sphere (Fig. 21), which is what most empirical models for the characterization of tephra deposits are based on (e.g. Carey and Sparks 1986).

Shape factor

Clasts collected at both outcrops display shape factor F between 0.3 and 0.95, with most values strongly diverging from the assumption of sphericity (F=1) (Fig. 23). Such a result arise questions on the applicability of empirical methods based on the assumption of spherical particles, such as the method of Carey and Sparks (1986). Even though F does not discriminate for shape, we consider F=0.3 a plausible threshold for the application of the method of Carey and Sparks (1986) because clasts with F<0.3 show discrepancies in terminal velocity with respect to spheres <20% (Fig. 24). In addition, the analysis of shape factor is also important for the choice of averaging technique. In fact, if F<<1, the discrepancy between values obtained using the 1-axis techniques (i.e. 1/3 and 1/5) and the 3-axes techniques (e.g. 3/5, 3/10, 3/12) are much larger.

Outliers

Results have shown that useful information is only given by size outliers. In fact, density outliers are impossible to measure in the field because of the different weight between wet and dry clasts, and shape outliers do not give information on the actual divergence from the assumption of sphere. In order to overcome density and shape anomalies, analyses should only be carried out on lithics of same nature (which are typically characterized by a narrower spread of densities with respect to

pumices) and on clasts with F>0.3 (Fig. 24). However, the issue of size outliers remains. Traditionally volcanologists have dealt with outliers by rejecting them on the basis of subjective criteria. As a result, if subjective deletion is typically chosen as the best strategy to deal with outliers, a standard technique should be proposed. However, our exercise has shown that both the boxplot method and the Dixon's test are not well suited for the evaluation of the largest clast, the former being not appropriate for small-size population and the second being too subjective on the choice of the population considered (Table 11 and Appendix D).

An alternative to outlier rejection is the strategy of outlier accommodation (e.g. Barnett and Lewis 1998). Such an alternative is even more valuable if we exclude the cause of outliers being due to measurement error (given that the identification of outliers is mostly done in the field). The only other reason to exclude outliers could be due to the possibility of execution errors, related, for example, to the presence in the outcrop of clasts that are not in place. Such a possibility needs to be analyzed in detail also based on the outcrop characteristics (e.g. sloping, possible slumping and reworking). Finally, if outliers are due to inherent variability, accommodation techniques should be preferred.

As an example of accommodation strategy, we have tested the use of the median of a population as supposed to the arithmetic mean (commonly used), because the median is typically less affected by extreme values. However, results show that (for the populations analyzed) median and mean have similar trends. Another possible accommodation strategy is related to data transformation (e.g. logarithmic scale, square-root values). In the case of the evaluation of the largest clast, plotting the data as survivor functions could represent an alternative strategies because it does not require outlier identification (e.g., Figs 31 and 34).

Choice of section size

Collection strategy: specified-area sections

Appendix F show that depositional areas up to 1 m^2 for outcrop 1 ($Md_\phi \approx -3$) and up to 0.2 m^2 for outcrop 2 ($Md_\phi = -1.5$) are not sufficient to stabilize the data. However, Appendix J and Figs 35 to 40 show good agreement between lithic values of the 1 m^2 and 4 m^2 sections of outcrop 1 and both lithic and pumice values of the 0.5 m^2 and 1 m^2 of outcrop 2. Pumices of outcrop 1 never reach a plateau (Figs 37a and 38a). As a result, the effect sampling-area size on the evaluation of the largest clasts depends on the total grainsize distribution of the outcrop investigated.

A 0.5 m^2 section for outcrop 2 is a good compromise between data quality and sampling time, and it gives discrepancies of about 21% and 19% for pumices and lithics of outcrop 1 (with respect to the largest area sampled at outcrop 1, i.e. 4 m^2). Percentage differences between values from the smallest and largest areas vary between 10 and 35% for pumice of outcrop 2 and both pumices and lithics of outcrop 1 and between 35 and 50% for lithics of outcrop 2 (Figs. 38 and 40).

Calibration with grainsize

The minimum volume (V_M) of material to be sampled in order to assure the representativeness of the largest-clast assessment for a given outcrop can be determined considering that:

$$V_M = \frac{N_T}{N_R} V_S \quad (1)$$

where N_T is the number of particles we want to sample for our assessment and N_R is the number of the largest particles collected in a sampled volume V_S. In addition, the resulting minimum area to be sampled is:

$$A_M = \frac{V_M}{T} \quad (2)$$

where T is the thickness of the outcrop. As an example, if we want to collect the 20 largest pumices from sample 1 in Table 6 (i.e. N_T = 20), the resulting minimum volume (V_M) and minimum area (A_M) to be sampled are 0.13 m^3 and 1.4 m^2 respectively (given that N_R = 2, V_S = 0.013 m^3 and T = 0.09 m; Table 6). If we want to collect the 20 largest lithics from the same sample, the resulting minimum volume (V_M) and minimum area (A_M) to be sampled are 0.26 m^3 and 2.9 m^2 respectively (given that N_R = 2, V_S = 0.013 m^3 and T = 0.09 m; Table 6).

On the other hand, if we want to collect only the 5 largest pumices and lithics (i.e. N_T = 5) the corresponding minimum volume (V_M) is 0.03 and 0.06 m^3 respectively and the minimum area (A_M) is 0.4 and 0.7 m^2 respectively. This is in good agreement with our results shown in Appendix J and Figs 35 to 40.

Collection strategy: unspecified area

Investigations carried out using the unspecified-area technique both in space and time show that both section length and collection time have a strong influence on the assessment of the largest clasts. In fact, small sections sampled over a long time (e.g. 2-m section sampled for 15 minutes) give a comparable result to a long section sampled for a short time (e.g. 4m section sampled for 2 minutes) (Fig. 35c and d). In addition, small sections (regardless collection time) and long sections sampled for short time resulted in the lowest values. Only values from the longest sections (i.e. 16 m at outcrop 1 and 4 m at outcrop 2) give similar results to the specified-area collection (with the exception of one of the 1-m sections of outcrop 2). In addition, long sections sampled for a long time gave, sometimes, comparable results to clast collections carried out over a 0.5-m^2 section (Fig. 35). However, values resulting from unspecified-area sections ranging between 2 and 16 m for outcrop 1 and between 0.5 and 4 m for outcrop 2 never stabilize (percentage difference between the

last two section mostly above 5%; Figs 41 and 42). In addition, Fig. 30 show the large discrepancy between clasts collected over 2 minutes and clasts collected over 15 minutes, with the 15-minute values being also more stable.

Choice of averaging technique

First of all, it is important to notice that the averaging technique is not strongly affected by the collection strategy (Fig. 43). Second, data on the largest clasts carried out at both outcrops show two clear populations of data: 1-axis techniques (1/3 and 1/5) and 3-axes techniques (A3/5, G3/5, A3/3, A3/10 and A3/12) (Appendix E). The percentage difference between the average values of each population (over all averaging techniques considered) varies between 27 and 34% for both pumices and lithics and both outcrops (with an average standard deviation within each population between 0.1 and 0.3cm). This implies that the choice of number of axes is more important than the choice of number of clast considered. This is even more true in situations where most clasts are characterized by $F<0.7$ (like lithics in our case). Third, in order to provide an objective reason for the choice between the 1-axis and 3-axes techniques we need to consider the use of the resulting values. These data are mostly used for the application of the model of Carey and Sparks (1986) for the determination of column height and wind speed at the time of the eruption, and given that such a method is based on the assumption of spherical particles, the 3-axis techniques are more appropriate. In addition, because of the assumption of spherical particles, the choice of the geometric mean of the three axes, as compared with the arithmetic mean, is more rigorous, as also suggested by Sparks et al. (1981). In fact, the geometric mean represents the diameter of a sphere with the same volume of an ellipsoid having the same axis of the measured clast.

Choice of collection strategy

As explained above, clast collection over a 0.5-m^2 depositional area represents a good compromise between data quality and sampling time for both outcrops, and resulting values are typically larger than the values obtained from the unspecified-area sampling on small sections (regardless time collection), whereas long sections sampled for a short time are the lowest (Figs 35 and 36). The unspecified-area collection strategy gave similar results to the specified-area collection only for the 16-m and 4-m sections for outcrop 1 and 2 respectively and for the 15-minute collections of 4-m sections at outcrop 1.

As a result, in situations where it is impossible to excavate a 0.5 m^2 section (e.g., poorly exposed deposits, archeological sites, densely populated areas), the unspecified-area collection strategy carried out for at least 15 minutes and over a long section can also provide good results. More attention should be given in case only short sections available, as shown by results in Fig. 35

(maybe sampling time should be increased?). In any case, when a 0.5 m^2 section cannot be excavated the resulting assessment of the largest clasts need to be considered as a minimum value.

Characterization of the largest clasts of a given outcrop

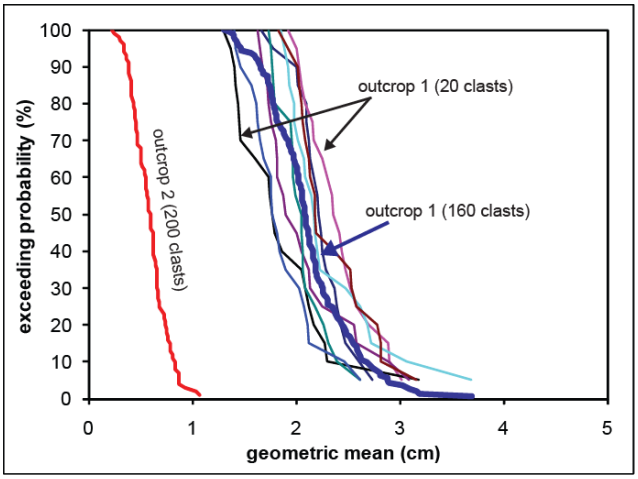

Fig. 45. Survivor functions for the lithic clasts collected at the eight 0.5 m^2 areas of outcrop 1 (A to H) and for the cumulative 0.5 m^2 area of outcrop 2 (A+B+C+D+E).

Based on the considerations above, our best large-clast characterization of outcrop 1 and 2 is given by the geometric mean of the 50th percentile of a 20-lithic-clast population collected over a 0.5 m^2 section (Fig. 45). This results in values of 2.1 ± 0.2 cm for outcrop 1 and 0.6 cm for outcrop 2. Standard deviation could not be determined at outcrop 2 because the 0.5 m^2 section results from the combination of 5 adjacent areas of 0.1 m^2. These values of 50th percentile are both 30% lower than the 5th percentile, which is the same discrepancy observed between the 50th and 5th percentile of the 0.1 m^2 sections (Appendix J). Same discrepancy is observed with respect to the G3/5 for same sampled area for both outcrops (0.5 m^2). In fact, the G3/5 technique for lithics of the 0.5 m^2 areas of outcrop 1 gave a value of 2.6 ± 0.3 cm and a value of 3.2 cm for the largest area investigated (4 m^2) (Appendix J). The G3/5 technique for lithics of the 0.5 m^2 area (A+B+C+D+E) of outcrop 2 gave a value of 1.0 cm and a value of 1.1 cm for the largest area investigated (1 m^2) (Appendix J).

The largest clasts of outcrop 1 calculated based on the G3/5 technique (2.6 cm) and the 50th percentile of the largest 20 clasts (2.1 cm) correspond to about the 5th and 10th percentile of the grainsize distribution of outcrop 1 (Appendix B). The largest clast of outcrop 2 calculated based on the G3/5 technique (1.0 cm) and the 50th percentile of the largest 20 clasts (0.6 cm) correspond to about the 10th and 25th percentile of the grainsize distribution of outcrop 2 (Appendix B). As a result, the G3/5 largest clast is 0.8 and 0.4 times the coarsest 1% for outcrop 1 and 2 respectively as supposed to 1.5 times as found by Sparks et al. (1981) for the Askja D deposit. Based on this large variability, we can conclude that the largest clast cannot be easily related to the grainsize distribution, which is expressed in weight percent and not in number of clasts.

5.0 FINAL REMARKS AND RECOMMENDATIONS

5.1 Relevance of the measure

Before deeply analyzing different options for the evaluation of the largest clasts of tephra deposits, it is important to understand and appreciate why this field methodology is important. In fact, defining the largest clasts is necessary for the compilation of isopleths maps, which are important for two main reasons: i) determination of column height when no direct observations are available (e.g. Carey and Sparks 1986 and Pyle 1989) and ii) definition of eruptive style (e.g. Pyle 1989). In particular, the determination of the column height is extremely valuable because it represents a critical input of tephra models and because it is used to derive information on the mass discharge rate and the duration of eruptions (i.e., ratio between erupted mass and mass eruption rate). In addition, recent advances in tephra modeling have shown that the column height cannot be uniquely constrained by inversion techniques (Connor and Connor 2006; Scollo et al. 2008). As a result, the application of the methods of Carey and Sparks (1986) and Pyle (1989) are often necessary to characterize volcanic eruptions. Nonetheless, our field exercise has shown the dependence of the results on different averaging and sampling techniques used confirming the need of a standardized strategy.

5.2 Can we estimate the maximum clast of a given outcrop?

An important philosophical, but fundamental, concept that needs to be clarified is the idea of the "maximum clast" of an outcrop. In fact, this value does not correspond, by definition, to the size of a single clast, but to a representative size obtained by averaging a certain number of the largest clasts collected in a given deposit. In addition, the large variation of the population of the largest clasts collected at any given outcrop show how it would be impossible to define the absolute maximum clast at any location (e.g. Fig. 34 and Appendix G).

Recommendation

The characterization of the population of the largest clasts that fell at a given distance from the vent is more appropriate than the definition of maximum clast.

5.3 Selection of sampling area

Special attention should be given to the choice of sampling area in order to avoid the presence of size outliers that could contaminate the clast population.

Recommendation

Sections on flat paleotopography should be preferred to sections on sloping paleotopography because they are likely to be less affected by reworking, slumping and secondary clast grainflows.

5.4 Collection strategy (specified- vs unspecified-area sections)

The assessment of the largest clasts strongly depend on the volume of material analyses and, therefore, on the sampled outcrop area. Sampling of unspecified-area sections typically results in the collection of the largest clasts only on the outcrop surface.

Recommendation

Specified-area sections should be preferred to unspecified-area sections when possible. In case sections cannot be excavated, unspecified-area sections should be sampled for at least 15 minutes on relatively long sections (e.g. 4 m section for outcrop 1 and 1 m section for outcrop 2). In this case, the resulting assessment of the largest clasts has to be considered as a minimum estimate.

5.5 Sampling area (area size)

The effect of the size of sampled area on the evaluation of the largest clasts depends on the general grainsize distribution of a given outcrop. Our exercise has shown that discrepancies in the assessment of the largest clasts are <20% for a 0.5-m^2 section at outcrop 1 ($Md\phi$ = -2.9 ϕ; σ=1.4) and a 0.2-m^2 section at outcrop 2 ($Md\phi$ = -1.5 ϕ; σ=1.4).

Recommendation

A sampling area of 0.5 m^2 is the best compromise between data quality and sampling time.

5.6 Juvenile or lithic?

As already suggested by Carey and Sparks (1986) and Sparks et al. (1981), lithic clasts should always be preferred to pumice clasts. This is due to several reasons. First, pumice clasts are characterized by a wider range of densities and particle properties (e.g. permeability, porosity). As a result, the aerodynamics characteristics of lithics are easier to constrain. Second, pumice clasts are typically more affected by breakage with impact with the ground, with larger clasts being more likely to break (Sparks et al. 1981).

Recommendation

When a sufficient number of good lithic fragments are present (i.e., lithics that are not altered and therefore are less likely to break), the additional collection of pumice clasts for the application of the method by Carey and Sparks (1986) is not necessary. In case of lithic-poor deposits (e.g., basaltic tephra), only the densest juveniles should be used.

5.7 Clast characterization (axis measurement and averaging technique)

Recommendation

In order to avoid large discrepancies from the assumptions of sphere considered in most empirical models (e.g. Carey and Sparks 1986), a clast should be characterized based on the geometric mean of its three axes taken perpendicularly between each other with the approximation of the minimum ellipsoid (Fig. 22). In addition, the 1-mm precision is not sufficient for clasts <1 cm, in which case we suggest the use of the micron digital caliper.

5.8 Choice of clast population

Dealing with outliers

Important potential outliers that should be considered during the evaluation of the largest clasts refer to density, shape and size. First, we overcome the problem of density outliers by selecting clasts from the same population of lithic clasts (supposedly characterized by a small density variation). Second, in order to avoid large discrepancies from the assumption of spherical particles used in most empirical methods, the definition of a shape threshold is more important than the definition of shape outliers. In particular, clasts with F<0.3 should be discarded. Third, based on our results of the application of two different methods for the identification and rejection of outliers, accommodation strategies are more appropriate in the evaluation of the largest clasts. This is also supported by the assumption that our measurements are not affected by measurement error (given that the outlier identification is firstly done visually in the field) and by execution error (assuming that the sampling section was carefully chosen). Obviously the execution error is affected by a certain level of uncertainty (due to the fact that we cannot be absolutely sure that a given clast is in place, discarding any sin-depositional reworking). However, size outliers are also expected to occur due to inherent variability of the system, e.g. particle diffusion, instability of eruption column. Given such an uncertainty on the origin of size outliers, the option of accommodating outliers in order to mitigate their effect on the final results seems more appropriate than rejecting them on a subjective basis. Our first attempt of accommodating the data by using the median instead of the mean did not improve the stability of the data (e.g. Table 12 and Fig. 25).

Another possible accommodation strategy is offered by data transformation. We have shown that values of the largest clasts found at a given outcrop can be plotted using a survivor function. The first advantage of this technique is the fact that outliers do not need to be identified and they do not affect the general trend of the population. Second, we have also seen that the 50^{th} percentile of this distribution is affected by less variability within the same outcrop than the largest values. In particular, we have seen that the 50^{th} percentile is affected by a standard deviation of 0.2 cm and an average percentage difference of about 30% from the 5^{th} percentile for the geometric mean of clasts

collected at both outcrops and for both 0.1 and 0.5 m^2 sections. Such a difference is of the same order of variability linked to the choice of collection strategy, sampled volume and averaging technique and can be accounted for in the final calculation. Third, the choice of characterizing a certain outcrop by plotting a survivor function eliminates the problem of choice of population size (i.e. number of clasts to be considered in the calculation). Finally, the survivor-function method could also speed up the field measurement by collecting the largest 20 clasts and only measuring the 10^{th} largest one, corresponding to the 50^{th} percentile of the population. In fact, the smallest clast of a 10-clast population corresponds to the 50^{th} percentile of a 20-clast population. As a result, we only need to collect the 10 largest clasts and measure the smallest one.

Recommendation

The method of the 50^{th} percentile is considered as the best way to assess the largest clasts because it has the advantages of: i) eliminating the problem of outlier identification based on a rigorous statistical approach, ii) offering a more reliable reproducibility of the characterization of a given outcrop than the measurement of a small population of large clasts (e.g. 3 or 5), iii) reducing analysis time in the field by requiring the measurement of only one clast (i.e., the smallest of the 11 largest clasts). In addition, the underestimation of values is in the same order of magnitude of the differences due to the choice of the collection strategy, sampled volume and averaging technique and can also be corrected when compiling the isopleth map. Further investigations on the stability of the discrepancy between 50^{th} percentile of a 20-clast population and the largest clasts found at a given outcrop should be carried out. Finally, the survivor-function data should also be calibrated with the method of Carey and Sparks (1986) in order to correct for the discrepancies with the 3- and 5-clast populations typically used.

Acknowledgments

All workshop participants (Appendix A) are especially thanked for their enthusiastic contribution and hard work to collect and characterize a large number of clasts in only one day! In fact, most data processing to determine the maximum clast was done during the second day of the workshop and preliminary results were discussed with the whole group. In particular, we would like to thank Mauro Rosi for the help in the identification of the best outcrops to use in this workshop and Chuck Connor for the “nearly real-time” statistical analysis of workshop data and innovative application of the survivor function for the determination of the maximum clast. Licia Costantini, Alain Volentik, Paola Del Carlo, Daniele Andronico and Claudia Principe are also thanked for the grainsize analysis carried out after the workshop (Appendix B) and Alvaro Amigo for the evaluation of the largest clasts resulting from all possible combinations of investigated areas for both outcrops (Appendix F).

References

Ablay GJ, Ernst GGJ, Marti J, Sparks RSJ (1995) The Similar-to-2 Ka Subplinian Eruption of Montana-Blanca, Tenerife. Bulletin of Volcanology 57(5):337-355

Adams NK, de Silva SL, Self S, Salas G, Schubring S, Permenter JL, Arbesman K (2001) The physical volcanology of the 1600 eruption of Huaynaputina, southern Peru. Bulletin of Volcanology 62(8):493-518

Andronico D, Cioni R (2002) Contrasting styles of Mount Vesuvius activity in the period between the Avellino and Pompeii Plinian eruptions, and some implications for assessment of future hazards. Bulletin of Volcanology 64(6):372-391

Aschenbrenner BC (1956) A new method of expressing particle sphericity. journal of Sedimentary Petrology 26(1):15-31

Barberi F, Coltelli M, Frullani A, Rosi M, Almeida E (1995) Chronology and dispersal characteristics of recently (last 5000 years) erupted tephra of Cotopaxi (Ecuador): implications for long-term eruptive forecasting. Journal of volcanology and geothermal research 69:217-239

Barnett V, Lewis T (1998) Outliers in Statistical Data. Wiely, Chichester

Biass S, Bonadonna C (2011) A quantitative uncertainty assessment of eruptive parameters derived from tephra deposits: the example of two large eruptions of cotopaxi volcano, ecuador. Bulletin of Volcanology

Bonadonna C, Ernst GGJ, Sparks RSJ (1998) Thickness variations and volume estimates of tephra fall deposits: the importance of particle Reynolds number. Journal of Volcanology and Geothermal Research 81(3-4):173-187

Bonadonna C, Houghton BF (2005) Total grainsize distribution and volume of tephra-fall deposits. Bulletin of Volcanology 67:441-456

Bryan SE, Cas RAF, Marti J (2000) The 0.57 Ma plinian eruption of the Granadilla Member, Tenerife (Canary Islands): an example of complexity in eruption dynamics and evolution. Journal of Volcanology and Geothermal Research 103(1-4):209-238

Bunte K, Abt SR (2001) Sampling Surface and Subsurface Particle-Size Distributions in Wadable Gravel- and Cobble-Bed Streams for Analyses in Sediment Transport, Hydraulics, and Streambed Monitoring. In: United States Department of Agriculture (Rocky Mountain Research Station),

Bursik MI, Sparks RSJ, Gilbert JS, Carey SN (1992) Sedimentation of tephra by volcanic plumes: I. Theory and its comparison with a study of the Fogo A plinian deposit, Sao Miguel (Azores). Bulletin of Volcanology 54:329-344

Carey S, Sigurdsson H (1987) Temporal Variations in Column Height and Magma Discharge Rate During the 79 Ad Eruption of Vesuvius. Geological Society of America Bulletin 99(2):303-314

Carey S, Sigurdsson H, Gardner JE, Criswell W (1990) Variations in column height and magma discharge during the May 18, 1980 eruption of Mount St Helens. Journal of Volcanology and Geothermal Research 43(1-4):99-112

Carey SN, Sigurdsson H (1986) The 1982 eruptions of El Chichon volcano, Mexico (2): observations and numerical modelling of tephra-fall distribution. Bulletin of Volcanology 48:127-141

Carey SN, Sparks RSJ (1986) Quantitative models of the fallout and dispersal of tephra from volcanic eruption columns. Bulletin of Volcanology 48:109-125

Coltelli M, Del Carlo P, Vezzoli L (1998) Discovery of a Plinian basaltic eruption of Roman age at Etna volcano, Italy. Geology 26(12):1095-1098

Connor LG, Connor CB (2006) Inversion is the key to dispersion: understanding eruption dynamics by inverting tephra fallout. In: Mader H, Cole S, Connor CB, Connor LG (eds) Statistics in Volcanology. Geological Society London, pp 231-242

Dixon WJ (1950) Analysis of extreme values. Annals of Mathematical Statistics 21(4):488-506

Evans M, Hastings N, Peacock B (2000) Statistical Distributions. Wiley, New York

Fierstein J, Hildreth W (1992) The plinian eruptions of 1912 at Novarupta, Katmai National Park, Alaska. Bulletin of Volcanology 54:646-684

Fierstein J, Nathenson M (1992) Another look at the calculation of fallout tephra volumes. Bulletin of Volcanology 54:156-167
Froggatt PC (1982) Review of methods estimating rhyolitic tephra volumes; applications to the Taupo Volcanic Zone, New Zealand. Journal of Volcanology and Geothermal Research 14:1-56
Gardner JE, Tait S (2000) The caldera-forming eruption of Volcan Ceboruco, Mexico. Bulletin of Volcanology 62(1):20-33
Giannetti B, De Casa G (2000) Stratigraphy, chronology, and sedimentology of ignimbrites from the white trachytic tuff, Roccamonfina Volcano, Italy. Journal of Volcanology and Geothermal Research 96(3-4):243-+
Hildreth W, Drake RE (1992) Volcano Quizapu, Chilean Andes. Bulletin of Volcanology 54:93-125
Jurado-Chichay Z, Walker GPL (2000) Stratigraphy and dispersal of the Mangaone Subgroup pyroclastic deposits, Okataina Volcanic Centre, New Zealand. Journal of Volcanology and Geothermal Research 104(1-4):319-383
Jurado-Chichay Z, Walker GPL (2001) The intensity and magnitude of the Mangaone subgroup plinian eruptions from Okataina Volcanic Centre, New Zealand. Journal of Volcanology and Geothermal Research 111(1-4):219-237
Kanisawa S, Yoshida T (1989) Genesis of the Extremely Low-K Tonalites from the Island-Arc Volcanism - Lithic Fragments in the Adachi-Medeshima Pumice Deposits, Northeast Japan. Bulletin of Volcanology 51(5):346-354
Limburg EM, Varekamp JC (1991) Young Pumice Deposits on Nisyros, Greece. Bulletin of Volcanology 54(1):68-77
Lirer L, Pescatore T, Booth B, Walker GPL (1973) Two Plinian pumice-fall deposits from Somma-Vesuvius, Italy. Geological Society of America Bulletin 84:759-772
Luhr JF (2000) The geology and petrology of Volcan San Juan (Nayarit, Mexico) and the compositionally zoned Tepic Pumice. Journal of Volcanology and Geothermal Research 95(1-4):109-156
McPhie J, Walker GPL, Christiansen RL (1990) Phreatomagmatic and phreatic fall and surge deposits from explosions at Kilauea volcano, Hawaii, 1790 A.D.: Keanakakoi Ash Member. Bulletin of Volcanology 52:334-354
Milner DM, Cole JW, Wood CP (2002) Asymmetric, multiple-block collapse at Rotorua Caldera, Taupo Volcanic Zone, New Zealand. Bulletin of Volcanology 64(2):134-149
Papale P, Rosi M (1993) A case of no-wind plinian fallout at Pululagua caldera (Ecuador): implications for model of clast dispersal. Bulletin of Volcanology 55:523-535
Pyle DM (1989) The thickness, volume and grainsize of tephra fall deposits. Bulletin of Volcanology 51(1):1-15
Rolandi G, Munno R, Postiglione I (2004) The AD 472 eruption of the Somma volcano. Journal of Volcanology and Geothermal Research 129(4):291-319
Scollo S, Tarantola S, Bonadonna C, Coltelli M, Saltelli A (2008) Sensitivity analysis and uncertainty estimation for tephra dispersal models. Journal of Geophisical Research 113(B06202)
Sigurdsson H, Carey S (1989) Plinian and co-ignimbrite tephra fall from the 1815 eruption of Tambora volcano. Bulletin of Volcanology 51:243-270
Sigurdsson H, Carey S, Cornell W, Pescatore T (1985) The Eruption of Vesuvius in AD 79. National Geographic Research 1(3):332-387
Sigurdsson H, Carey SN, Espindola JM (1984) The 1982 Eruptions of El Chichon Volcano, Mexico - Stratigraphy of Pyroclastic Deposits. Journal of Volcanology and Geothermal Research 23(1-2):11-37
Smith RT, Houghton BF (1995) Delayed Deposition of Plinian Pumice During Phreatoplinian Volcanism - the 1800-Yr-Bp Taupo Eruption, New-Zealand. Journal of Volcanology and Geothermal Research 67(4):221-226
Smith RT, Houghton BF (1995) Vent migration and changing eruptive style during the 1800a Taupo eruption: New evidence from the Hatepe and Rotongaio phreatoplinian ashes. Bulletin of Volcanology 57(6):432-439

Sottili G, Palladino DM, Zanon V (2004) Plinian activity during the early eruptive history of the Sabatini Volcanic District, central Italy. Journal of Volcanology and Geothermal Research 135(4):361-379
Sparks RSJ (1986) The dimensions and dynamics of volcanic eruption colums. Bulletin of Volcanology 48:3-15
Sparks RSJ, Wilson L, Sigurdsson H (1981) The pyroclastic deposits of the 1875 eruption of Askja, Iceland. Philosophical Transaction of the Royal Society of London 229:241-273
Suzuki T, Katsu Y, Nakamura T (1973) Size distribution of the Tarumai Ta-b pumice-fall deposit. Bulletin of the Volcanological Society of Japan 18:47-64
Suzukikamata K, Kamata H (1990) The Proximal Facies of the Tosu Pyroclastic-Flow Deposit Erupted from Aso Caldera, Japan. Bulletin of Volcanology 52(5):325-333
Thouret JC, Juvigne E, Gourgaud A, Boivin P, Davila J (2002) Reconstruction of the AD 1600 Huaynaputina eruption based on the correlation of geologic evidence with early Spanish chronicles. Journal of Volcanology and Geothermal Research 115(3-4):529-570
Tukey JW (1977) Exploratory Data Analysis. Addison-Wesley, Reading, MA
Turner JS (1979) Buoyancy effects in fluids. Cambridge University Press, Cambridge, p 368
Walker GPL (1973) Explosive volcanic eruptions - a new classification scheme. Geologische Rundschau 62:431-446
Walker GPL (1980) The Taupo Pumice: product of the most powerful known (Ultraplinian) eruption? Journal of Volcanology and Geothermal Research 8:69-94
Walker GPL (1981) Characteristics of two phreatoplinian ashes, and their water-flushed origin. Journal of Volcanology and Geothermal Research 9:395-407
Walker GPL (1981) The Waimihia and Hatepe plinian deposits from the rhyolitic Taupo Volcanic Centre. New Zealand Journal of Geology and Geophysics 24:305-324
Walker GPL, Croasdale R (1971) Two plinian-type eruptions in the Azores. Journal of the Geological Society of London 127:17-55
Walker GPL, Self S, Froggatt PC (1981) The Ground Layer of the Taupo Ignimbrite - a Striking Example of Sedimentation from a Pyroclastic Flow. Journal of Volcanology and Geothermal Research 10(1-3):1-11
Walker GPL, Self S, Wilson L (1984) Tarawera, 1886, New Zealand - A basaltic Plinian fissure eruption. Journal of Volcanology and Geothermal Research 21:61-78
Walker GPL, Wilson CJN, Froggatt PC (1981) An Ignimbrite Veneer Deposit - the Trail-Marker of a Pyroclastic Flow. Journal of Volcanology and Geothermal Research 9(4):409-421
Williams SN, Self S (1983) The October 1902 Plinian eruption of Santa Maria volcano, Guatemala. Journal of Volcanology and Geothermal Research 16:33-56
Wilson L, Huang TC (1979) The influence of shape on the atmospheric settling velocity of volcanic ash particles. Earth and Planetary Sciences Letters 44:311-324
Wilson L, Walker GPL (1987) Explosive volcanic-eruptions .6. Ejecta dispersal in plinian eruptions - the control of eruption conditions and atmospheric properties. Geophysical Journal of the Royal Astronomical Society 89(2):657-679
Woods AW (1988) The fluid-dynamics and thermodynamics of eruption columns. Bulletin of Volcanology 50(3):169-193

Appendix A

Participants

	Name	Institution
1	Amigo Alvaro	University of Bristol, UK
2	Andronico Daniele	INGV –Catania, Italy
3	Bonadonna Costanza	University of Geneva, Switzerland
4	Browne Brandon L.	California State University, USA
5	Bull Kate	Alaska Volcano Observatory, USA
6	Carey Rebecca	University of Hawaii, USA
7	Cashman Kathy	University of Oregon, USA
8	Cioni Raffaello	University of Cagliari, Italy
9	Coltelli Mauro	INGV – Catania, Italy
10	Connor Chuck	University of South Florida, USA
11	Connor Laura	University of South Florida, USA
12	Costantini Licia	University of Geneva, Switzerland
13	Del Carlo Paola	INGV – Catania, Italy
14	Houghton Bruce	University of Hawaii, USA
15	Jenkins Susanna	Macquarie University, Australia
16	Jutzeler Martin	University of Lausanne, Switzerland
17	Kobs Shannon	SUNY Buffalo, USA
18	Landi Patrizia	INGV – Pisa, Italy
19	Lautze Nicole	University of Hawaii, USA
20	Magill Christina	Macquarie University, Australia
21	Melendez Christyanne	Northern Arizona University, USA
22	Pioli Laura	University of Pisa, Italy
23	Pistolesi Marco	University of Pisa, Italy
24	Principe Claudia	CNR – Pisa, Italy
25	Rosi Mauro	University of Pisa, Italy
26	Salani Flavia Maria	Universidad de Buenos Aires, Argentina
27	Scollo Simona	INGV – Catania, Italy
28	Sruoga Patricia	Ser. Geologico Minero, Argentina
29	Swanson Don	USGS – HVO, USA
30	Takarada Shinji	Geological Survey of Japan, Japan
31	Volentik Alain	University of South Florida, USA
32	Wright Heather	University of Oregon, USA

APPENDIX B

Grainsize data

SIEVING

PHI	Pisa (1B)	Tampa (1C)	Catania (1D)	Standard deviation
-5	0.401413	0.409724	0.405716	0.0
-4	14.27204	14.56752	14.42502	0.1
-3	32.922	33.6036	33.27489	0.3
-2	22.71472	21.98722	22.55926	0.4
-1	17.90641	18.12626	18.46529	0.3
0	7.51071	7.73686	7.68954	0.1
1	1.241641	1.15364	1.187557	0.0
2	0.389534	0.360201	0.806615	0.2
3	0.547783	0.444857	0.466076	0.1
4	0.499091	0.405019	0.720038	0.2
>4	1.594656	1.205098	0	0.8

PHI	Pisa (2B)	Tampa (2C)	Catania (2D)	Standard deviation
-5	0	0	0	0.0
-4	13.64262	13.70	13.90912	0.1
-3	34.16195	34.31	34.82927	0.4
-2	22.06597	22.84	24.54234	1.3
-1	18.08557	17.82	16.75656	0.7
0	7.629109	7.63	7.157599	0.3
1	1.326802	1.25	1.224179	0.1
2	0.426472	0.43	0.436507	0.0
3	0.473858	0.58	0.558226	0.1
4	0.568629	1.30	0.586207	0.4
>4	1.619014	0.14	0	0.9

SIEVING AND PHARMAVISION (SAMPLE 1C)

PHI	Sieving	Sieving + pharmavision	Standard deviation
-5	0.409724	0.412392	0.0
-4	14.56752	14.66239	0.1
-3	33.6036	33.1712	0.3
-2	21.98722	22.13041	0.1
-1	18.12626	18.24431	0.1
0	7.73686	7.787245	0.0
1	1.15364	0	0.8
2	0.360201	0.682256	0.2
3	0.444857	0.954912	0.4
4	0.405019	0.725468	0.2
5	1.205098	0.762834	0.3
6	-	0.387279	
7	-	0.057594	
8	-	0.01874	

SIEVING (three samples of same outcrop)

PHI	Tamoa (1C)	Tampa (1C)	Tampa (area F)	Standard deviation
-5	0.41	0	0	0.2
-4	14.57	13.70	15.20	0.8
-3	33.60	34.31	32.03	1.2
-2	21.99	22.84	25.31	1.7
-1	18.13	17.82	16.62	0.8
0	7.74	7.63	7.80	0.1
1	1.15	1.25	1.52	0.2
2	0.36	0.43	0.33	0.0
3	0.44	0.58	0.28	0.1
4	0.41	1.30	0.69	0.5
>4	1.21	0.14	0.22	0.6

SIEVING AND PHARMAVISION (SAMPLE 1C and AREA A)

PHI	1C	Area A	Standard deviation
-5	0.4	0	0.3
-4	14.7	11.1	2.5
-3	33.2	32.9	0.2
-2	22.1	26.5	3.1
-1	18.2	17.8	0.3
0	7.8	7.7	0.0
1	0.0	0.0	0.0
2	0.7	1.1	0.3
3	1.0	0.4	0.4
4	0.7	0.6	0.1
5	0.8	1.1	0.2
6	0.4	0.7	0.2
7	0.1	0.1	0.0
8	0.0	0.0	0.0

SIEVING AND PHARMAVISION (SAMPLE 1C and outcrop 2)

PHI	1C (outcrop 1)	Outcrop 2
-5	0.4	0.00
-4	14.7	2.23
-3	33.2	13.04
-2	22.1	22.50
-1	18.2	25.85
0	7.8	22.55
1	0.0	7.78
2	0.7	0.59
3	1.0	1.52
4	0.7	1.37
5	0.8	1.37
6	0.4	0.93
7	0.1	0.1
8	0.0	0.0

APPENDIX C

Axis measurement (data)

Diameter of equivalent sphere (cm)	GM1 (cm)	GM2 (cm)	GM3 (cm)	GM4 (cm)	GM5 (cm)	GM6 (cm)	GM7 (cm)	average (cm)	STDEV (cm)
2.79	3.30	3.00	3.19	3.01	3.34	3.23	2.97	3.15	0.15
2.45	2.58	2.49	2.32	2.36	2.55	2.65	2.42	2.48	0.12
2.73	3.28	2.77	2.74	2.82	2.95	2.99	2.92	2.92	0.18
2.42	2.67	2.69	2.58	2.81	2.79	2.75	2.68	2.71	0.08
3.32	3.42	3.03	3.46	3.02	3.40	3.33	3.51	3.31	0.20
2.34	2.46	2.38	2.41	2.35	2.51	2.51	2.48	2.44	0.06
2.33	2.49	2.35	2.22	2.47	2.37	2.63	2.40	2.42	0.13
1.73	2.03	1.73	1.99	1.56	1.96	1.84	1.86	1.85	0.16
1.51	1.77	1.54	1.65	1.63	1.67	1.74	1.63	1.66	0.08
1.39	1.63	1.52	1.43	1.59	1.66	1.63	1.57	1.58	0.08

Table C1. GM: geometric mean. Diameter of equivalent sphere is determined from the volume derived using the Archimede's principle. The average and standard deviation are calculated only for the values of geometric mean.

	% diff. 1	% diff. 2	% diff. 3	% diff. 4	% diff. 5	% diff. 6	% diff. 7	average (cm)
clast 1	-18.48	-7.70	-14.63	-7.84	-19.78	-15.78	-6.74	-12.99
clast 2	-5.10	-1.51	5.34	3.74	-4.17	-8.13	1.11	-1.24
clast 3	-20.08	-1.43	-0.43	-3.29	-7.97	-9.69	-6.94	-7.12
clast 4	-9.98	-10.91	-6.37	-15.70	-14.98	-13.36	-10.66	-11.71
clast 5	-2.96	8.77	-4.17	8.94	-2.29	-0.20	-5.66	0.35
clast 6	-5.05	-1.65	-2.81	-0.62	-7.41	-7.41	-6.20	-4.45
clast 7	-7.00	-0.69	4.62	-5.81	-1.67	-12.76	-3.07	-3.77
clast 8	-17.55	-0.20	-15.01	9.69	-13.27	-6.64	-7.52	-7.22
clast 9	-17.33	-1.89	-9.35	-8.27	-10.41	-15.12	-8.27	-10.09
clast 10	-16.87	-9.16	-2.31	-14.36	-18.78	-16.87	-12.83	-13.03
Average	-12.04	-2.64	-4.51	-3.35	-10.07	-10.60	-6.68	-7.13

Table C2. Percentage difference between the geometric mean (from table C1) and the diameter of the equivalent sphere determined from the volume derived using the Archimede's principle. Percentage difference is determined using the following formula: $\frac{value2 - value1}{value1} \times 100$.

	USER1			USER4			USER7		
axis (cm)	4	3	3	3.9	2.4	2.9	3.9	2.5	2.7
axis (cm)	3.1	2.9	1.9	2.7	2.7	1.8	3.1	2.7	1.7
axis (cm)	4.4	4	2	4	3.5	1.6	4.2	3.7	1.6
axis (cm)	4.3	2.1	2.1	4	2.4	2.3	4.2	2	2.3
axis (cm)	4.6	3.1	2.8	3.3	3.1	2.7	4.8	3.1	2.9
axis (cm)	3.2	2.9	1.6	3	2.9	1.5	3.3	3.1	1.5
axis (cm)	3.4	2.4	1.9	3.4	2.1	2.1	3.3	2.1	2
axis (cm)	2.6	1.9	1.7	1.6	1.7	1.4	2.1	1.8	1.7
axis (cm)	2.4	2.1	1.1	2.2	1.8	1.1	2.2	1.8	1.1
axis (cm)	2.4	2	0.9	2.3	2.2	0.8	2.4	1.8	0.9
	USER2			USER5					
axis (cm)	4	2.6	2.6	4	3.1	3			
axis (cm)	3	2.7	1.9	3.3	2.8	1.8			
axis (cm)	3.4	3.9	1.6	4.1	3.9	1.6			
axis (cm)	3.4	2.6	2.2	4.3	2.4	2.1			
axis (cm)	3.2	2.8	3.1	4.5	3	2.9			
axis (cm)	2.9	2.9	1.6	3.2	3.1	1.6			
axis (cm)	3.4	1.9	2	3.5	2	1.9			
axis (cm)	1.8	1.7	1.7	2.6	1.7	1.7			
axis (cm)	2.2	1.5	1.1	2.8	1.5	1.1			
axis (cm)	2.2	2	0.8	2.4	2.1	0.9			
	USER3			USER6					
axis (cm)	3.8	2.6	3.3	4	3	2.8			
axis (cm)	3.2	2.6	1.5	3.1	3	2			
axis (cm)	3.9	3.3	1.6	4.3	3.9	1.6			
axis (cm)	4.3	2.1	1.9	4.3	2.3	2.1			
axis (cm)	4.6	3.1	2.9	4.7	2.9	2.7			
axis (cm)	3.2	2.9	1.5	3.2	3.1	1.6			
axis (cm)	3.4	1.9	1.7	3.6	2.4	2.1			
axis (cm)	2.3	1.9	1.8	2.2	1.9	1.5			
axis (cm)	2.4	1.7	1.1	2.8	1.7	1.1			
axis (cm)	2.3	2.1	0.6	2.4	2	0.9			

Table C3. Axis of 10 clasts measured by 7 different users (cm)

APPENDIX D

Application of the Dixon's test

The Dixon's test is a convenient and robust statistical test used to identify values that appear diverging from the considered population (Dixon 1950). This technique is recommended for use in small populations (as small as three) and for situations where data are normally distributed but the mean or variance change slowly over time (Chernick 1982). The main limitation is that it requires the assumption of normality. It is most useful for spotting individual outliers rather than group outliers.

Application: the N values comprising the set of observations are arranged in ascending order: $Y_1<Y_2<\ldots<Y_N$. The statistic experimental ratio R_x is calculated based on the observations (where x=10, 11, 21 and 22 depending on the population size; Table D1). If $R_x > R_{crit}$, then the suspect value can be characterized as an outlier and it can be rejected. If not, the suspect value must be retained and used in all subsequent calculations. R_{crit} is determined with Table D1 based on population size and critical value α.

n	0.1	∪ 0.05	0.01	
3	0.886	0.941	0.988	R10=(Y2-Y1)/(Yn-Y1)
4	0.679	0.765	0.889	
5	0.557	0.642	0.780	
6	0.482	0.560	0.698	
7	0.434	0.507	0.637	
8	0.479	0.554	0.683	R11=(Y2-Y1)/(Y(n-1)-Y1)
9	0.441	0.512	0.635	
10	0.409	0.477	0.597	
11	0.517	0.576	0.679	R21=(Y3-Y1)/(Y(n-1)-Y1)
12	0.490	0.546	0.642	
13	0.467	0.521	0.615	
14	0.492	0.546	0.641	R22=(Y3-Y1)/(Y(n-2)-Y1)
15	0.472	0.525	0.616	
16	0.454	0.507	0.595	
17	0.438	0.490	0.577	
18	0.424	0.475	0.561	
19	0.412	0.462	0.547	
20	0.401	0.450	0.535	
21	0.391	0.440	0.524	
22	0.382	0.430	0.514	∪ is the critical value (10, 5 or 1%)
23	0.374	0.421	0.505	R is the statistical test
24	0.367	0.413	0.497	n is the sample size
25	0.360	0.406	0.489	

Table D1

Appendix E

Plots of the largest clasts as derived from different sampled areas and using different collection strategies at both outcrops

OUTCROP 1 0.1 m^2 area plots

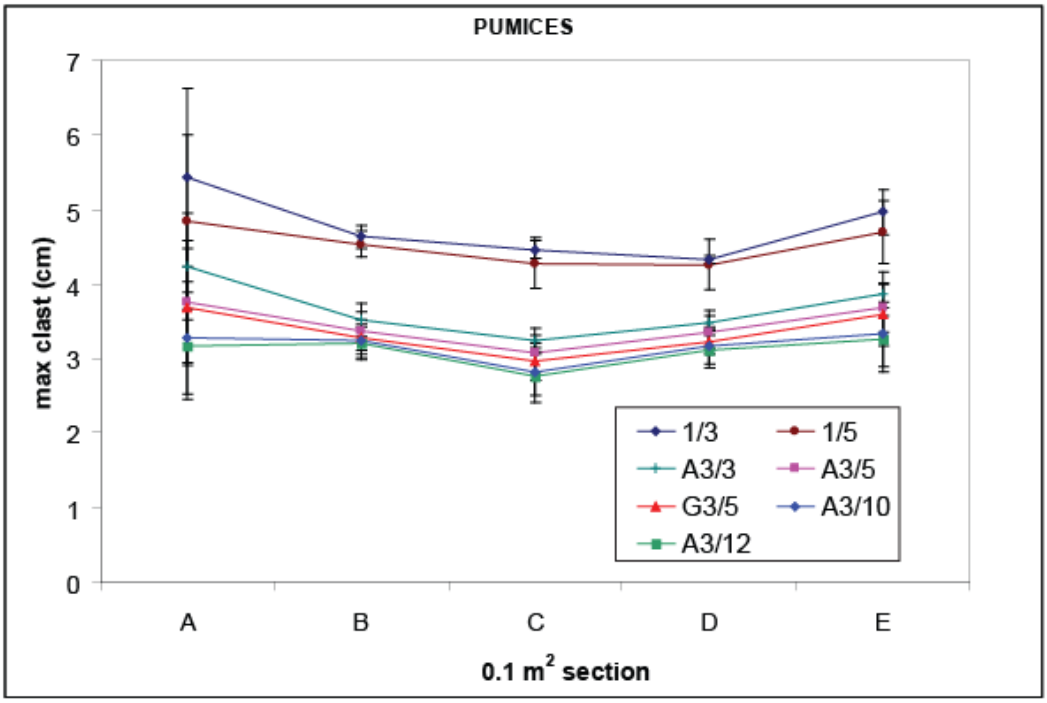

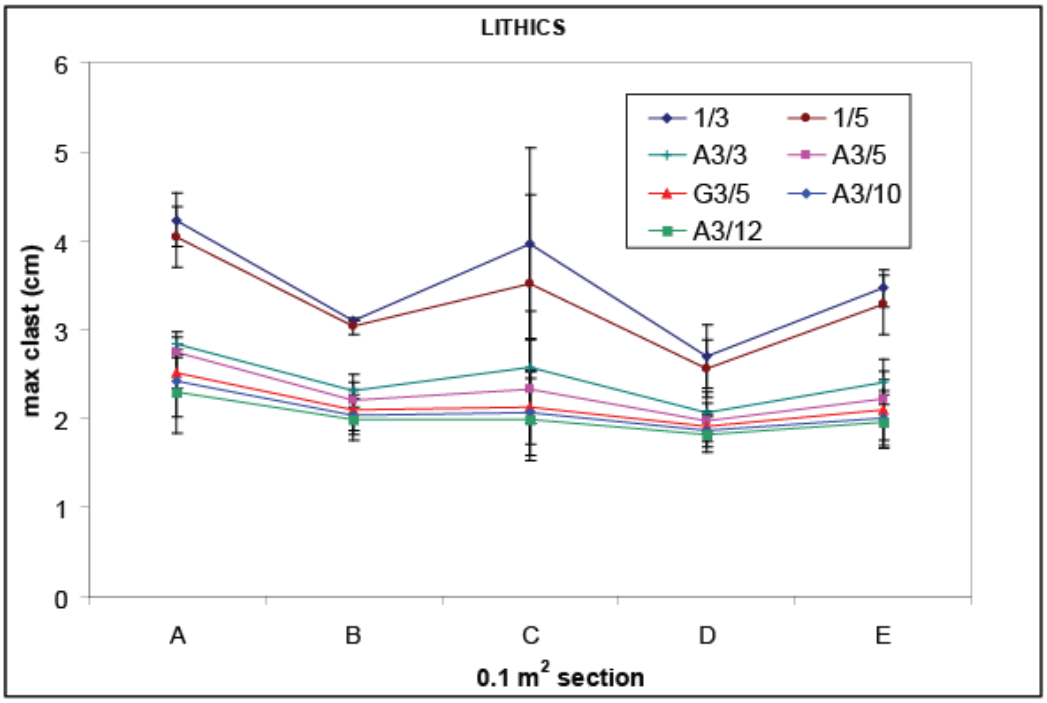

Outcrop 1

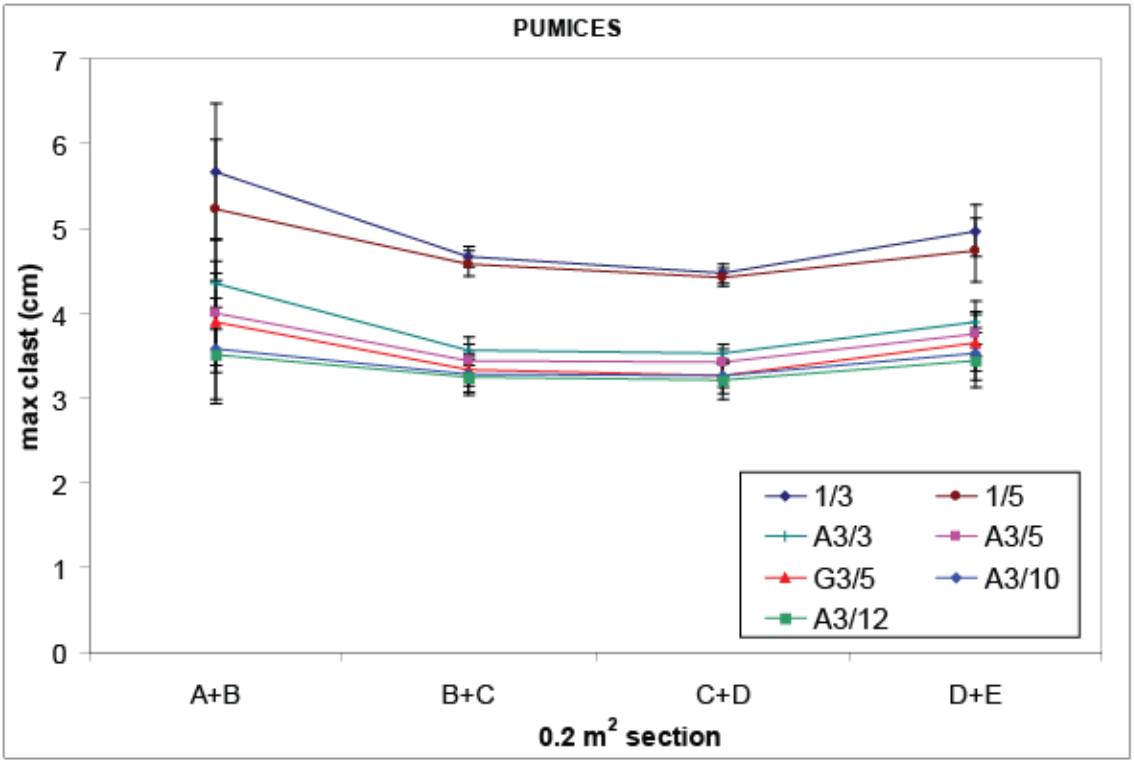
PUMICES
max clast (cm)
0
1
2
3
4
5
6
7
A+B
B+C
C+D
D+E
0.2 m² section
1/3
1/5
A3/3
A3/5
G3/5
A3/10
A3/12

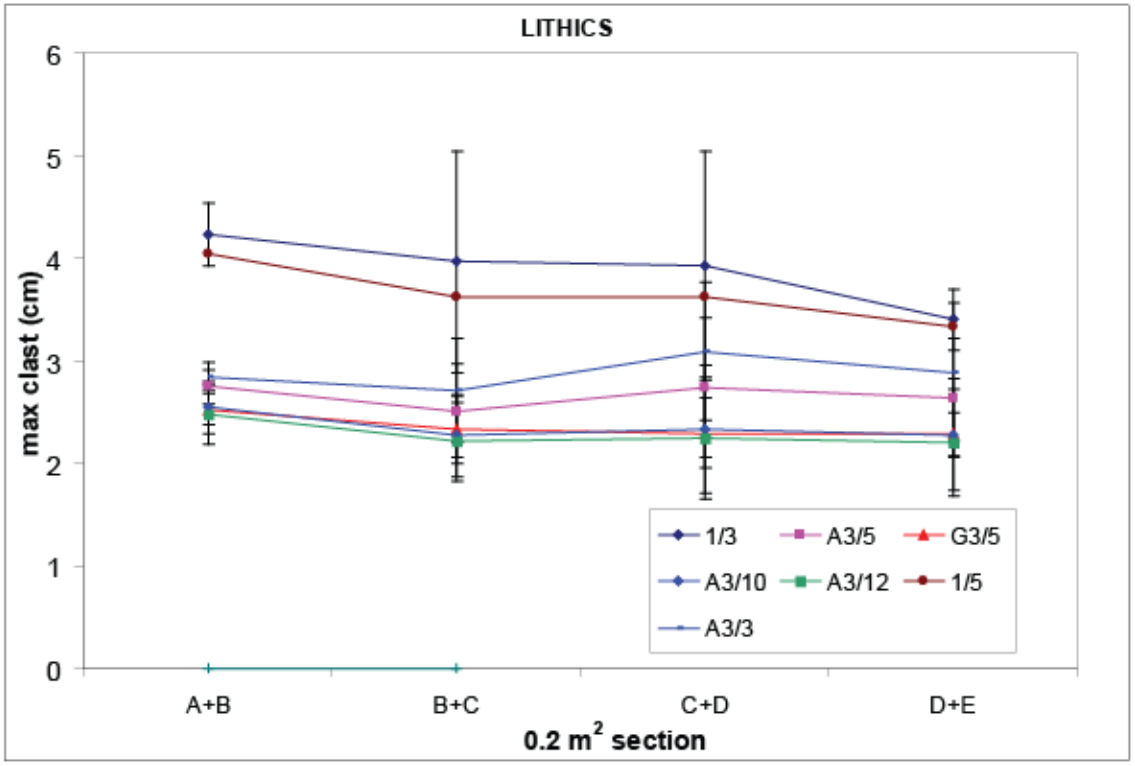
LITHICS
max clast (cm)
0
1
2
3
4
5
6
A+B
B+C
C+D
D+E
0.2 m² section
1/3
A3/5
G3/5
A3/10
A3/12
1/5
A3/3

Outcrop 1

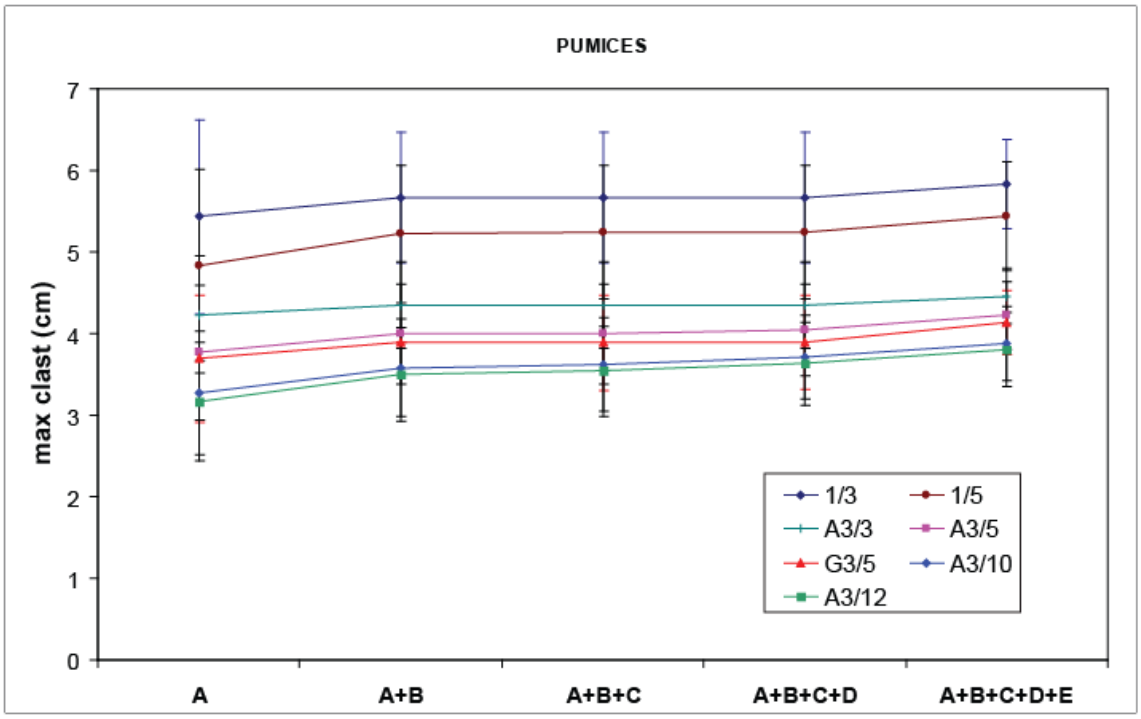
PUMICES
max clast (cm)
0
1
2
3
4
5
6
7
A
A+B
A+B+C
A+B+C+D
A+B+C+D+E
1/3
1/5
A3/3
A3/5
G3/5
A3/10
A3/12

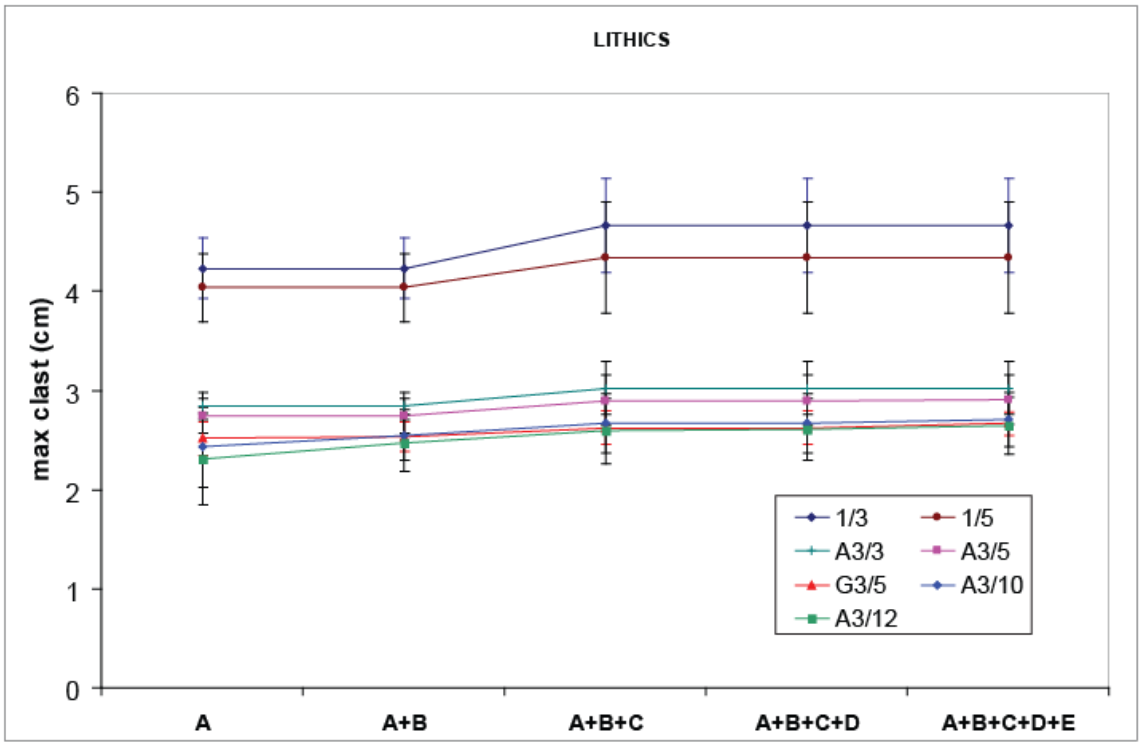
LITHICS
max clast (cm)
0
1
2
3
4
5
6
A
A+B
A+B+C
A+B+C+D
A+B+C+D+E
1/3
1/5
A3/3
A3/5
G3/5
A3/10
A3/12

Outcrop 1

OUTCROP 1 0.5 m^2 area plots

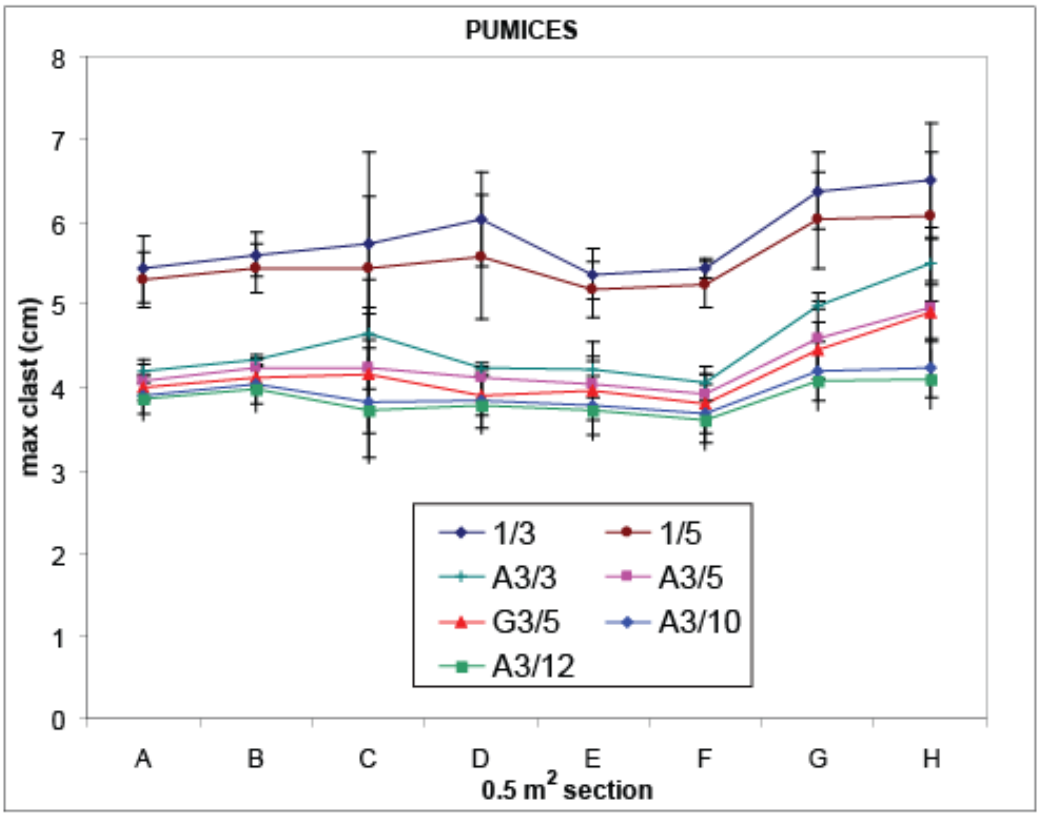

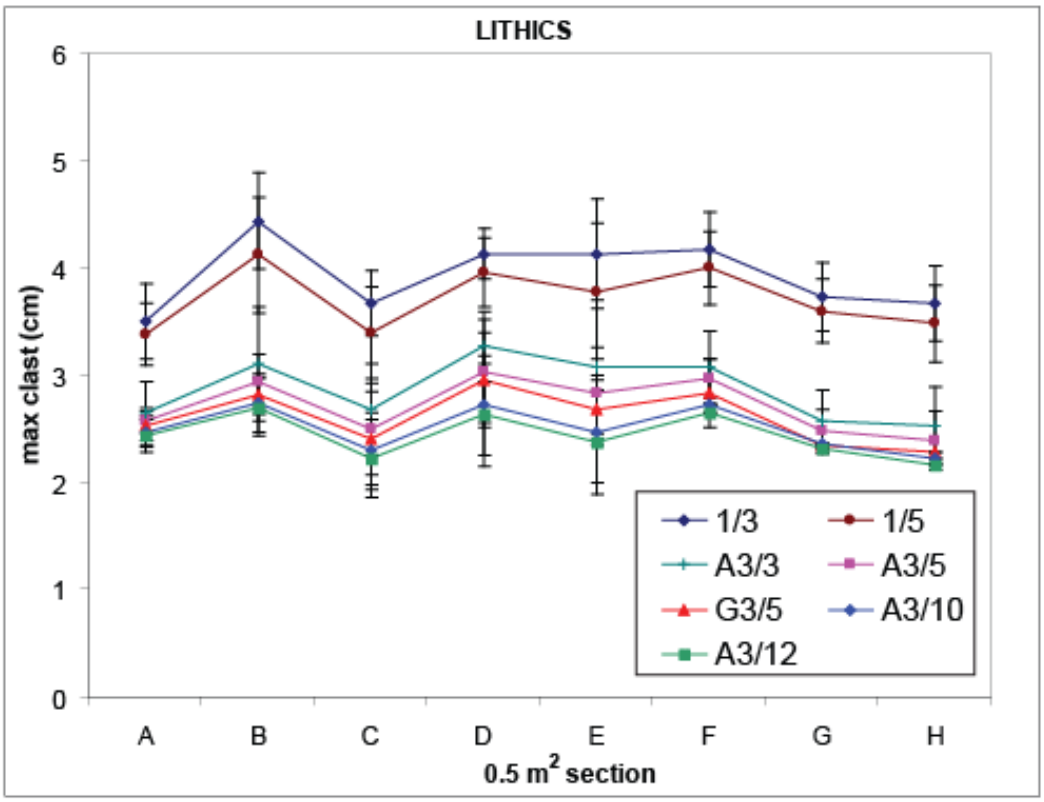

Outcrop 1

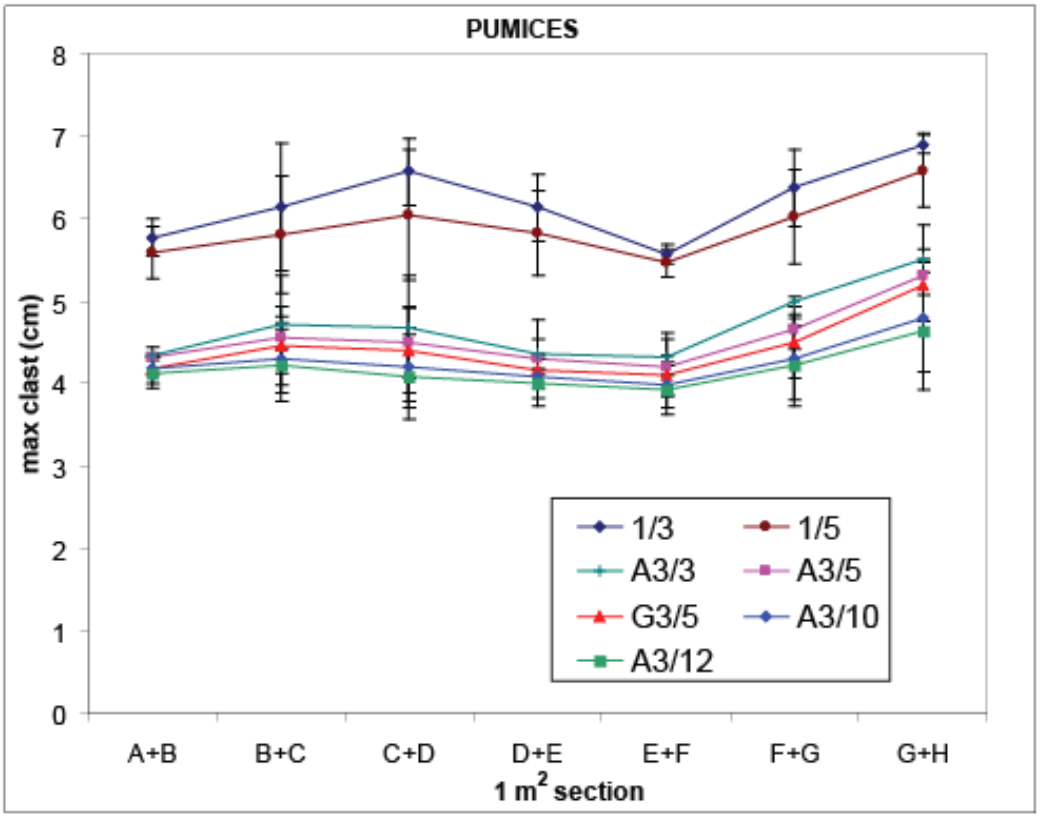
PUMICES
max clast (cm)
0
1
2
3
4
5
6
7
8
A+B
B+C
C+D
D+E
E+F
F+G
G+H
1 m2 section
1/3
1/5
A3/3
A3/5
G3/5
A3/10
A3/12

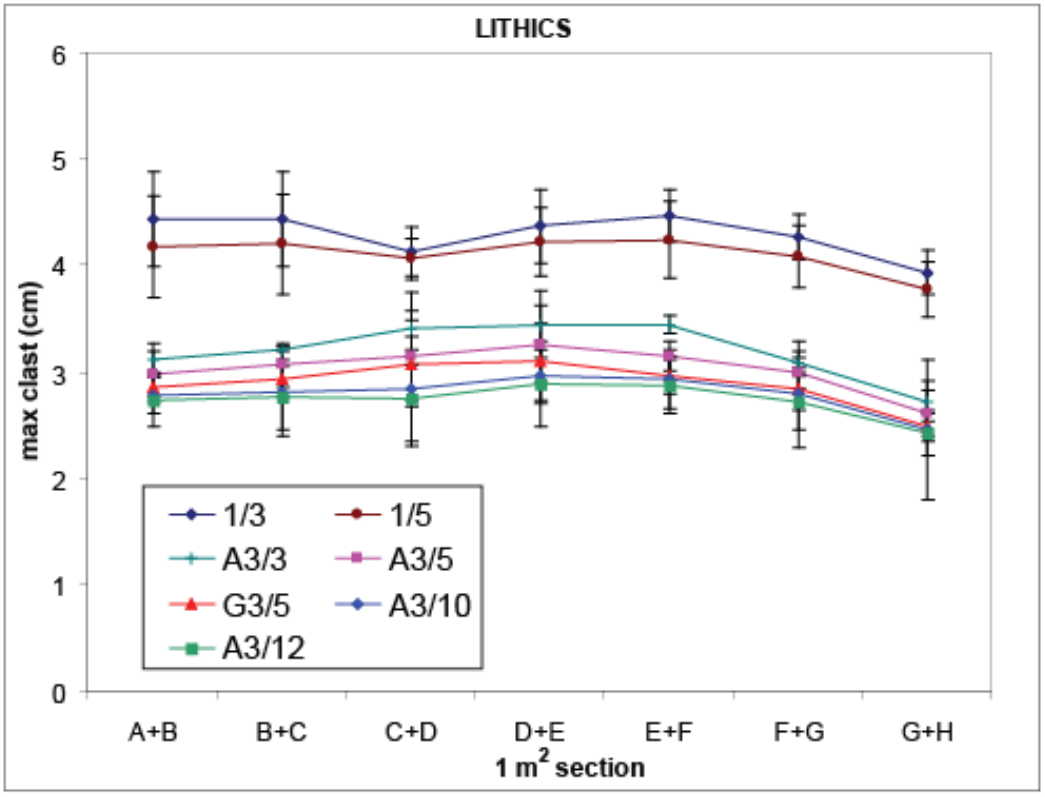
LITHICS
max clast (cm)
0
1
2
3
4
5
6
A+B
B+C
C+D
D+E
E+F
F+G
G+H
1 m2 section
1/3
1/5
A3/3
A3/5
G3/5
A3/10
A3/12

Outcrop 1

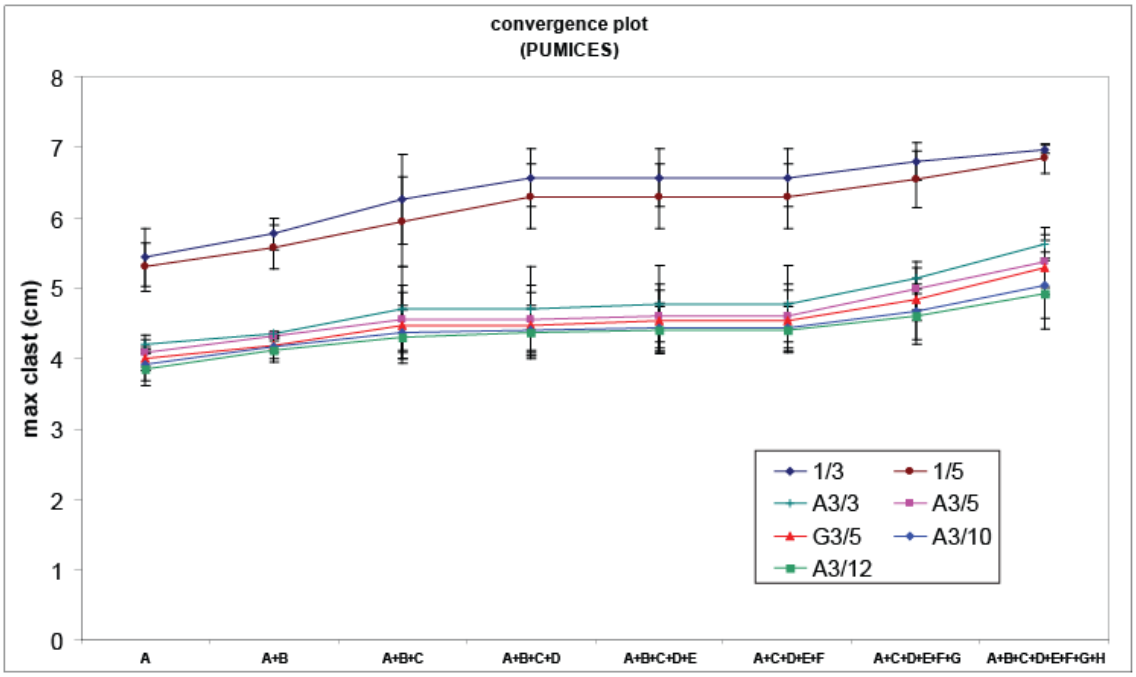
convergence plot
(PUMICES)
max clast (cm)
0
1
2
3
4
5
6
7
8
A
A+B
A+B+C
A+B+C+D
A+B+C+D+E
A+C+D+E+F
A+C+D+E+F+G
A+B+C+D+E+F+G+H
1/3
1/5
A3/3
A3/5
G3/5
A3/10
A3/12

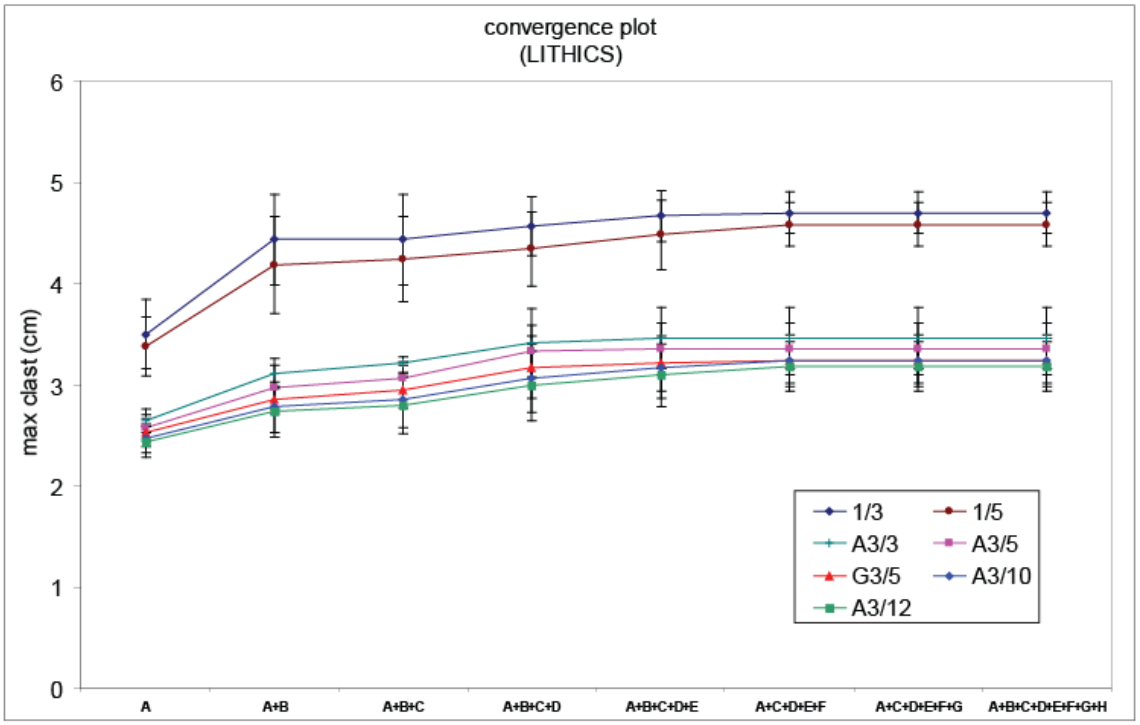
convergence plot
(LITHICS)
max clast (cm)
0
1
2
3
4
5
6
A
A+B
A+B+C
A+B+C+D
A+B+C+D+E
A+C+D+E+F
A+C+D+E+F+G
A+B+C+D+E+F+G+H
1/3
1/5
A3/3
A3/5
G3/5
A3/10
A3/12

Outcrop 1

OUTCROP 1 unspecified-area plots

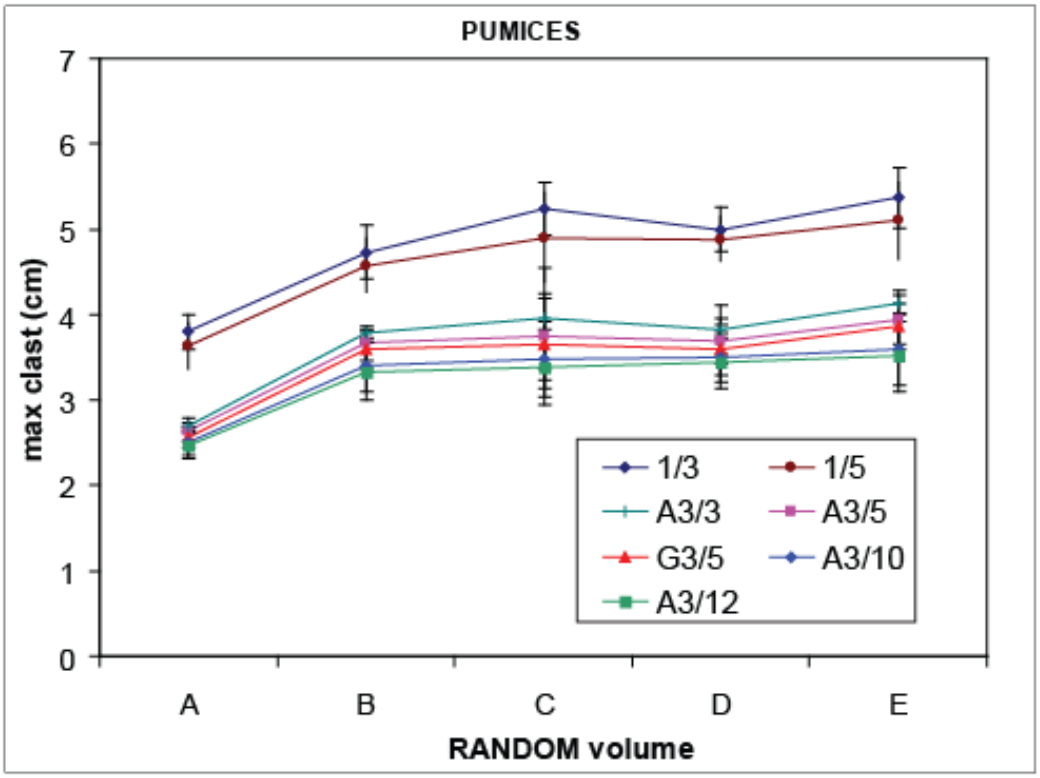

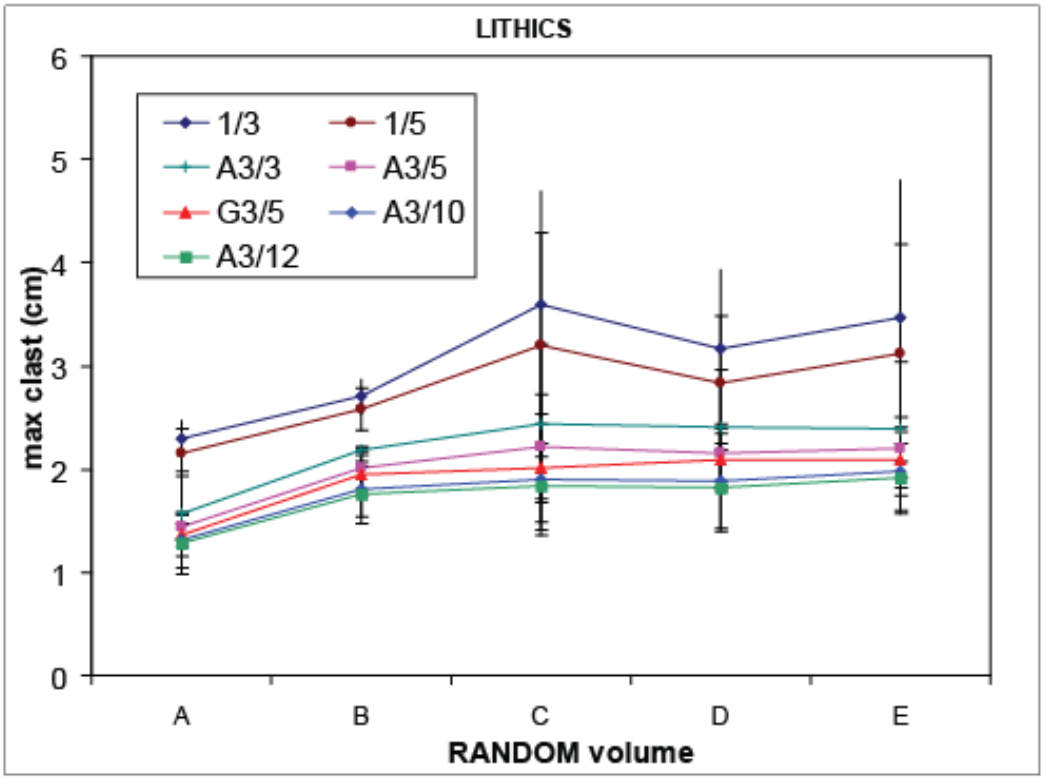

Outcrop 1

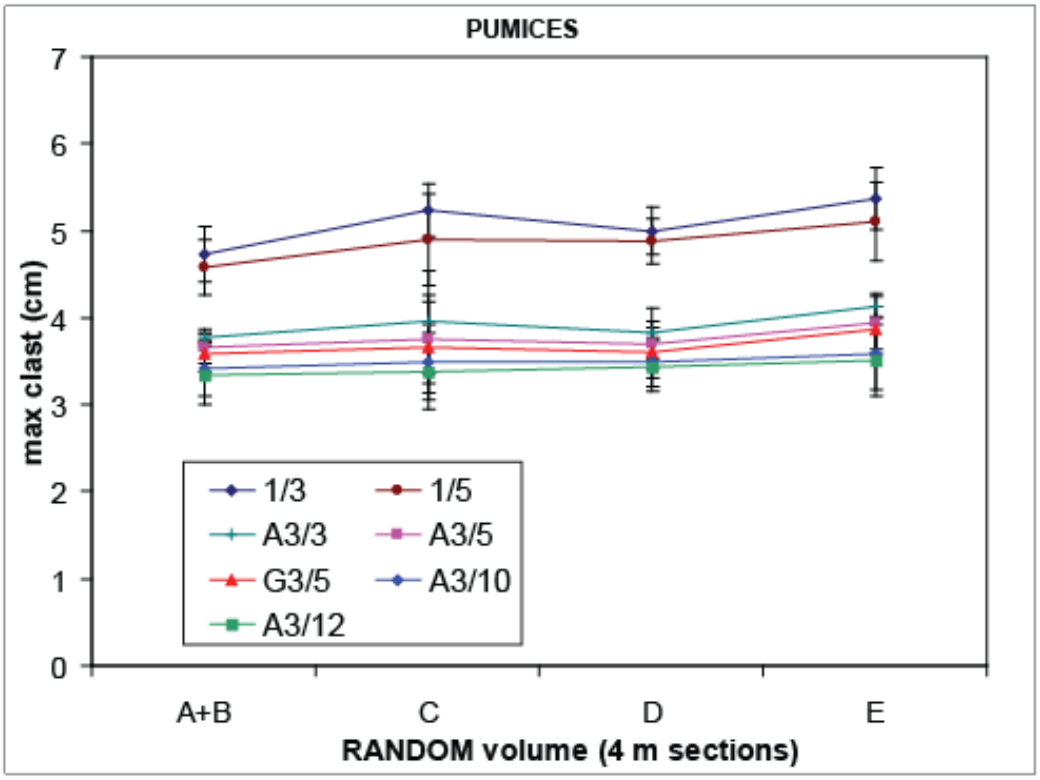
PUMICES
max clast (cm)
0
1
2
3
4
5
6
7
1/3
1/5
A3/3
A3/5
G3/5
A3/10
A3/12
A+B
C
D
E
RANDOM volume (4 m sections)

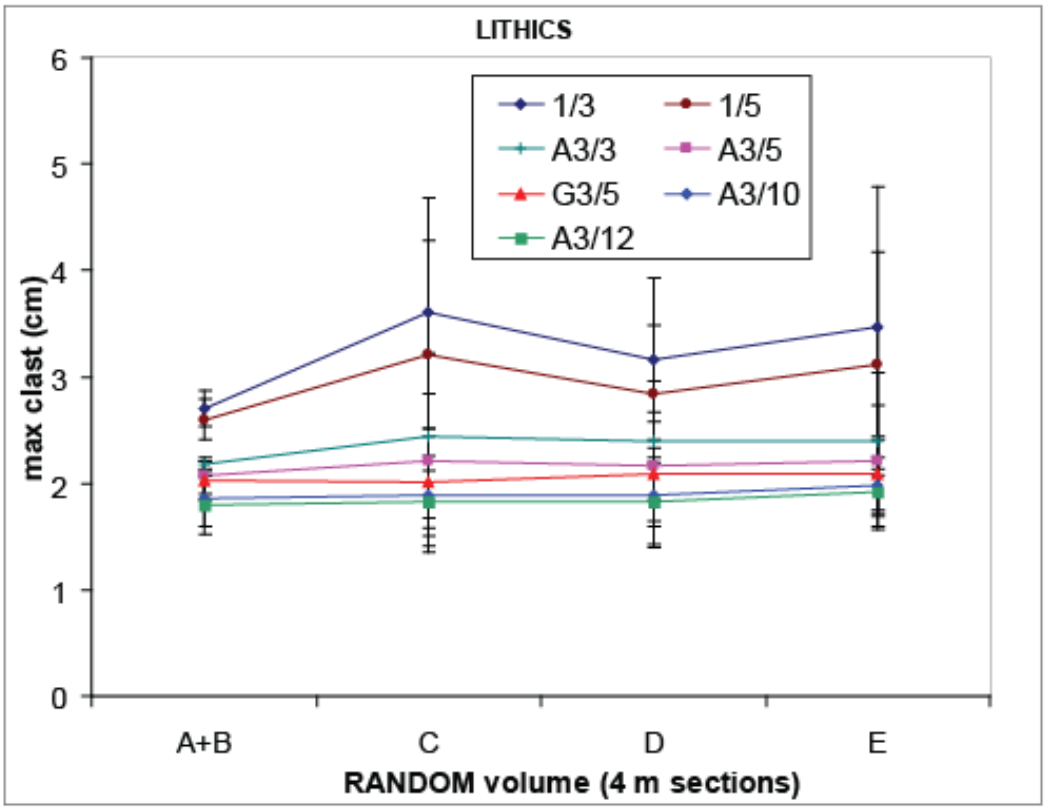
LITHICS
max clast (cm)
0
1
2
3
4
5
6
1/3
1/5
A3/3
A3/5
G3/5
A3/10
A3/12
A+B
C
D
E
RANDOM volume (4 m sections)

Outcrop 1

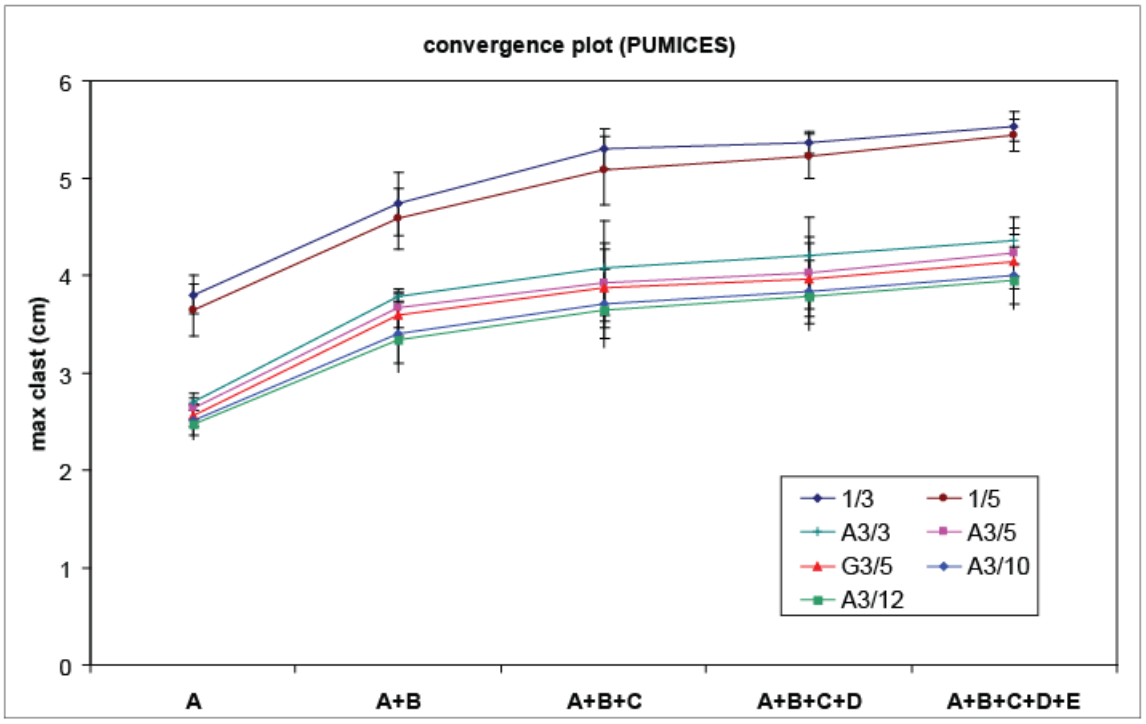
convergence plot (PUMICES)
max clast (cm)
0
1
2
3
4
5
6
A
A+B
A+B+C
A+B+C+D
A+B+C+D+E
1/3
1/5
A3/3
A3/5
G3/5
A3/10
A3/12

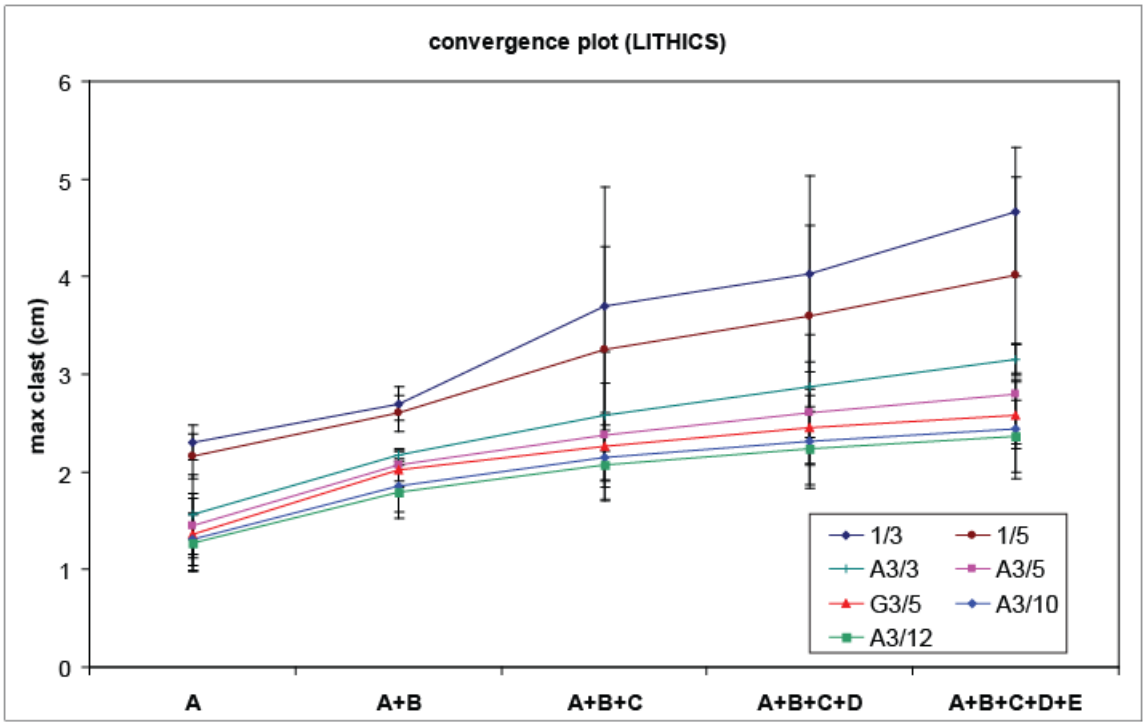
convergence plot (LITHICS)
max clast (cm)
0
1
2
3
4
5
6
A
A+B
A+B+C
A+B+C+D
A+B+C+D+E
1/3
1/5
A3/3
A3/5
G3/5
A3/10
A3/12

Outcrop 1

OUTCROP 1 unspecified-area plots (time)

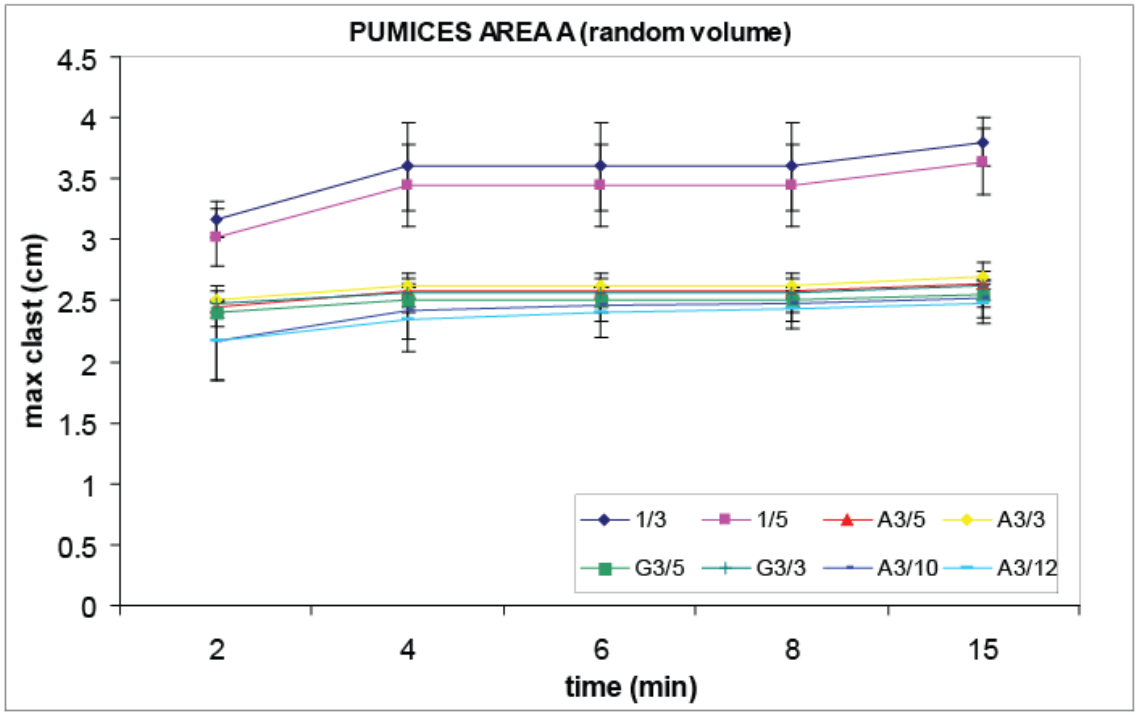

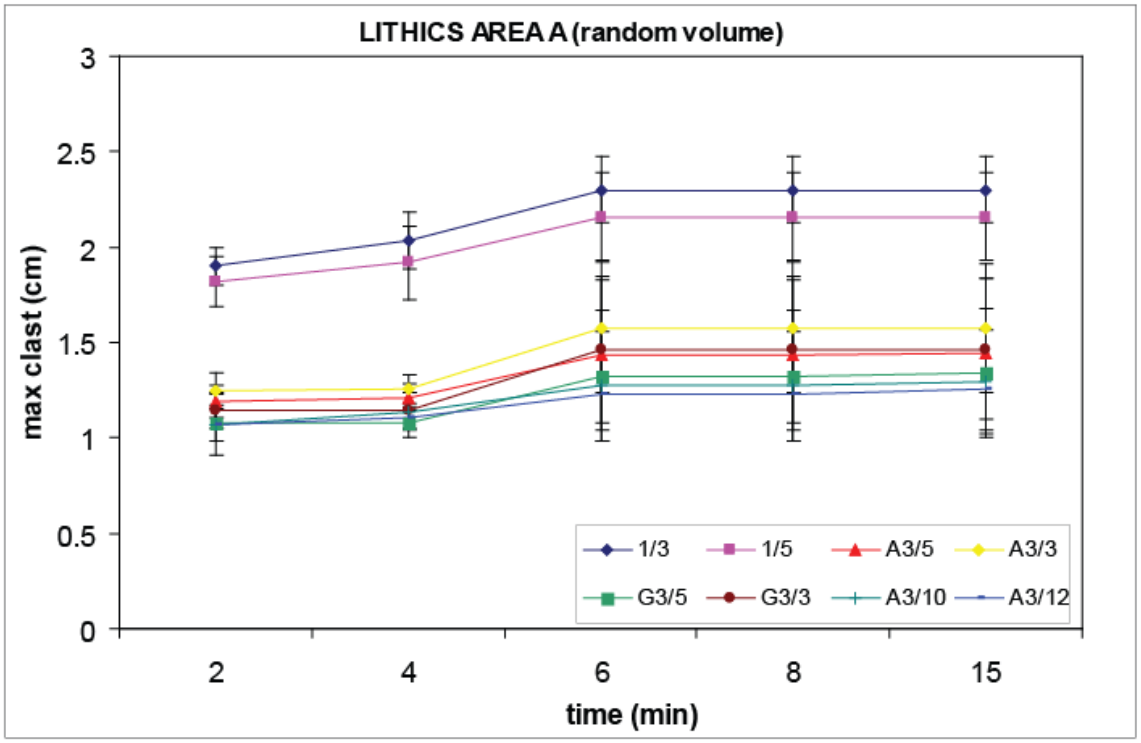

Outcrop 1

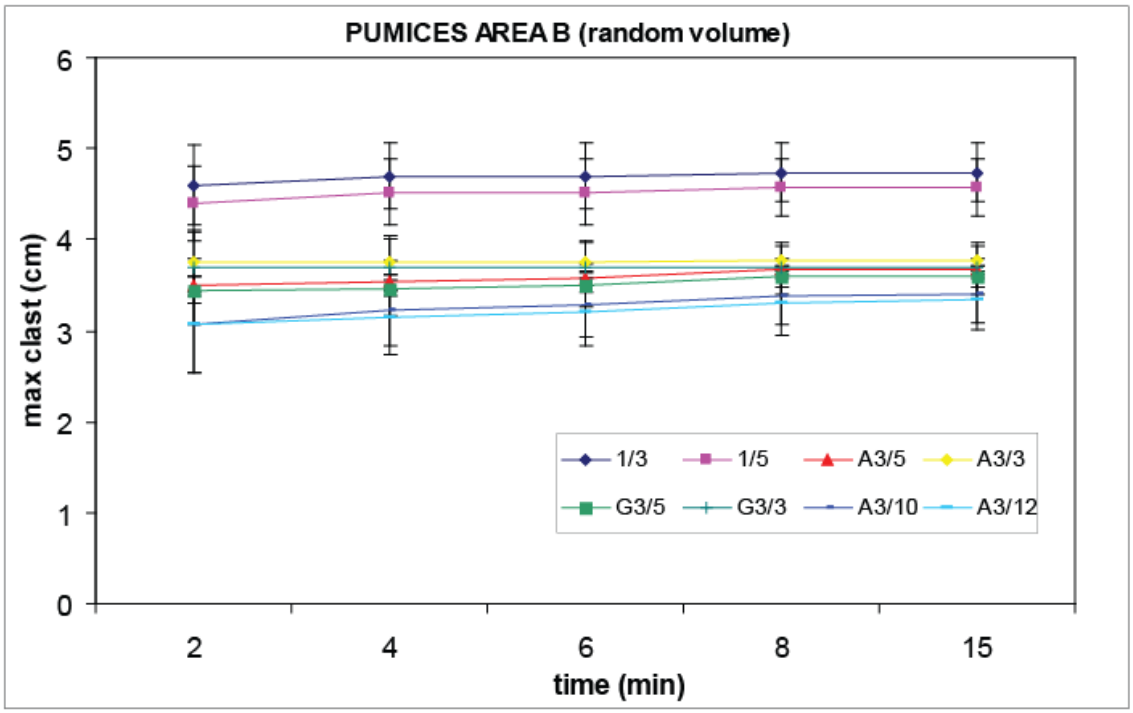
PUMICES AREA B (random volume)
max clast (cm)
time (min)
0
1
2
3
4
5
6
2
4
6
8
15
1/3
1/5
A3/5
A3/3
G3/5
G3/3
A3/10
A3/12

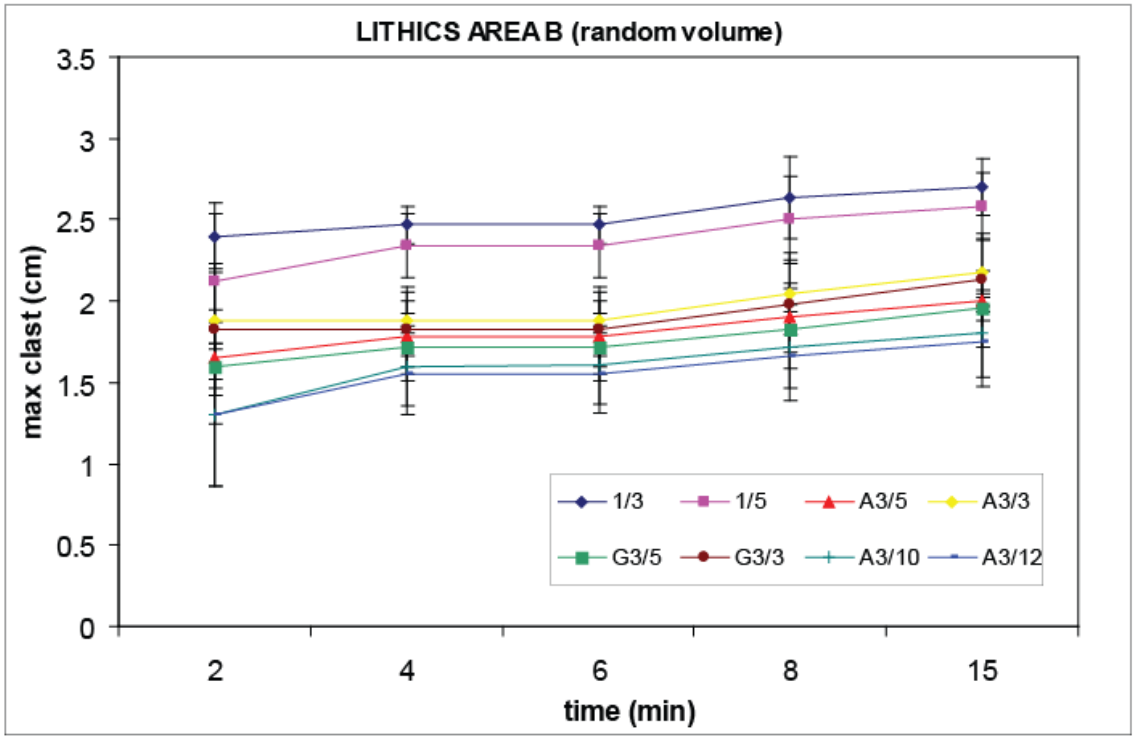
LITHICS AREA B (random volume)
max clast (cm)
time (min)
0
0.5
1
1.5
2
2.5
3
3.5
2
4
6
8
15
1/3
1/5
A3/5
A3/3
G3/5
G3/3
A3/10
A3/12

Outcrop 1

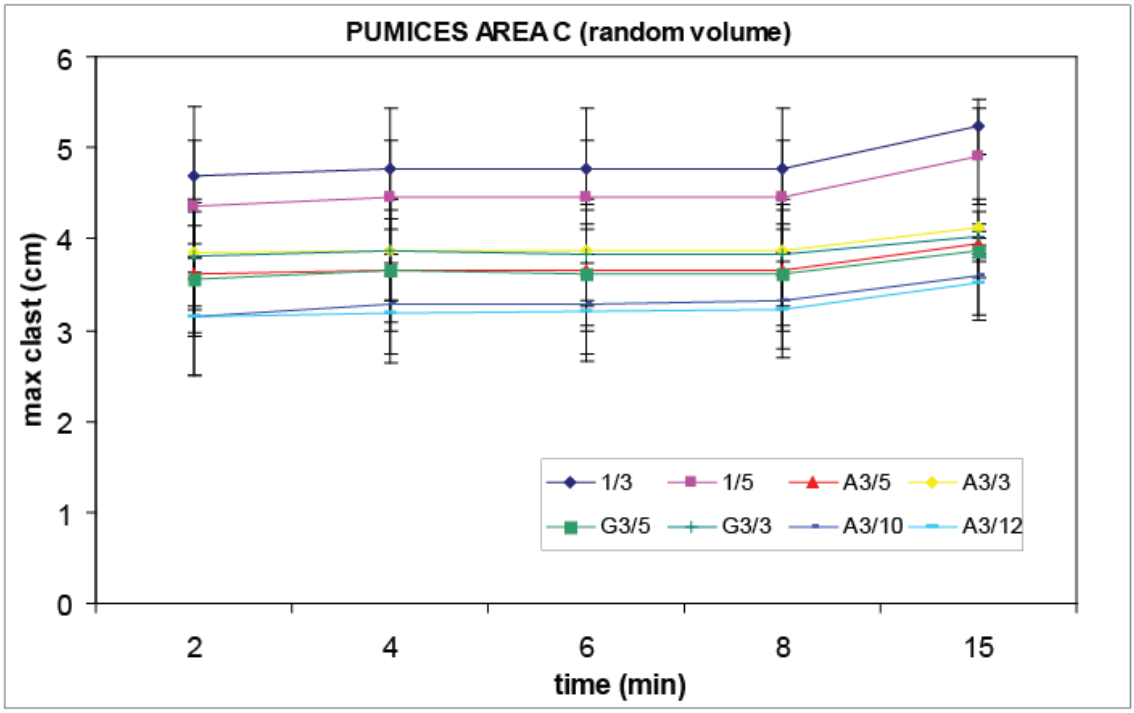
PUMICES AREA C (random volume)
max clast (cm)
time (min)
0
1
2
3
4
5
6
2
4
6
8
15
1/3
1/5
A3/5
A3/3
G3/5
G3/3
A3/10
A3/12

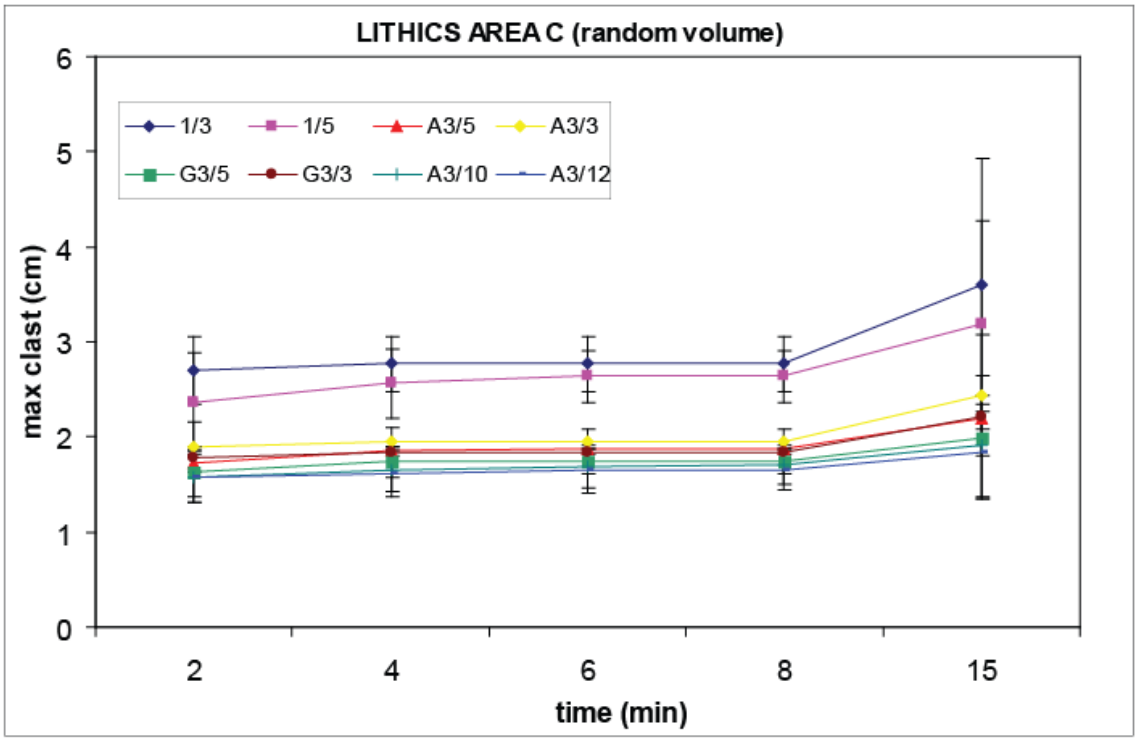
LITHICS AREA C (random volume)
max clast (cm)
time (min)
0
1
2
3
4
5
6
2
4
6
8
15
1/3
1/5
A3/5
A3/3
G3/5
G3/3
A3/10
A3/12

Outcrop 1

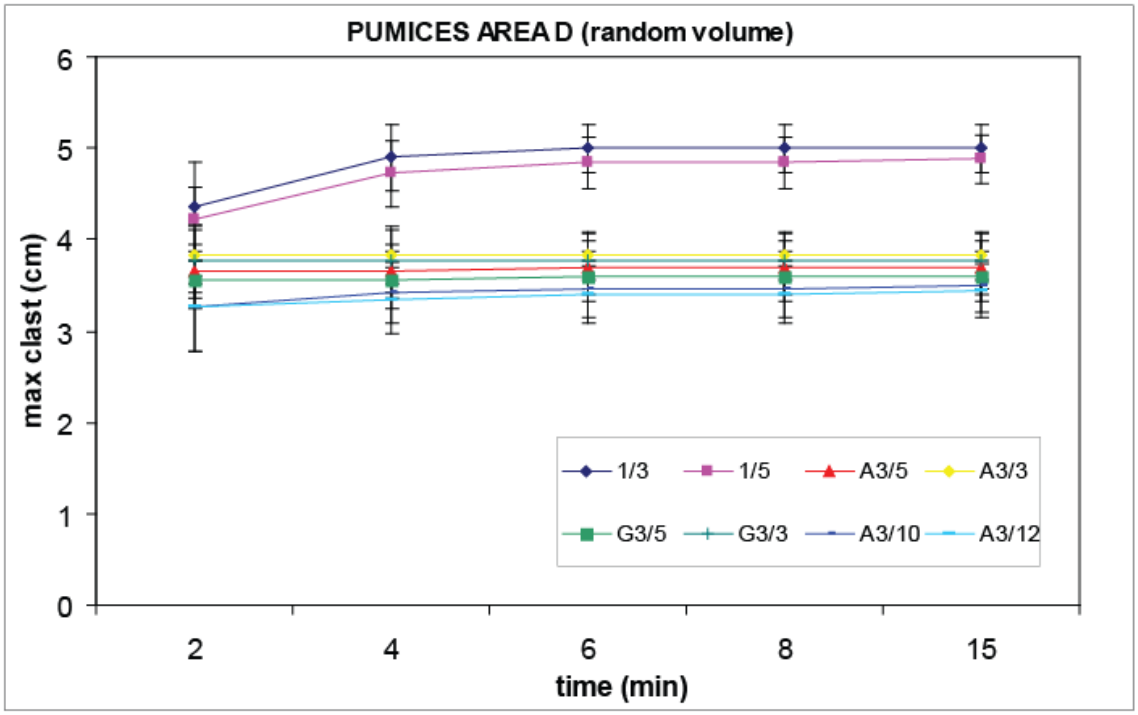
PUMICES AREA D (random volume)
max clast (cm)
time (min)
1/3
1/5
A3/5
A3/3
G3/5
G3/3
A3/10
A3/12

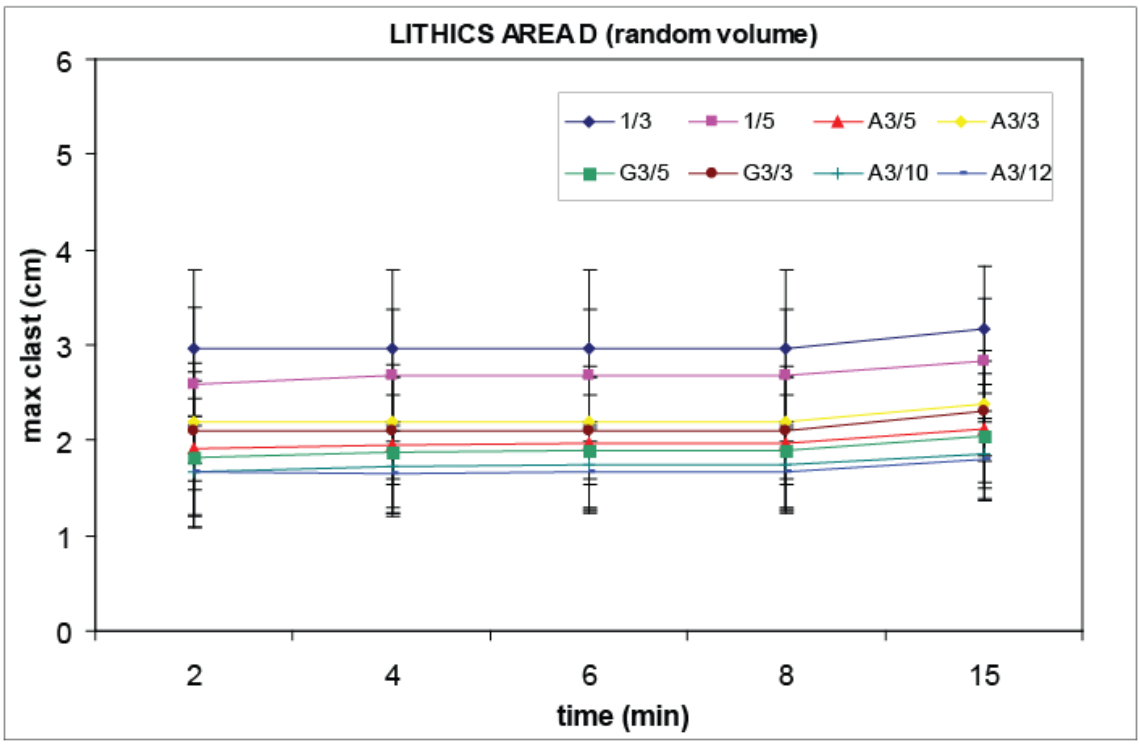
LITHICS AREA D (random volume)
max clast (cm)
time (min)
1/3
1/5
A3/5
A3/3
G3/5
G3/3
A3/10
A3/12

Outcrop 1

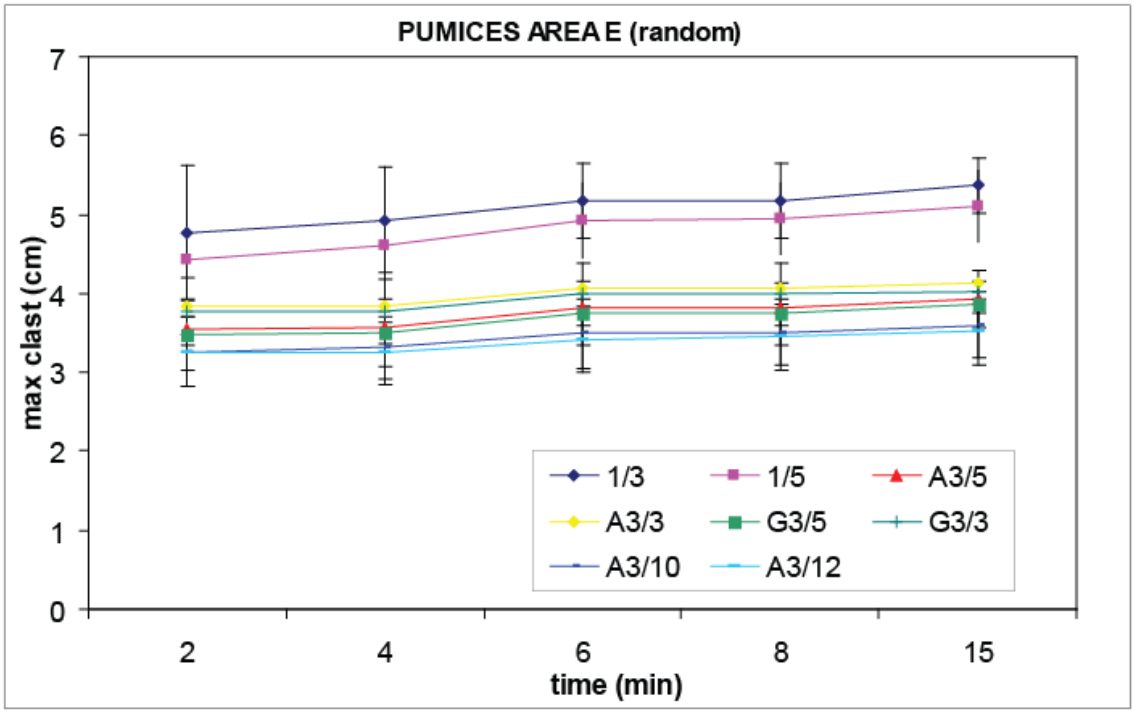
PUMICES AREA E (random)
max clast (cm)
time (min)
1/3
1/5
A3/5
A3/3
G3/5
G3/3
A3/10
A3/12

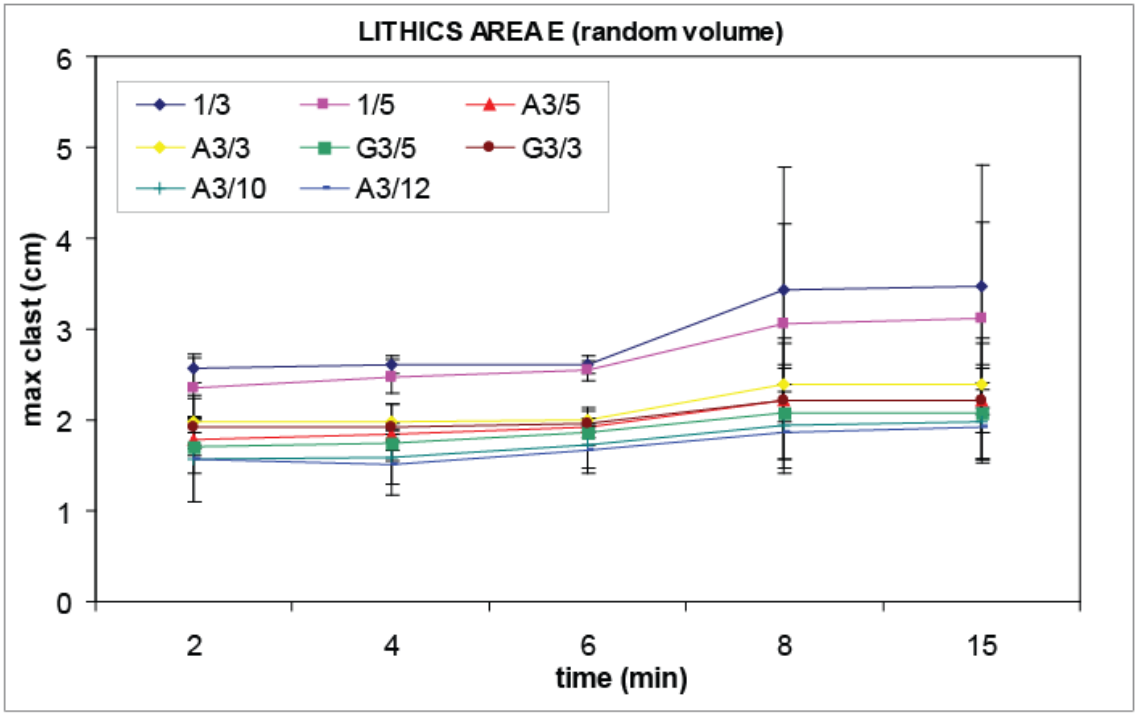
LITHICS AREA E (random volume)
max clast (cm)
time (min)
1/3
1/5
A3/5
A3/3
G3/5
G3/3
A3/10
A3/12

Outcrop 1

OUTCROP 2 0.1 m^2 area plots

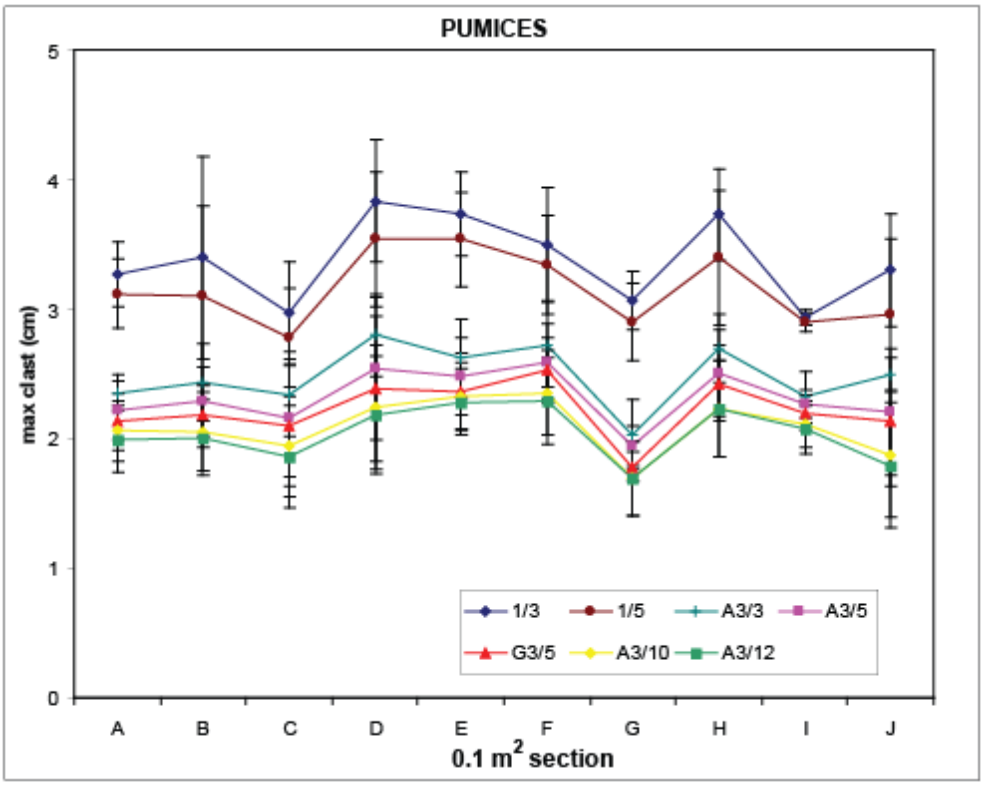

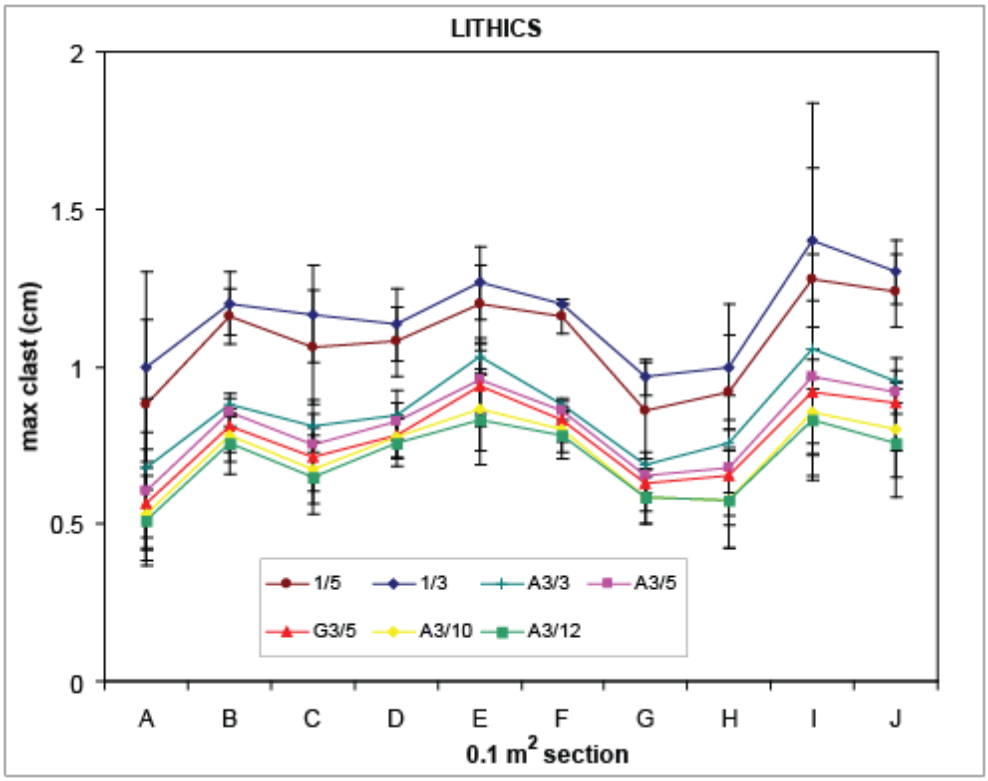

Outcrop 2

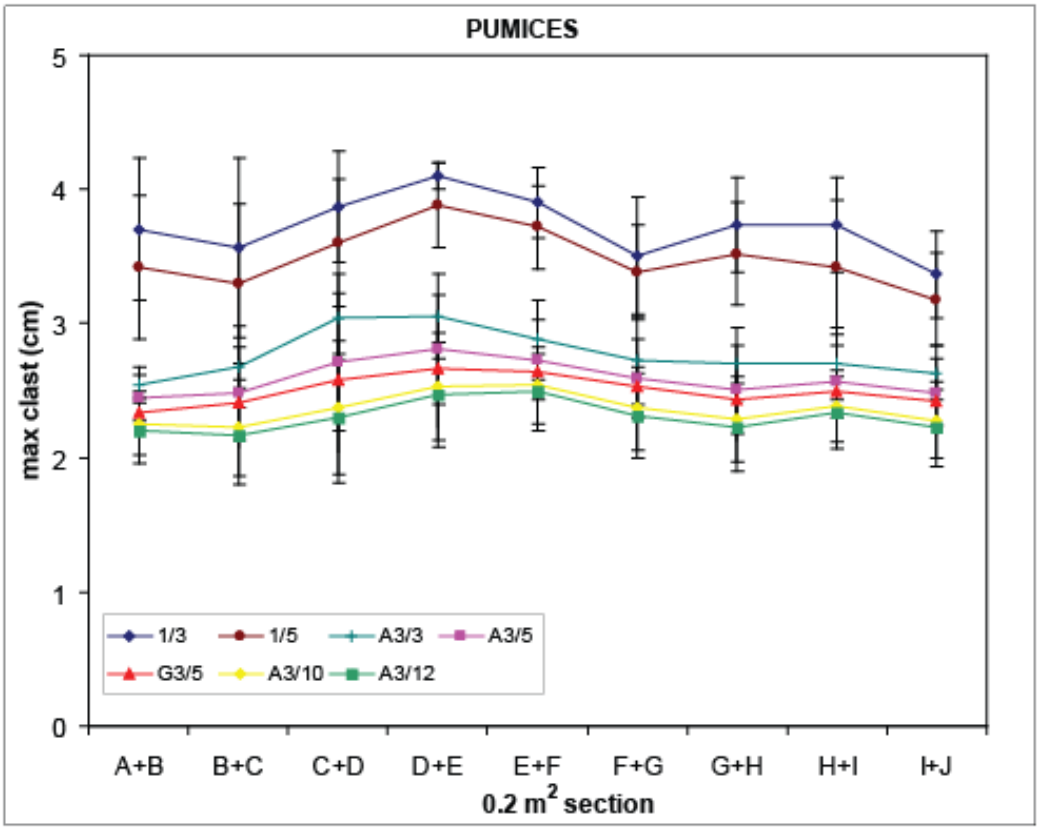
PUMICES
max clast (cm)
0
1
2
3
4
5
A+B
B+C
C+D
D+E
E+F
F+G
G+H
H+I
I+J
0.2 m2 section
1/3
1/5
A3/3
A3/5
G3/5
A3/10
A3/12

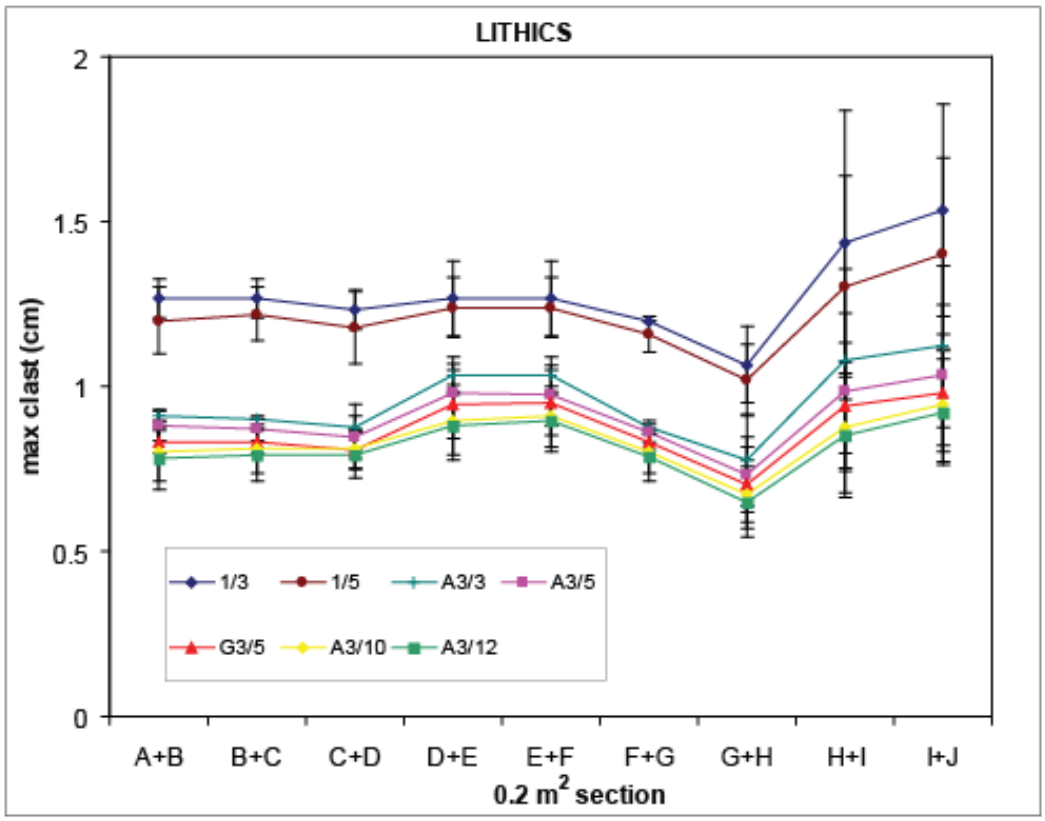
LITHICS
max clast (cm)
0
0.5
1
1.5
2
A+B
B+C
C+D
D+E
E+F
F+G
G+H
H+I
I+J
0.2 m2 section
1/3
1/5
A3/3
A3/5
G3/5
A3/10
A3/12

Outcrop 2

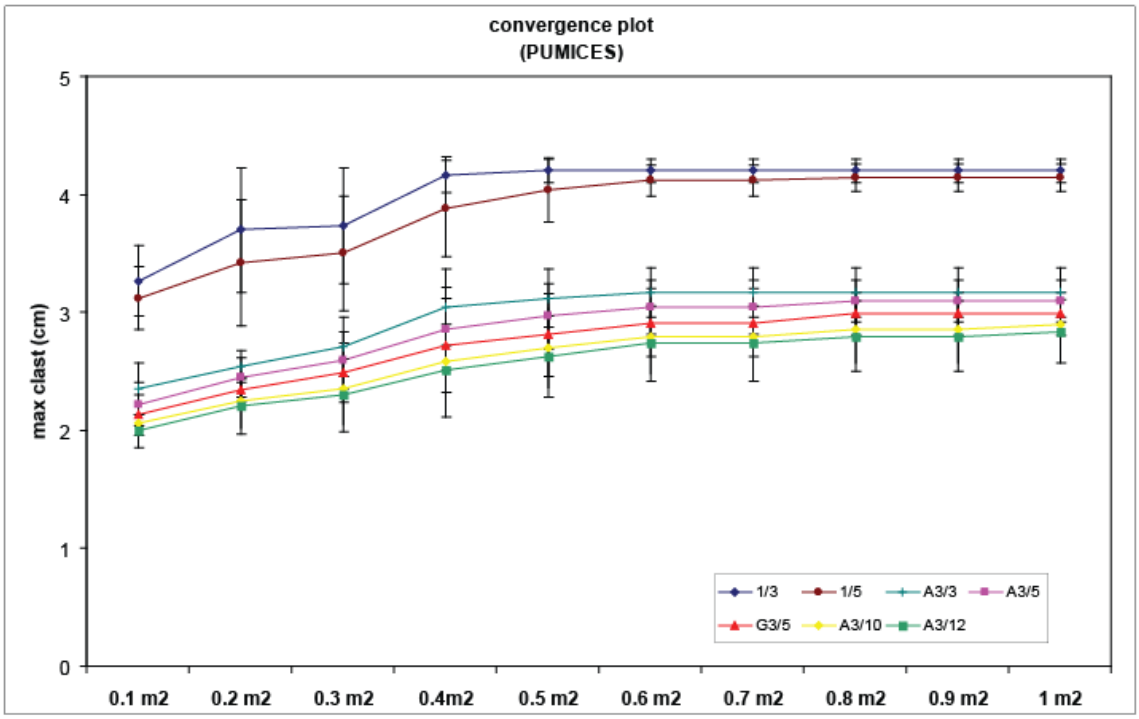
convergence plot
(PUMICES)
max clast (cm)
0
1
2
3
4
5
0.1 m2
0.2 m2
0.3 m2
0.4m2
0.5 m2
0.6 m2
0.7 m2
0.8 m2
0.9 m2
1 m2
1/3
1/5
A3/3
A3/5
G3/5
A3/10
A3/12

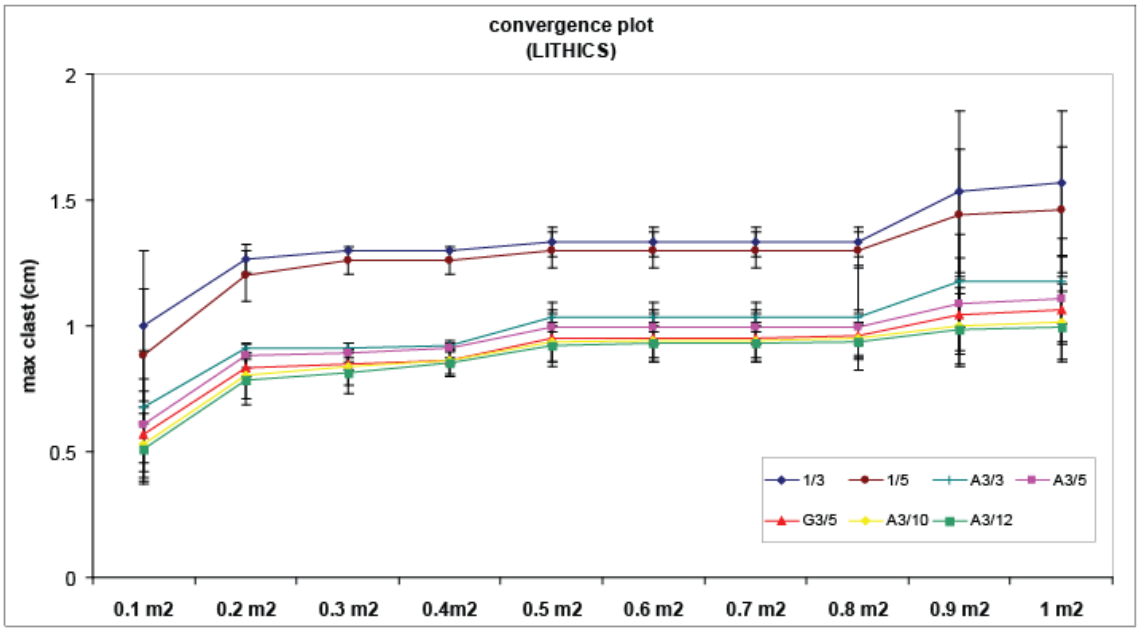
convergence plot
(LITHICS)
max clast (cm)
0
0.5
1
1.5
2
0.1 m2
0.2 m2
0.3 m2
0.4m2
0.5 m2
0.6 m2
0.7 m2
0.8 m2
0.9 m2
1 m2
1/3
1/5
A3/3
A3/5
G3/5
A3/10
A3/12

Outcrop 2

OUTCROP 2 unspecified-area plots plots

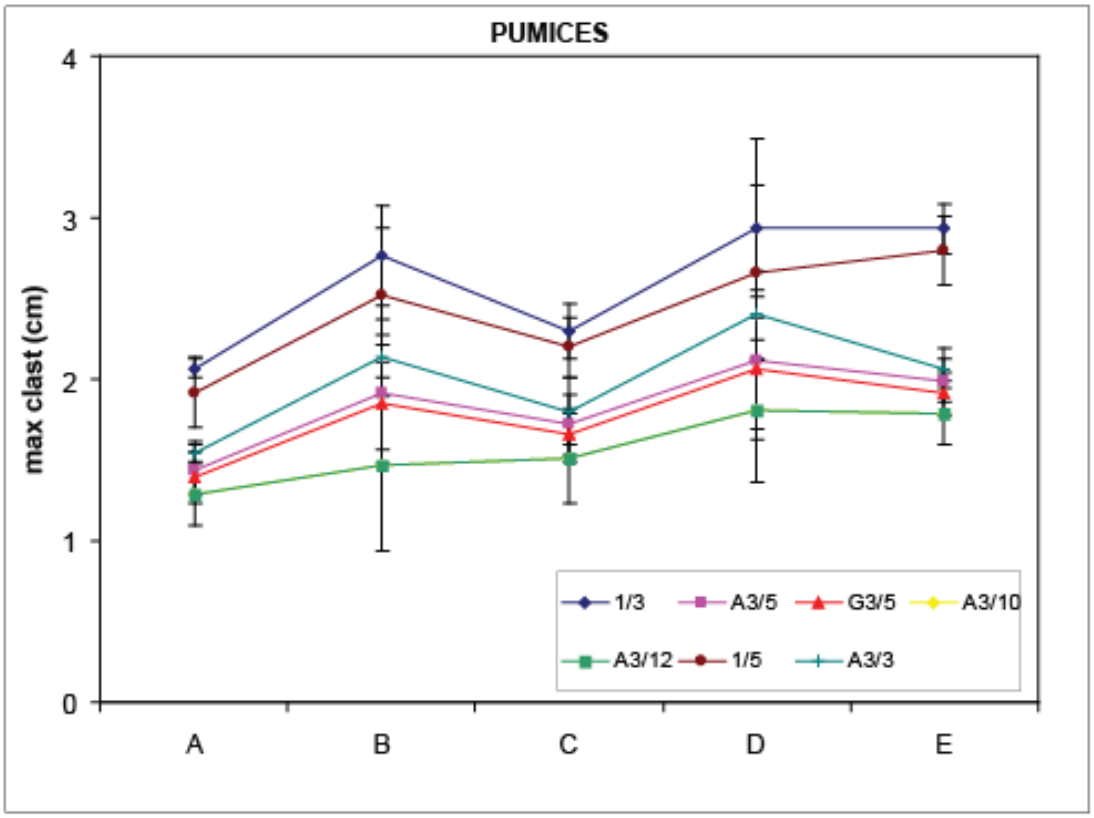

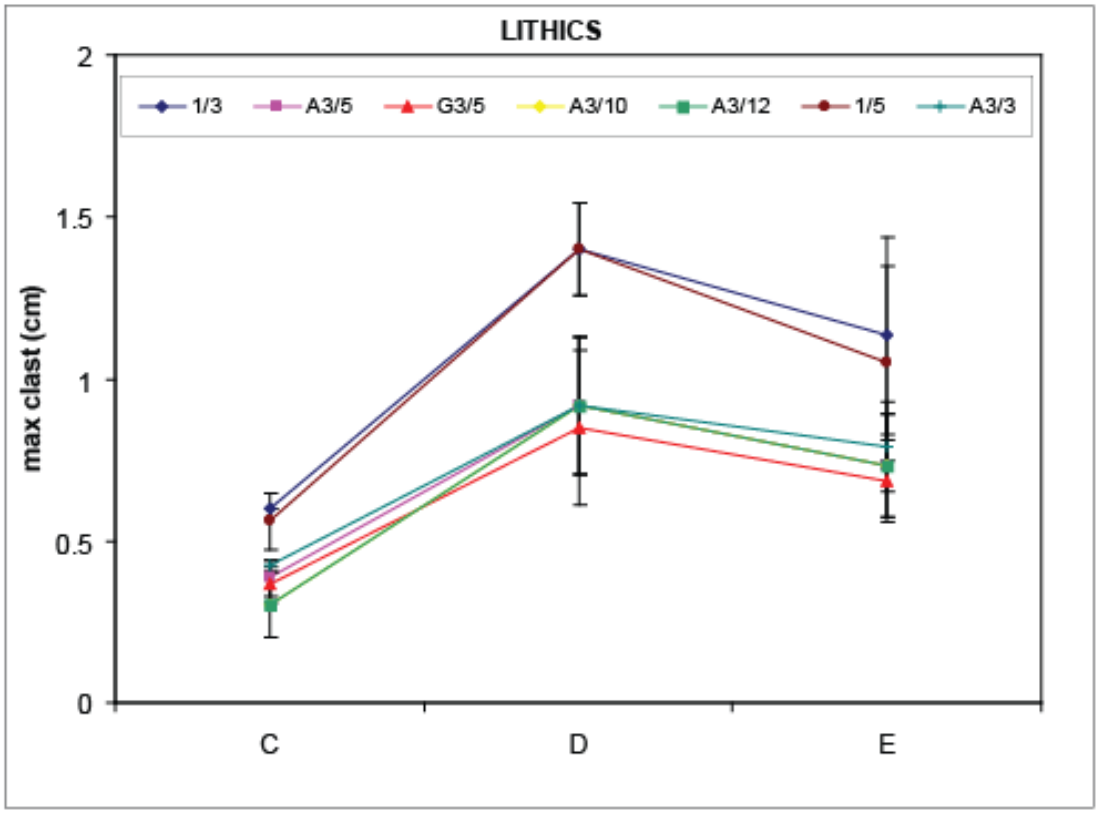

Outcrop 2

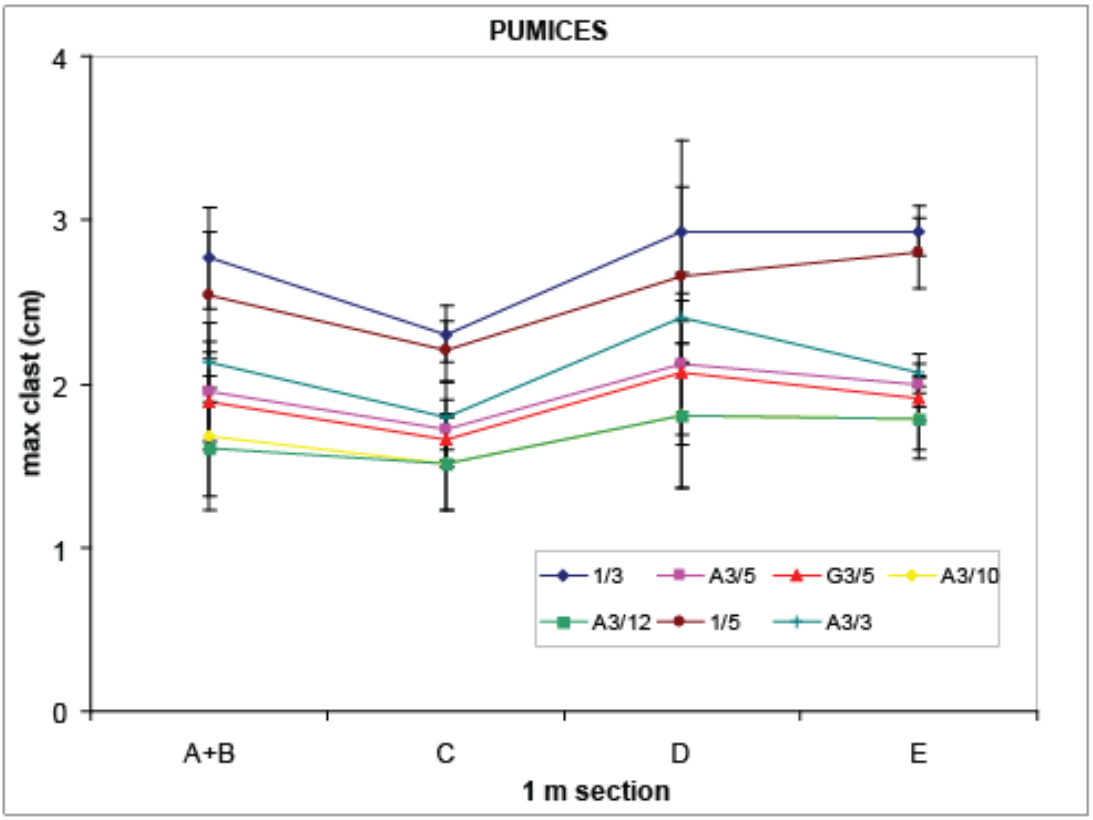
PUMICES
max clast (cm)
4
3
2
1
0
A+B
C
D
E
1 m section
1/3
A3/5
G3/5
A3/10
A3/12
1/5
A3/3

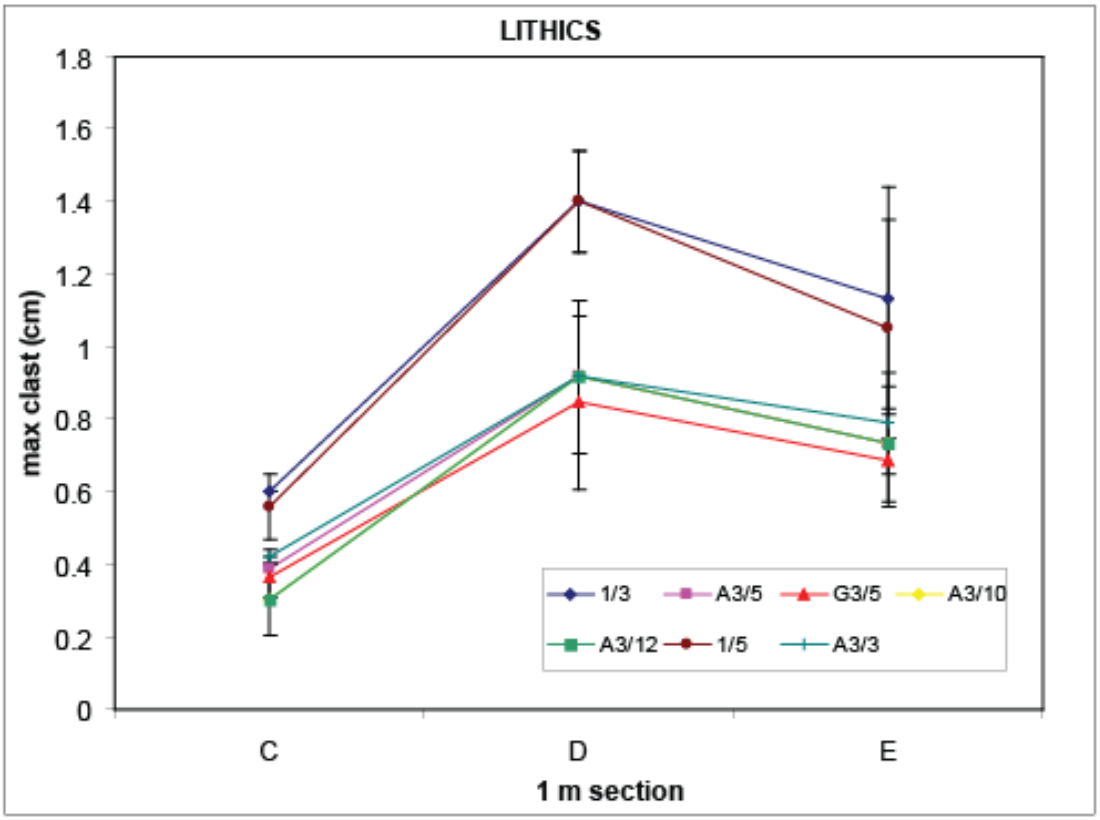
LITHICS
max clast (cm)
1.8
1.6
1.4
1.2
1
0.8
0.6
0.4
0.2
0
C
D
E
1 m section
1/3
A3/5
G3/5
A3/10
A3/12
1/5
A3/3

Outcrop 2

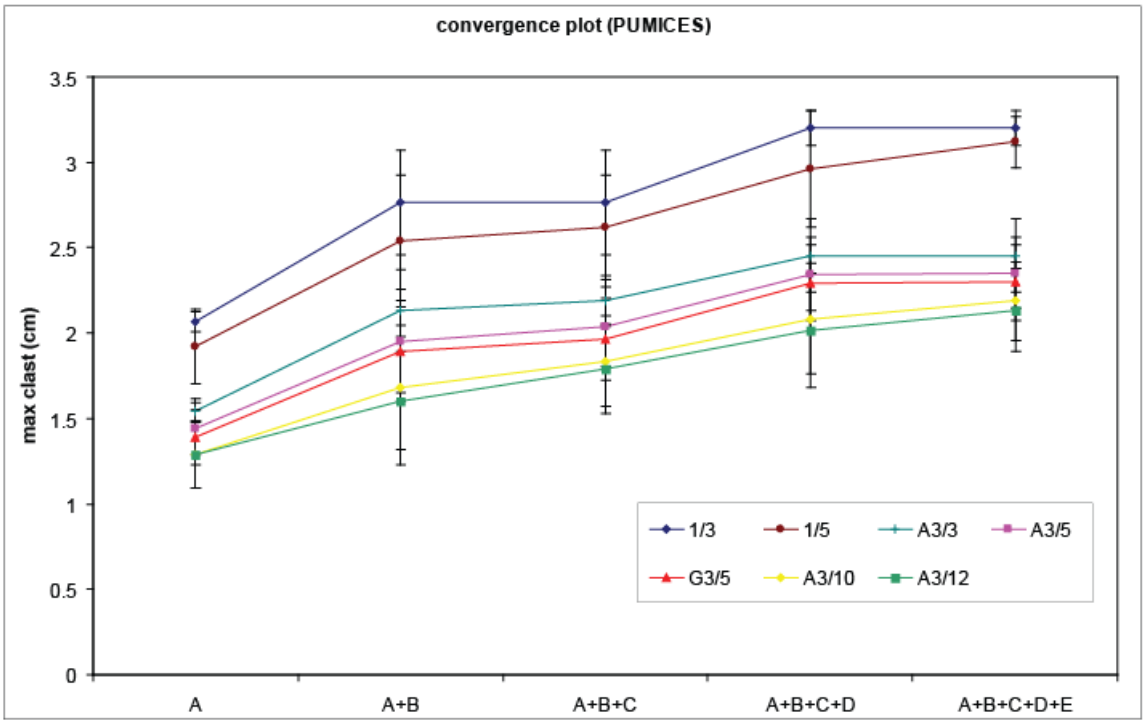
convergence plot (PUMICES)
max clast (cm)
3.5
3
2.5
2
1.5
1
0.5
0
A
A+B
A+B+C
A+B+C+D
A+B+C+D+E
1/3
1/5
A3/3
A3/5
G3/5
A3/10
A3/12

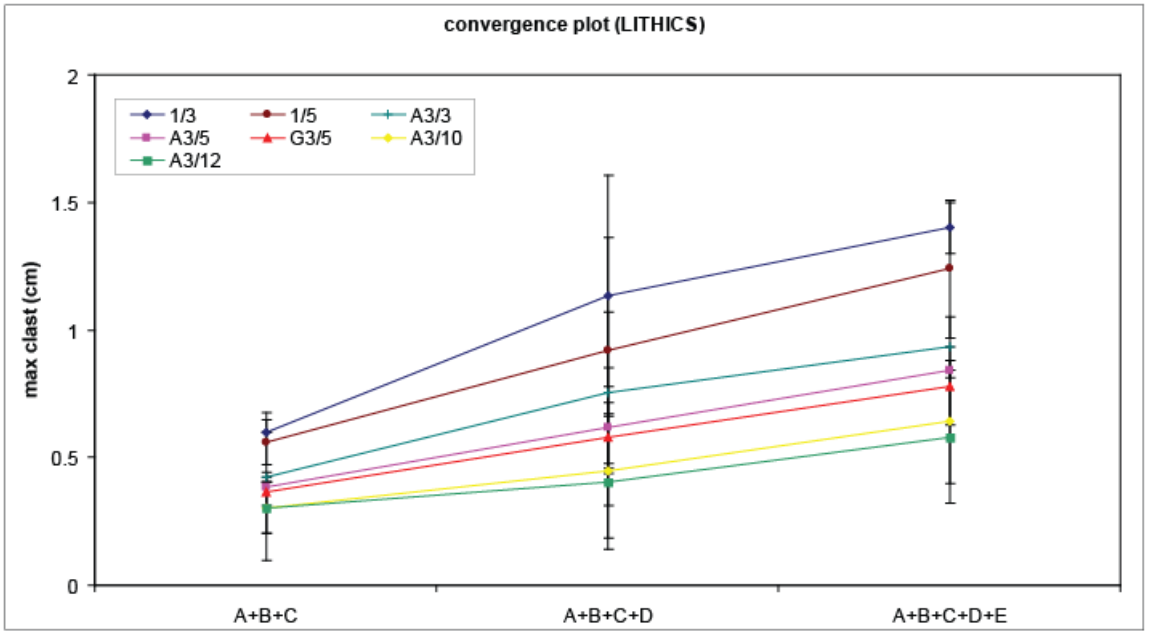
convergence plot (LITHICS)
max clast (cm)
2
1.5
1
0.5
0
A+B+C
A+B+C+D
A+B+C+D+E
1/3
1/5
A3/3
A3/5
G3/5
A3/10
A3/12

Outcrop 2

APPENDIX F

Evaluation of the largest clasts resulting from all possible combinations of investigated areas for both outcrops

The effect of the size of outcrop area analyzed on the evaluation of the maximum clast is investigated by plotting results from all possible combinations of original measurements for both outcrop 1 and 2 and averaging the maximum axis and the 3 axis of a different number of clasts (both arithmetic and geometric mean):

- OUTCROP 1: combinations of 2 areas of 0.1 m^2 (tot=0.2m^2) for lithics and pumices; [10 combinations] A+B, A+C, A+D, …, D+E (3, 5 clasts) (Fig. F1)

- OUTCROP 1: combinations of 2 areas of 0.5 m^2 (tot=1 m^2) for lithics and pumices; [28 combinations] A+B, A+C, A+D, …,G+H (3, 5, 10, 12 clasts) (Fig. F2)

- OUTCROP 2: combinations of 2 areas of 0.1 m^2 (tot=0.2m^2) for lithics and pumices; [45 combinations] A+B, A+C, A+D, … , I+J (3, 5, 10, 12 clasts) (Fig. F3)

- OUTCROP 1: combinations of 3 and 4 areas of 0.5m^2 for lithics and pumices; [56 and 70 combinations] (3, 5, 10, 12 clasts) (Fig. F4)

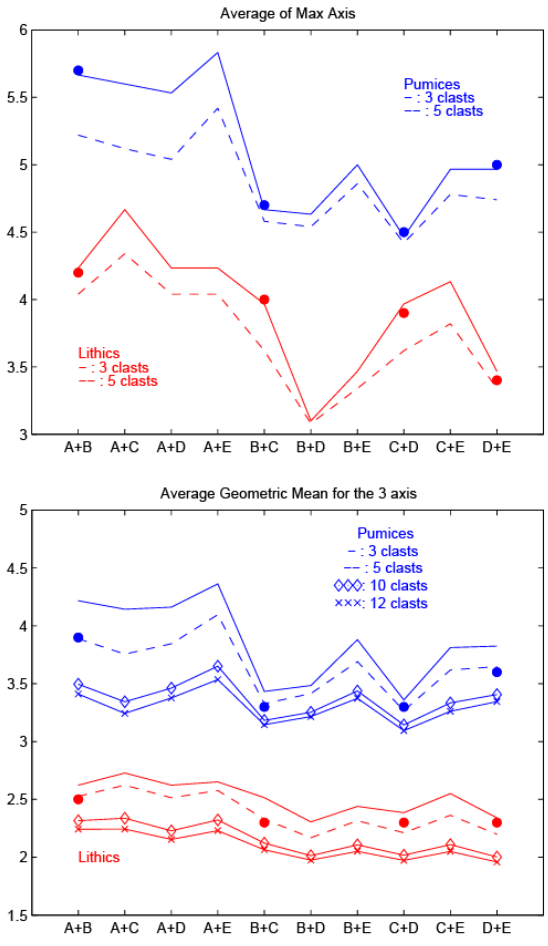

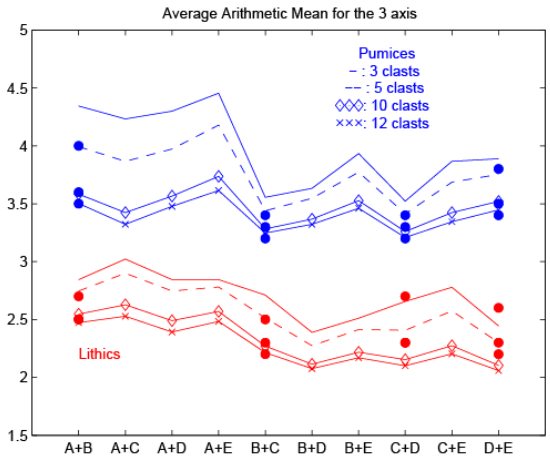

Fig. F1. All possible combinations of deriving areas of 0.2 m^2 from areas of 0.1 m^2 (Outcrop 1; 10 combinations)

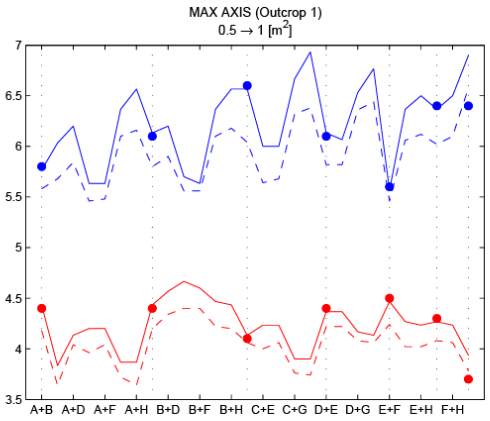

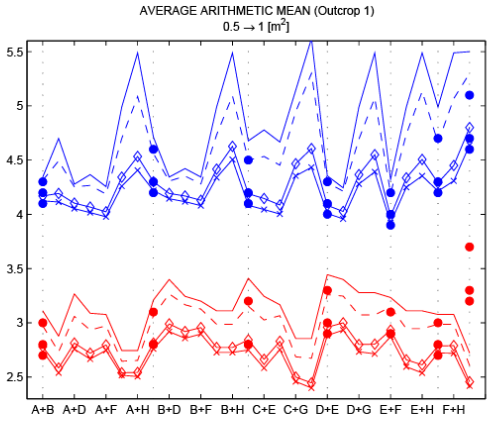

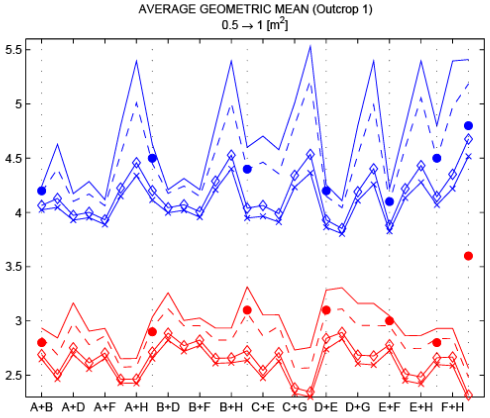

Fig. F2. All possible combinations of deriving areas of 1 m^2 from areas of 0.5 m^2 (Outcrop 1; 28 combinations). Legend in Fig. F1.

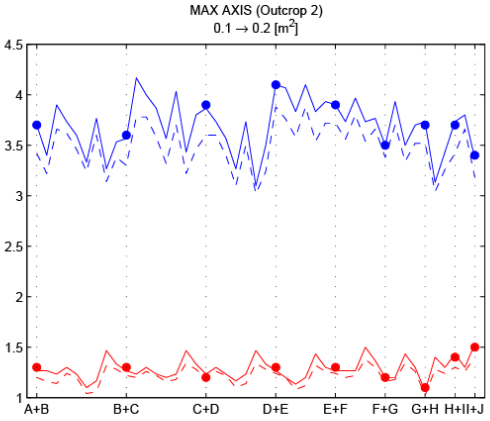

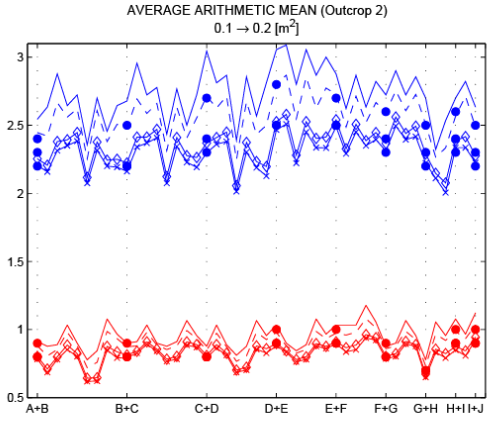

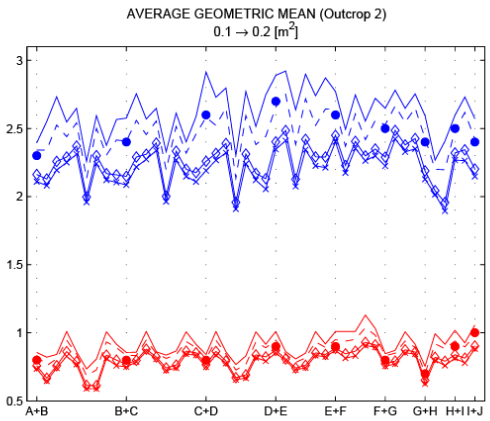

Fig. F3. All possible combinations of deriving areas of 0.1 m^2 from areas of 0.2 m^2 (Outcrop 2; 45 combinations). Legend in Fig. F1.

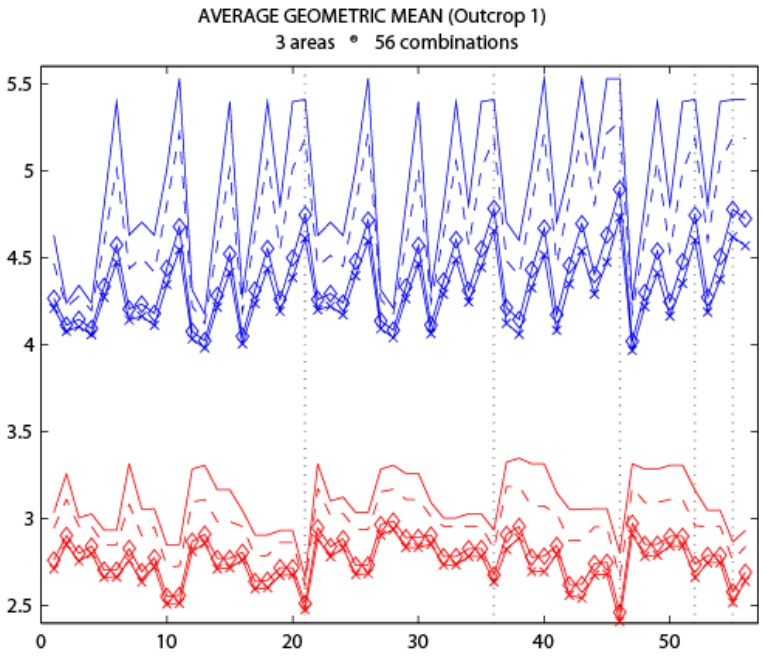

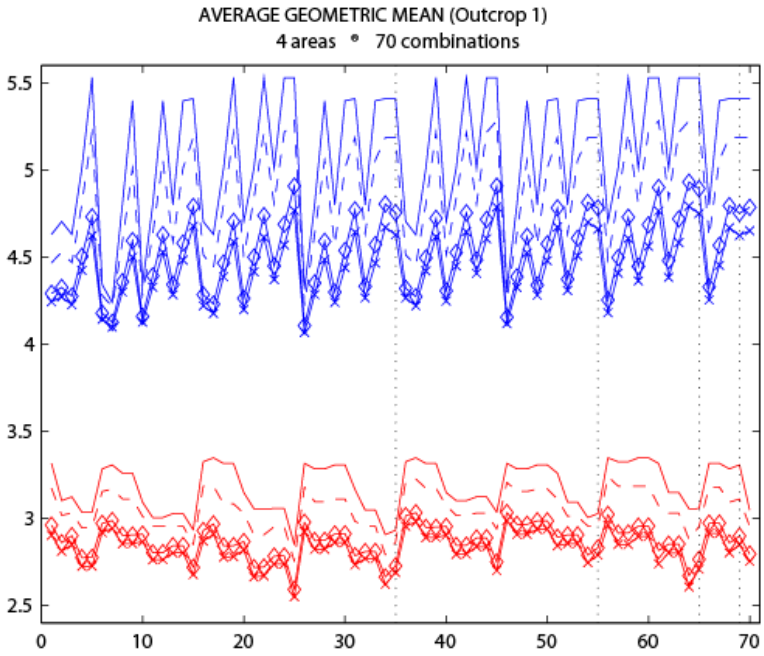

Fig. F4. All possible combinations of 3 and 4 areas of 0.5 m^2 (Outcrop 1; 56 and 70 combinations respectively)

Appendix G

Survivor plots and data

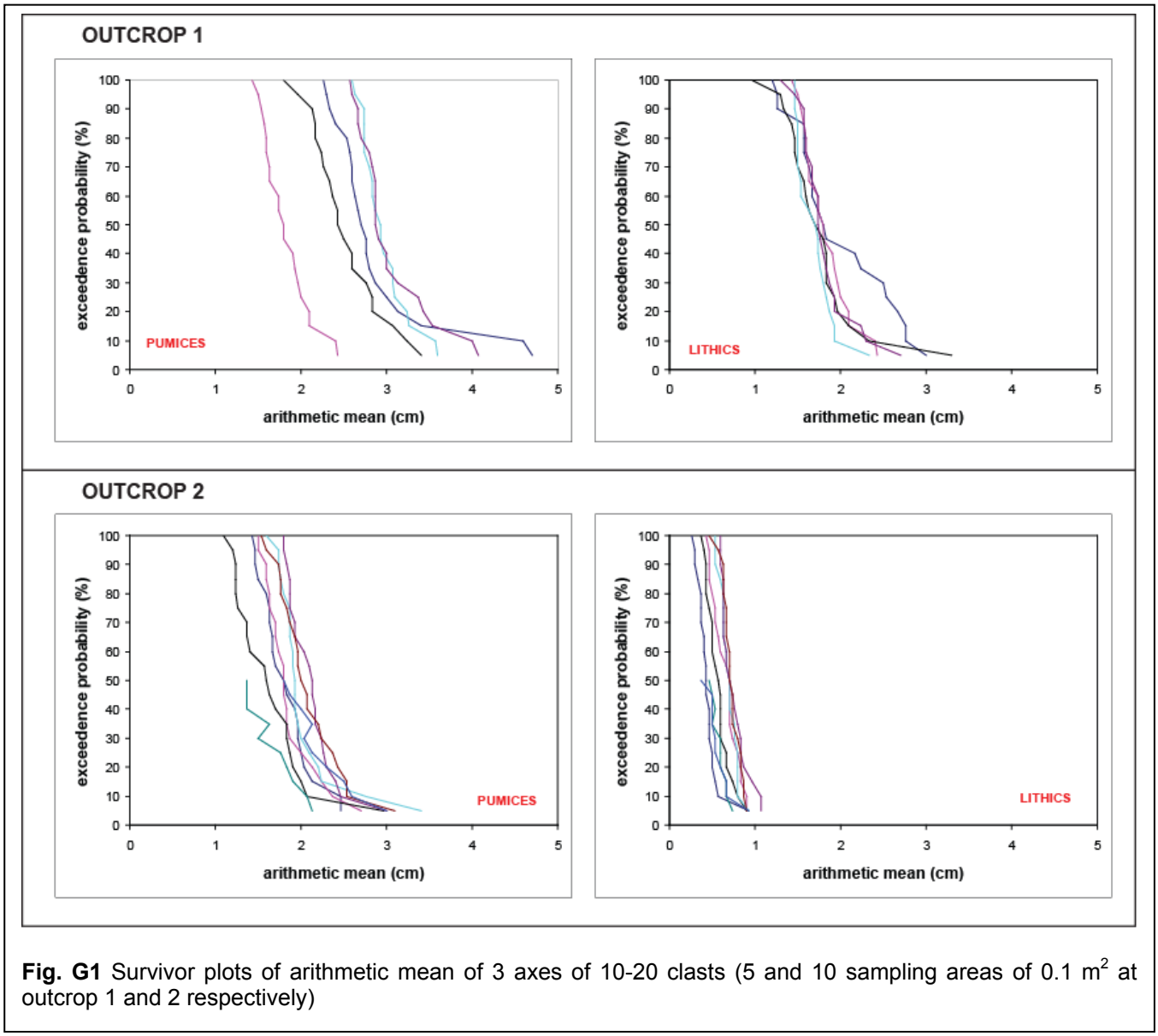

Fig. G1 Survivor plots of arithmetic mean of 3 axes of 10-20 clasts (5 and 10 sampling areas of 0.1 m^2 at outcrop 1 and 2 respectively)

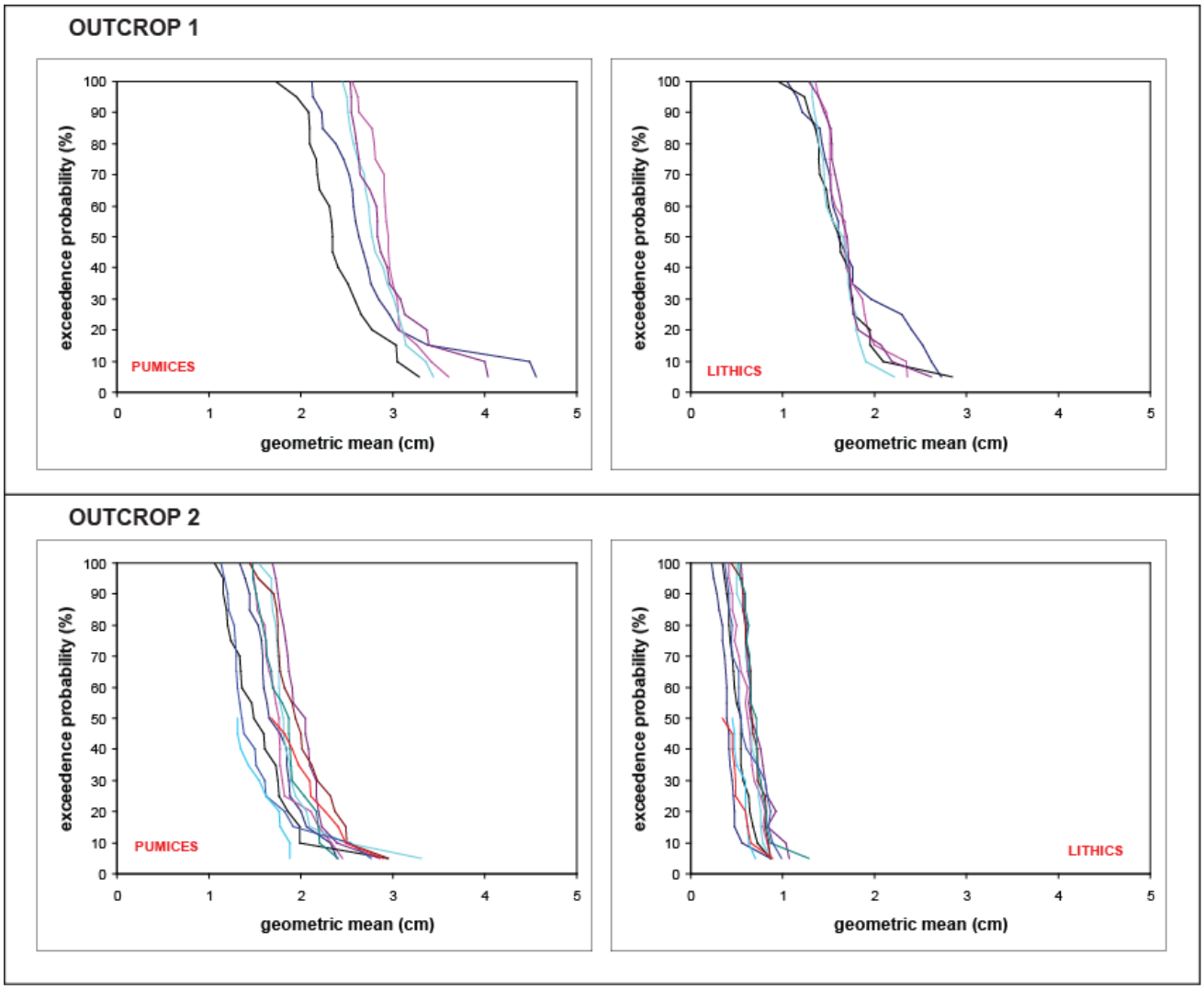

Fig. G2 Survivor plots of geometric mean of 3 axes of 10-20 clasts (5 and 10 sampling areas of 0.1 m^2 at outcrop 1 and 2 respectively)

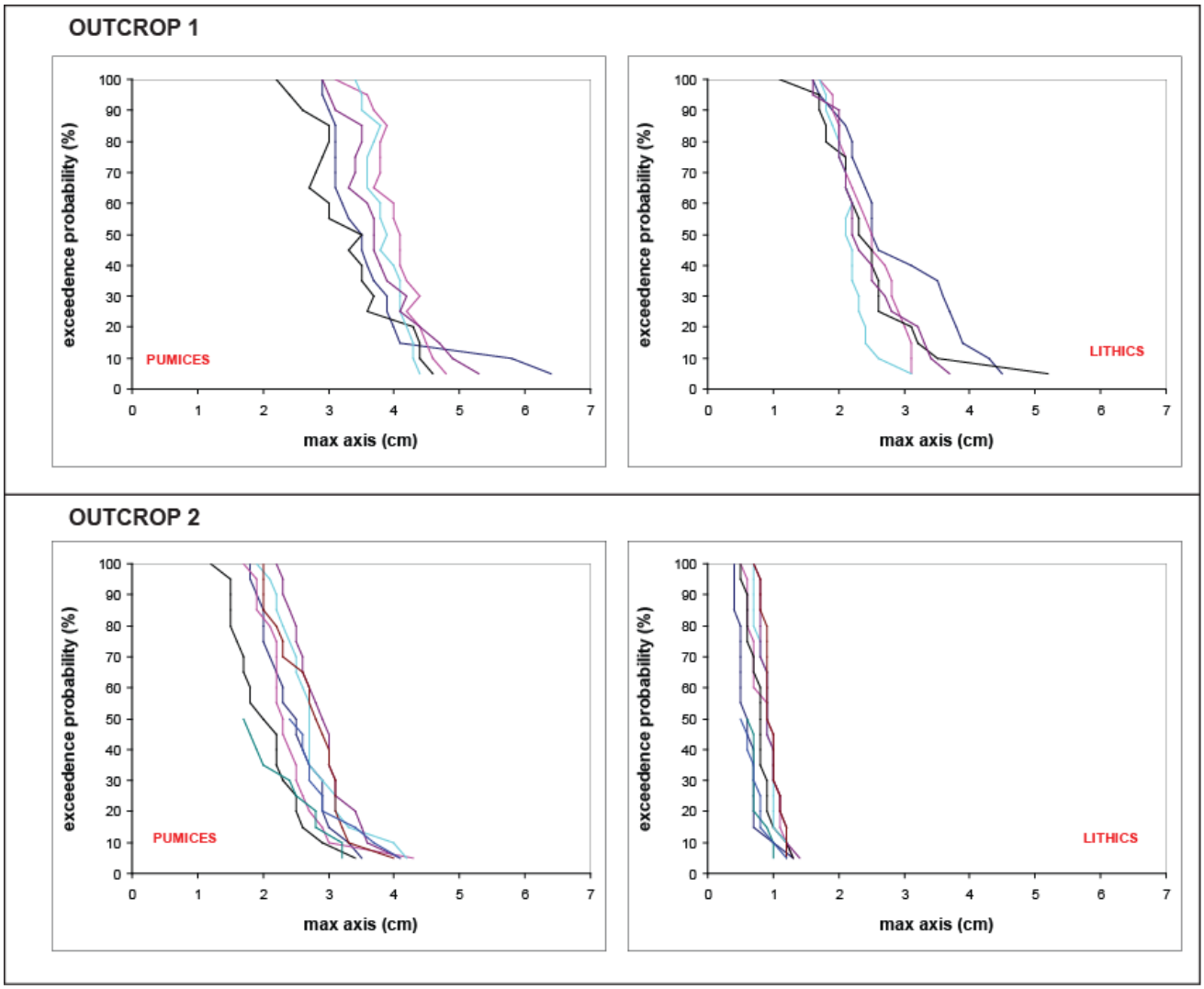

Fig. G3 Survivor plots of max axis of 10-20 clasts (5 and 10 sampling areas of 0.1 m^2 at outcrop 1 and 2 respectively)

A	B	C	D	E	STDEV
2.1	2.6	1.7	2.5	2.5	0.4
2.1	2.6	1.9	2.5	2.5	0.3
2.2	2.6	2.1	2.5	2.6	0.2
2.2	2.8	2.1	2.5	2.6	0.3
2.4	2.8	2.1	2.6	2.6	0.3
2.5	2.8	2.2	2.6	2.6	0.2
2.5	2.9	2.2	2.7	2.6	0.3
2.6	2.9	2.2	2.7	2.7	0.3
2.6	2.9	2.3	2.7	2.8	0.2
2.6	2.9	2.3	2.8	2.8	0.2
2.6	3.0	2.3	2.8	2.8	0.2
2.7	3.0	2.3	2.8	2.9	0.2
2.7	3.0	2.4	2.9	2.9	0.2
2.8	3.0	2.5	2.9	3.0	0.2
2.8	3.1	2.6	3.0	3.1	0.2
3.0	3.1	2.7	3.1	3.1	0.2
3.1	3.1	2.8	3.1	3.4	0.2
3.4	3.3	3.0	3.1	3.4	0.2
4.5	3.4	3.0	3.4	4.0	0.6
4.6	3.6	3.3	3.4	4.0	0.5

Table G1 Outcrop 1, Pumices, Geometric mean

A	B	C	D	E	STDEV
1.0	1.4	1.0	1.3	1.3	0.2
1.2	1.4	1.2	1.3	1.4	0.1
1.2	1.5	1.3	1.4	1.5	0.1
1.4	1.5	1.4	1.4	1.5	0.1
1.4	1.5	1.4	1.4	1.5	0.1
1.5	1.5	1.4	1.4	1.5	0.1
1.5	1.5	1.4	1.5	1.6	0.1
1.5	1.5	1.5	1.5	1.6	0.1
1.5	1.6	1.5	1.5	1.6	0.1
1.6	1.7	1.5	1.5	1.6	0.1
1.6	1.7	1.6	1.7	1.7	0.0
1.7	1.7	1.6	1.7	1.7	0.0
1.8	1.7	1.7	1.7	1.7	0.0
1.8	1.8	1.7	1.7	1.7	0.0
2.0	1.9	1.8	1.7	1.7	0.1
2.3	1.9	1.8	1.8	1.8	0.2
2.4	1.9	2.0	1.8	1.8	0.2
2.5	2.0	2.0	1.8	2.1	0.3
2.6	2.3	2.1	1.9	2.2	0.3
2.7	2.4	2.8	2.2	2.6	0.3

Table G2 Outcrop 1, Lithics, Geometric mean

A	B	C	D	E	STDEV
2.3	1.4	1.8	2.6	2.6	0.5
2.3	1.5	2.0	2.6	2.6	0.5
2.3	1.5	2.1	2.7	2.7	0.5
2.4	1.6	2.2	2.7	2.7	0.5
2.5	1.6	2.2	2.7	2.7	0.5
2.6	1.6	2.2	2.7	2.8	0.5
2.6	1.6	2.3	2.8	2.8	0.5
2.6	1.6	2.3	2.8	2.9	0.5
2.6	1.7	2.4	2.8	2.9	0.5
2.7	1.7	2.4	2.9	2.9	0.5
2.7	1.8	2.4	2.9	2.9	0.5
2.8	1.8	2.5	2.9	2.9	0.5
2.8	1.9	2.6	3.0	3.0	0.4
2.8	1.9	2.6	3.1	3.0	0.5
2.9	2.0	2.8	3.1	3.1	0.5
3.0	2.0	2.8	3.1	3.4	0.5
3.1	2.1	2.8	3.2	3.4	0.5
3.4	2.1	3.1	3.3	3.5	0.6
4.6	2.4	3.2	3.6	4.0	0.8
4.7	2.4	3.4	3.6	4.1	0.8

Table G3 Outcrop 1, Pumices, Arithmetic mean

A	B	C	D	E	STDEV
1.2	1.4	1.0	1.5	1.3	0.2
1.3	1.5	1.3	1.5	1.5	0.1
1.3	1.5	1.3	1.5	1.6	0.1
1.6	1.6	1.4	1.5	1.6	0.1
1.6	1.6	1.5	1.5	1.6	0.1
1.6	1.6	1.5	1.5	1.6	0.1
1.6	1.6	1.5	1.5	1.7	0.1
1.7	1.6	1.6	1.5	1.7	0.1
1.7	1.7	1.6	1.5	1.7	0.1
1.7	1.7	1.6	1.6	1.7	0.1
1.8	1.8	1.7	1.7	1.7	0.1
1.8	1.8	1.8	1.7	1.8	0.0
2.2	1.9	1.8	1.7	1.8	0.2
2.2	1.9	1.8	1.8	1.8	0.2
2.5	2.0	1.8	1.8	1.9	0.3
2.5	2.0	1.9	1.8	1.9	0.3
2.7	2.1	2.0	1.9	1.9	0.3
2.8	2.1	2.1	1.9	2.2	0.3
2.8	2.4	2.3	1.9	2.3	0.3
3.0	2.4	3.3	2.3	2.7	0.4

Table G4 Outcrop 1, Lithics, Arithmetic mean

A	B	C	D	E	STDEV
2.9	3.1	2.2	3.4	2.9	0.4
2.9	3.6	2.4	3.5	3.0	0.5
3.0	3.7	2.6	3.5	3.1	0.4
3.1	3.9	3.0	3.8	3.5	0.4
3.1	3.8	3.0	3.7	3.5	0.4
3.1	3.8	2.9	3.6	3.4	0.4
3.1	3.8	2.8	3.6	3.4	0.4
3.1	3.7	2.7	3.6	3.3	0.4
3.2	4.0	3.0	3.8	3.6	0.4
3.3	4.0	3.0	3.8	3.7	0.4
3.5	4.1	3.5	3.9	3.7	0.3
3.5	4.1	3.3	3.8	3.7	0.3
3.6	4.1	3.5	4.0	3.8	0.3
3.7	4.2	3.5	4.1	3.9	0.3
3.9	4.4	3.7	4.1	4.2	0.3
3.9	4.2	3.6	4.1	4.1	0.2
4.0	4.4	4.3	4.2	4.4	0.2
4.1	4.5	4.4	4.3	4.7	0.2
5.8	4.6	4.4	4.3	4.9	0.6
6.4	4.8	4.6	4.4	5.3	0.8

Table G5 Outcrop 1, Pumices, Max Axis

A	B	C	D	E	STDEV
1.6	1.7	1.1	1.7	1.6	0.3
1.7	1.9	1.7	1.8	1.6	0.1
1.9	1.9	1.7	1.8	2.0	0.1
2.1	2.0	1.8	1.9	2.0	0.1
2.2	2.1	1.8	2.0	2.0	0.1
2.2	2.0	2.1	2.0	2.0	0.1
2.3	2.1	2.1	2.1	2.1	0.1
2.4	2.2	2.1	2.1	2.1	0.1
2.5	2.5	2.2	2.2	2.2	0.1
2.5	2.4	2.3	2.1	2.2	0.2
2.5	2.3	2.3	2.1	2.2	0.2
2.6	2.5	2.5	2.2	2.3	0.2
3.1	2.7	2.5	2.2	2.5	0.3
3.5	2.8	2.6	2.2	2.5	0.5
3.6	2.8	2.6	2.3	2.7	0.5
3.7	2.9	2.6	2.3	2.8	0.5
3.8	3.0	3.1	2.4	3.2	0.5
3.9	3.1	3.2	2.4	3.3	0.5
4.3	3.1	3.5	2.6	3.4	0.6
4.5	3.1	5.2	3.1	3.7	0.9

Table G6 Outcrop 1, Lithics, Max Axis

A	B	C	D	E	F	G	H	I	J	STDEV
1.3	1.5	1.1	1.5	1.7	1.4			1.5	1.1	0.2
1.4	1.5	1.2	1.7	1.7	1.5			1.5	1.2	0.2
1.4	1.5	1.2	1.7	1.8	1.7			1.5	1.2	0.2
1.4	1.5	1.2	1.7	1.8	1.7			1.5	1.2	0.2
1.5	1.6	1.2	1.7	1.8	1.8			1.6	1.3	0.2
1.6	1.6	1.2	1.7	1.8	1.8			1.6	1.3	0.2
1.6	1.6	1.3	1.7	1.9	1.8			1.6	1.3	0.2
1.6	1.7	1.3	1.8	1.9	1.8			1.7	1.3	0.2
1.6	1.7	1.4	1.8	1.9	1.8			1.7	1.3	0.2
1.6	1.7	1.5	1.8	1.9	1.9			1.8	1.3	0.2
1.7	1.8	1.5	1.8	2.0	1.9	1.3	1.7	1.9	1.4	0.2
1.8	1.8	1.6	1.8	2.0	2.0	1.3	1.8	1.9	1.4	0.2
1.8	1.8	1.6	1.8	2.1	2.0	1.3	1.9	1.9	1.5	0.2
1.8	1.8	1.7	1.9	2.1	2.1	1.4	2.0	1.9	1.5	0.2
1.9	1.8	1.8	1.9	2.2	2.2	1.5	2.1	1.9	1.6	0.2
1.9	1.8	1.8	1.9	2.2	2.3	1.6	2.1	2.0	1.6	0.2
2.0	2.1	1.9	2.1	2.2	2.4	1.8	2.3	2.2	1.8	0.2
2.1	2.2	2.0	2.1	2.2	2.5	1.8	2.4	2.2	1.9	0.2
2.3	2.3	2.0	2.5	2.4	2.5	1.9	2.5	2.2	2.5	0.2
2.4	2.5	2.9	3.3	2.9	3.0	1.9	2.9	2.4	2.8	0.4

Table G7 Outcrop 2, Pumices, Geometric mean

A	B	C	D	E	F	G	H	I	J	STDEV
0.2	0.4	0.3	0.5	0.6	0.4			0.5	0.4	0.1
0.3	0.4	0.4	0.5	0.6	0.5			0.5	0.4	0.1
0.3	0.4	0.4	0.5	0.6	0.6			0.6	0.4	0.1
0.3	0.4	0.4	0.6	0.6	0.6			0.6	0.4	0.1
0.3	0.5	0.4	0.6	0.6	0.6			0.6	0.5	0.1
0.3	0.5	0.4	0.6	0.6	0.6			0.6	0.4	0.1
0.4	0.5	0.5	0.6	0.6	0.6			0.6	0.5	0.1
0.4	0.6	0.5	0.6	0.6	0.7			0.6	0.5	0.1
0.4	0.6	0.5	0.7	0.7	0.7			0.7	0.5	0.1
0.4	0.6	0.5	0.7	0.6	0.7			0.7	0.5	0.1
0.4	0.6	0.5	0.7	0.7	0.7	0.4	0.3	0.7	0.6	0.1
0.4	0.6	0.5	0.7	0.7	0.7	0.5	0.4	0.7	0.6	0.1
0.4	0.7	0.6	0.7	0.8	0.7	0.5	0.5	0.7	0.6	0.1
0.4	0.7	0.6	0.7	0.8	0.7	0.5	0.5	0.7	0.7	0.1
0.4	0.7	0.6	0.7	0.8	0.7	0.6	0.5	0.8	0.8	0.1
0.5	0.8	0.6	0.7	0.8	0.8	0.6	0.5	0.8	0.8	0.1
0.5	0.8	0.6	0.8	0.9	0.8	0.6	0.6	0.8	0.9	0.1
0.5	0.8	0.7	0.8	0.8	0.8	0.6	0.6	0.8	0.8	0.1
0.6	0.8	0.7	0.8	1.0	0.9	0.6	0.7	0.9	0.9	0.1
0.9	0.9	0.9	0.9	1.1	0.9	0.7	0.9	1.3	1.0	0.2

Table G8 Outcrop 2, Lithics, Geometric mean

A	B	C	D	E	F	G	H	I	J	STDEV
1.4	1.5	1.1	1.6	1.8	1.5			1.6	1.2	0.2
1.5	1.5	1.2	1.7	1.8	1.6			1.6	1.2	0.2
1.5	1.6	1.2	1.7	1.8	1.7			1.6	1.3	0.2
1.5	1.6	1.2	1.8	1.9	1.8			1.6	1.3	0.2
1.6	1.6	1.2	1.8	1.9	1.8			1.7	1.3	0.2
1.6	1.6	1.3	1.9	1.9	1.8			1.7	1.3	0.2
1.6	1.7	1.4	1.9	1.9	1.9			1.7	1.4	0.2
1.7	1.7	1.4	1.9	1.9	1.9			1.8	1.4	0.2
1.7	1.7	1.4	1.9	2.0	2.0			1.8	1.4	0.2
1.7	1.8	1.6	1.9	2.1	2.0			1.9	1.4	0.2
1.8	1.8	1.6	1.9	2.1	2.0	1.4	1.8	1.9	1.4	0.2
1.8	1.8	1.6	1.9	2.1	2.1	1.4	1.9	2.0	1.5	0.2
1.9	1.8	1.7	1.9	2.2	2.1	1.4	2.0	2.0	1.5	0.2
2.0	1.8	1.8	2.0	2.2	2.2	1.6	2.1	2.0	1.5	0.2
2.0	1.9	1.8	2.0	2.2	2.2	1.5	2.0	2.0	1.7	0.2
2.0	2.0	1.9	2.1	2.3	2.4	1.8	2.1	2.1	1.7	0.2
2.0	2.1	1.9	2.2	2.3	2.4	1.8	2.3	2.2	1.9	0.2
2.1	2.2	2.0	2.2	2.4	2.5	1.9	2.5	2.2	2.0	0.2
2.5	2.4	2.1	2.8	2.5	2.5	2.1	2.6	2.3	2.6	0.2
2.5	2.7	3.0	3.4	3.0	3.1	2.1	3.0	2.4	2.8	0.4

Table G9 Outcrop 2, Pumices, Arithmetic mean

A	B	C	D	E	F	G	H	I	J	STDEV
0.3	0.4	0.4	0.5	0.6	0.5			0.6	0.4	0.1
0.3	0.5	0.4	0.5	0.6	0.6			0.6	0.4	0.1
0.3	0.5	0.4	0.5	0.6	0.6			0.6	0.4	0.1
0.3	0.5	0.4	0.6	0.6	0.6			0.6	0.4	0.1
0.4	0.5	0.4	0.6	0.6	0.6			0.6	0.5	0.1
0.4	0.5	0.5	0.6	0.6	0.7			0.7	0.5	0.1
0.4	0.5	0.5	0.6	0.6	0.7			0.7	0.5	0.1
0.4	0.6	0.5	0.6	0.6	0.7			0.7	0.5	0.1
0.4	0.6	0.5	0.7	0.7	0.7			0.7	0.5	0.1
0.4	0.7	0.5	0.7	0.7	0.7			0.7	0.5	0.1
0.4	0.7	0.6	0.7	0.7	0.7	0.5	0.4	0.7	0.6	0.1
0.4	0.7	0.6	0.7	0.7	0.7	0.5	0.5	0.7	0.6	0.1
0.5	0.7	0.6	0.7	0.8	0.7	0.5	0.5	0.7	0.6	0.1
0.5	0.7	0.6	0.8	0.8	0.7	0.5	0.5	0.7	0.7	0.1
0.5	0.7	0.6	0.8	0.8	0.8	0.6	0.5	0.8	0.8	0.1
0.5	0.8	0.7	0.8	0.8	0.8	0.6	0.5	0.8	0.9	0.1
0.5	0.8	0.7	0.8	0.9	0.8	0.6	0.6	0.8	0.9	0.1
0.5	0.8	0.7	0.8	1.0	0.9	0.7	0.7	0.9	0.9	0.1
0.6	0.9	0.8	0.8	1.1	0.9	0.7	0.7	0.9	0.9	0.1
0.9	0.9	0.9	0.9	1.1	0.9	0.7	0.9	1.4	1.0	0.2

Table G10 Outcrop 2, Lithics, Arithmetic mean

A	B	C	D	E	F	G	H	I	J	STDEV
1.8	1.7	1.2	1.9	2.2	2			1.9	1.4	0.3
1.8	1.9	1.5	2.1	2.3	2			1.9	1.6	0.3
1.9	1.9	1.5	2.2	2.3	2			2	1.7	0.3
2	1.9	1.5	2.2	2.4	2			2.1	1.7	0.3
2	2.1	1.5	2.3	2.5	2.2			2.1	1.8	0.3
2	2.2	1.6	2.4	2.5	2.3			2.1	1.8	0.3
2.1	2.2	1.7	2.5	2.6	2.3			2.2	1.8	0.3
2.2	2.2	1.7	2.5	2.6	2.6			2.2	1.9	0.3
2.3	2.2	1.8	2.6	2.7	2.7			2.3	1.9	0.3
2.3	2.2	1.8	2.7	2.8	2.7			2.4	1.9	0.4
2.5	2.3	2	2.7	2.9	2.8	1.7	2.4	2.5	2	0.4
2.5	2.3	2.2	2.7	3	2.9	1.8	2.6	2.5	2	0.4
2.6	2.4	2.2	2.7	3	3	1.9	2.6	2.6	2	0.4
2.7	2.5	2.2	2.7	3	3	2	2.7	2.6	2.2	0.3
2.9	2.5	2.3	2.9	3.1	3.1	2.4	2.7	2.6	2.2	0.3
2.9	2.6	2.5	3.1	3.1	3.1	2.5	2.9	2.8	2.2	0.3
2.9	2.7	2.5	3.1	3.4	3.1	2.8	2.9	2.9	2.7	0.3
3	2.9	2.6	3.3	3.5	3.2	2.8	3.4	2.9	2.8	0.3
3.3	3	2.9	4	3.6	3.3	3.2	3.7	2.9	3.5	0.4
3.5	4.3	3.4	4.2	4.1	4	3.2	4.1	3	3.6	0.5

Table G11 Outcrop 2, Pumices, Max axis

A	B	C	D	E	F	G	H	I	J	STDEV
0.4	0.5	0.5	0.7	0.7	0.7			0.8	0.5	0.1
0.4	0.6	0.5	0.7	0.8	0.8			0.9	0.6	0.2
0.4	0.6	0.6	0.7	0.8	0.8			0.7	0.6	0.1
0.4	0.6	0.6	0.7	0.8	0.8			0.7	0.6	0.1
0.5	0.6	0.6	0.7	0.8	0.9			0.9	0.6	0.2
0.5	0.7	0.6	0.8	0.8	0.9			0.9	0.6	0.1
0.5	0.7	0.7	0.8	0.8	0.9			0.9	0.6	0.1
0.5	0.7	0.7	0.9	0.9	0.9			0.9	0.7	0.1
0.5	0.7	0.8	0.9	0.9	0.9			0.9	0.7	0.1
0.5	0.9	0.8	0.9	0.9	0.9			0.9	0.8	0.1
0.6	0.9	0.8	0.9	0.9	0.9	0.6	0.5	0.9	0.8	0.2
0.6	1.0	0.8	0.9	0.9	1.0	0.7	0.6	0.9	0.8	0.1
0.7	1.0	0.8	1.0	1.0	1.0	0.7	0.6	1.1	0.9	0.2
0.7	1.0	0.8	1.0	1.0	1.0	0.7	0.7	1.1	1.0	0.2
0.7	1.0	0.9	1.0	1.0	1.0	0.7	0.7	1.1	1.1	0.2
0.7	1.1	0.9	1.0	1.1	1.1	0.7	0.8	1.0	1.1	0.2
0.7	1.1	0.9	1.0	1.1	1.1	0.7	0.8	1.0	1.2	0.2
0.7	1.1	1.0	1.0	1.2	1.2	0.9	0.8	1.0	1.2	0.2
1.0	1.2	1.2	1.2	1.2	1.2	1.0	1.0	1.2	1.3	0.1
1.3	1.3	1.3	1.2	1.4	1.2	1.0	1.2	1.9	1.4	0.2

Table G12 Outcrop 2, Lithics, Max axis

APPENDIX H

Percentage difference amongst different averaging techniques (data)

Values in yellow cells are the actual clast average (cm) derived from:
1/3 = arithmetic average of the maximum axis of the 3 largest clasts
1/5 = arithmetic average of the maximum axis of the 5 largest clasts
A3/3 = arithmetic average of the arithmetic average of the 3 axis of the 3 largest clasts
A3/5 = arithmetic average of the arithmetic average of the 3 axis of the 5 largest clasts
A3/10 = arithmetic average of the arithmetic average of the 3 axis of the 10 largest clasts
A3/12 = arithmetic average of the arithmetic average of the 3 axis of the 12 largest clasts
G3/5 = arithmetic average of the geometric mean of the 3 axis of the 5 largest clasts (i.e. diameter of the equivalent sphere)

Values in white cells are the percentage difference amongst different techniques (considering the formula: $\frac{value2 - value1}{value1} \times 100$)

PUMICES	1/3	1/5	A3/3	A3/5	G3/5	A3/10	A3/12
1/3	5.4	12.5	28.6	42.1	45.9	63.6	68.8
1/5	-11.1	4.8	14.3	26.3	29.7	45.5	50.0
A3/3	-22.2	-12.5	4.2	10.5	13.5	27.3	31.3
A3/5	-29.6	-20.8	-9.5	3.8	2.7	15.2	18.8
G3/5	-31.5	-22.9	-11.9	-2.6	3.7	12.1	15.6
A3/10	-38.9	-31.3	-21.4	-13.2	-10.8	3.3	3.1
A3/12	-40.7	-33.3	-23.8	-15.8	-13.5	-3.0	3.2

Table H1. Outcrop 1, Area A (0.1 m^2) (Pumices)

LITHICS	1/3	1/5	A3/3	A3/5	G3/5	A3/10	A3/12
1/3	4.2	5.0	50.0	55.6	68.0	75.0	82.6
1/5	-4.8	4.0	42.9	48.1	60.0	66.7	73.9
A3/3	-33.3	-30.0	2.8	3.7	12.0	16.7	21.7
A3/5	-35.7	-32.5	-3.6	2.7	8.0	12.5	17.4
G3/5	-40.5	-37.5	-10.7	-7.4	2.5	4.2	8.7
A3/10	-42.9	-40.0	-14.3	-11.1	-4.0	2.4	4.3
A3/12	-45.2	-42.5	-17.9	-14.8	-8.0	-4.2	2.3

Table H2. Outcrop 1, Area A (0.1 m^2) (Lithics)

PUMICES	1/3	1/5	A3/3	A3/5	G3/5	A3/10	A3/12
1/3	5.7	9.6	32.6	42.5	46.2	58.3	62.9
1/5	-8.8	5.2	20.9	30.0	33.3	44.4	48.6
A3/3	-24.6	-17.3	4.3	7.5	10.3	19.4	22.9
A3/5	-29.8	-23.1	-7.0	4.0	2.6	11.1	14.3
G3/5	-31.6	-25.0	-9.3	-2.5	3.9	8.3	11.4
A3/10	-36.8	-30.8	-16.3	-10.0	-7.7	3.6	2.9
A3/12	-38.6	-32.7	-18.6	-12.5	-10.3	-2.8	3.5

Table H3. Outcrop 1, Area A+B (0.2 m^2) (Pumices)

LITHICS	1/3	1/5	A3/3	A3/5	G3/5	A3/10	A3/12
1/3	4.2	5.0	50.0	55.6	68.0	68.0	68.0
1/5	-4.8	4.0	42.9	48.1	60.0	60.0	60.0
A3/3	-33.3	-30.0	2.8	3.7	12.0	12.0	12.0
A3/5	-35.7	-32.5	-3.6	2.7	8.0	8.0	8.0
G3/5	-40.5	-37.5	-10.7	-7.4	2.5	0.0	0.0
A3/10	-40.5	-37.5	-10.7	-7.4	0.0	2.5	0.0
A3/12	-40.5	-37.5	-10.7	-7.4	0.0	0.0	2.5

Table H4. Outcrop 1, Area A+B (0.2 m^2) (Lithics)

PUMICES	1/3	1/5	A3/3	A3/5	G3/5	A3/10	A3/12
1/3	5.7	9.6	32.6	42.5	46.2	58.3	62.9
1/5	-8.8	5.2	20.9	30.0	33.3	44.4	48.6
A3/3	-24.6	-17.3	4.3	7.5	10.3	19.4	22.9
A3/5	-29.8	-23.1	-7.0	4.0	2.6	11.1	14.3
G3/5	-31.6	-25.0	-9.3	-2.5	3.9	8.3	11.4
A3/10	-36.8	-30.8	-16.3	-10.0	-7.7	3.6	2.9
A3/12	-38.6	-32.7	-18.6	-12.5	-10.3	-2.8	3.5

Table H5. Outcrop 1, Area A+B+C (0.3 m^2) (Pumices)

LITHICS	1/3	1/5	A3/3	A3/5	G3/5	A3/10	A3/12
1/3	4.7	9.3	56.7	62.1	80.8	74.1	80.8
1/5	-8.5	4.3	43.3	48.3	65.4	59.3	65.4
A3/3	-36.2	-30.2	3.0	3.4	15.4	11.1	15.4
A3/5	-38.3	-32.6	-3.3	2.9	11.5	7.4	11.5
G3/5	-44.7	-39.5	-13.3	-10.3	2.6	-3.7	0.0
A3/10	-42.6	-37.2	-10.0	-6.9	3.8	2.7	3.8
A3/12	-44.7	-39.5	-13.3	-10.3	0.0	-3.7	2.6

Table H6. Outcrop 1, Area A+B+C (0.3 m^2) (Lithics)

PUMICES	1/3	1/5	A3/3	A3/5	G3/5	A3/10	A3/12
1/3	5.7	9.6	32.6	42.5	46.2	54.1	58.3
1/5	-8.8	5.2	20.9	30.0	33.3	40.5	44.4
A3/3	-24.6	-17.3	4.3	7.5	10.3	16.2	19.4
A3/5	-29.8	-23.1	-7.0	4.0	2.6	8.1	11.1
G3/5	-31.6	-25.0	-9.3	-2.5	3.9	5.4	8.3
A3/10	-35.1	-28.8	-14.0	-7.5	-5.1	3.7	2.8
A3/12	-36.8	-30.8	-16.3	-10.0	-7.7	-2.7	3.6

Table H7. Outcrop 1, Area A+B+C+D (0.4 m^2) (Pumices)

LITHICS	1/3	1/5	A3/3	A3/5	G3/5	A3/10	A3/12
1/3	4.7	9.3	56.7	62.1	80.8	74.1	80.8
1/5	-8.5	4.3	43.3	48.3	65.4	59.3	65.4
A3/3	-36.2	-30.2	3.0	3.4	15.4	11.1	15.4
A3/5	-38.3	-32.6	-3.3	2.9	11.5	7.4	11.5
G3/5	-44.7	-39.5	-13.3	-10.3	2.6	-3.7	0.0
A3/10	-42.6	-37.2	-10.0	-6.9	3.8	2.7	3.8
A3/12	-44.7	-39.5	-13.3	-10.3	0.0	-3.7	2.6

Table H8. Outcrop 1, Area A+B+C+D (0.4 m^2) (Lithics)

PUMICES	1/3	1/5	A3/3	A3/5	G3/5	A3/10	A3/12
1/3	5.8	7.4	28.9	38.1	41.5	48.7	52.6
1/5	-6.9	5.4	20.0	28.6	31.7	38.5	42.1
A3/3	-22.4	-16.7	4.5	7.1	9.8	15.4	18.4
A3/5	-27.6	-22.2	-6.7	4.2	2.4	7.7	10.5
G3/5	-29.3	-24.1	-8.9	-2.4	4.1	5.1	7.9
A3/10	-32.8	-27.8	-13.3	-7.1	-4.9	3.9	2.6
A3/12	-34.5	-29.6	-15.6	-9.5	-7.3	-2.6	3.8

Table H9. Outcrop 1, Area A+B+C+D+E (0.5 m^2) (Pumices)

LITHICS	1/3	1/5	A3/3	A3/5	G3/5	A3/10	A3/12
1/3	4.7	9.3	56.7	62.1	74.1	74.1	80.8
1/5	-8.5	4.3	43.3	48.3	59.3	59.3	65.4
A3/3	-36.2	-30.2	3.0	3.4	11.1	11.1	15.4
A3/5	-38.3	-32.6	-3.3	2.9	7.4	7.4	11.5
G3/5	-42.6	-37.2	-10.0	-6.9	2.7	0.0	3.8
A3/10	-42.6	-37.2	-10.0	-6.9	0.0	2.7	3.8
A3/12	-44.7	-39.5	-13.3	-10.3	-3.7	-3.7	2.6

Table H10. Outcrop 1, Area A+B+C+D+E (0.5 m^2) (Lithics)

PUMICES	1/3	1/5	A3/3	A3/5	G3/5	A3/10	A3/12
1/3	3.3	6.5	37.5	50.0	57.1	57.1	65.0
1/5	-6.1	3.1	29.2	40.9	47.6	47.6	55.0
A3/3	-27.3	-22.6	2.4	9.1	14.3	14.3	20.0
A3/5	-33.3	-29.0	-8.3	2.2	4.8	4.8	10.0
G3/5	-36.4	-32.3	-12.5	-4.5	2.1	0.0	5.0
A3/10	-36.4	-32.3	-12.5	-4.5	0.0	2.1	5.0
A3/12	-39.4	-35.5	-16.7	-9.1	-4.8	-4.8	2.0

Table H11. Outcrop 2, Area A (0.1 m^2) (Pumices)

LITHICS	1/3	1/5	A3/3	A3/5	G3/5	A3/10	A3/12
1/3	1.0	11.1	42.9	66.7	66.7	100.0	100.0
1/5	-10.0	0.9	28.6	50.0	50.0	80.0	80.0
A3/3	-30.0	-22.2	0.7	16.7	16.7	40.0	40.0
A3/5	-40.0	-33.3	-14.3	0.6	0.0	20.0	20.0
G3/5	-40.0	-33.3	-14.3	0.0	0.6	20.0	20.0
A3/10	-50.0	-44.4	-28.6	-16.7	-16.7	0.5	0.0
A3/12	-50.0	-44.4	-28.6	-16.7	-16.7	0.0	0.5

Table H12. Outcrop 2, Area A (0.1 m^2) (Lithics)

PUMICES	1/3	1/5	A3/3	A3/5	G3/5	A3/10	A3/12
1/3	3.7	8.8	48.0	54.2	60.9	60.9	68.2
1/5	-8.1	3.4	36.0	41.7	47.8	47.8	54.5
A3/3	-32.4	-26.5	2.5	4.2	8.7	8.7	13.6
A3/5	-35.1	-29.4	-4.0	2.4	4.3	4.3	9.1
G3/5	-37.8	-32.4	-8.0	-4.2	2.3	0.0	4.5
A3/10	-37.8	-32.4	-8.0	-4.2	0.0	2.3	4.5
A3/12	-40.5	-35.3	-12.0	-8.3	-4.3	-4.3	2.2

Table H13. Outcrop 2, Area A+B (0.2 m^2) (Pumices)

LITHICS	1/3	1/5	A3/3	A3/5	G3/5	A3/10	A3/12
1/3	1.3	8.3	44.4	44.4	62.5	62.5	62.5
1/5	-7.7	1.2	33.3	33.3	50.0	50.0	50.0
A3/3	-30.8	-25.0	0.9	0.0	12.5	12.5	12.5
A3/5	-30.8	-25.0	0.0	0.9	12.5	12.5	12.5
G3/5	-38.5	-33.3	-11.1	-11.1	0.8	0.0	0.0
A3/10	-38.5	-33.3	-11.1	-11.1	0.0	0.8	0.0
A3/12	-38.5	-33.3	-11.1	-11.1	0.0	0.0	0.8

Table H14. Outcrop 2, Area A+B (0.2 m^2) (Lithics)

PUMICES	1/3	1/5	A3/3	A3/5	G3/5	A3/10	A3/12
1/3	3.7	5.7	37.0	42.3	48.0	54.2	60.9
1/5	-5.4	3.5	29.6	34.6	40.0	45.8	52.2
A3/3	-27.0	-22.9	2.7	3.8	8.0	12.5	17.4
A3/5	-29.7	-25.7	-3.7	2.6	4.0	8.3	13.0
G3/5	-32.4	-28.6	-7.4	-3.8	2.5	4.2	8.7
A3/10	-35.1	-31.4	-11.1	-7.7	-4.0	2.4	4.3
A3/12	-37.8	-34.3	-14.8	-11.5	-8.0	-4.2	2.3

Table H15. Outcrop 2, Area A+B+C (0.3 m^2) (Pumices)

LITHICS	1/3	1/5	A3/3	A3/5	G3/5	A3/10	A3/12
1/3	1.3	0.0	44.4	44.4	62.5	62.5	62.5
1/5	0.0	1.3	44.4	44.4	62.5	62.5	62.5
A3/3	-30.8	-30.8	0.9	0.0	12.5	12.5	12.5
A3/5	-30.8	-30.8	0.0	0.9	12.5	12.5	12.5
G3/5	-38.5	-38.5	-11.1	-11.1	0.8	0.0	0.0
A3/10	-38.5	-38.5	-11.1	-11.1	0.0	0.8	0.0
A3/12	-38.5	-38.5	-11.1	-11.1	0.0	0.0	0.8

Table H16. Outcrop 2, Area A+B+C (0.3 m^2) (Lithics)

PUMICES	1/3	1/5	A3/3	A3/5	G3/5	A3/10	A3/12
1/3	4.2	7.7	40.0	44.8	55.6	61.5	68.0
1/5	-7.1	3.9	30.0	34.5	44.4	50.0	56.0
A3/3	-28.6	-23.1	3.0	3.4	11.1	15.4	20.0
A3/5	-31.0	-25.6	-3.3	2.9	7.4	11.5	16.0
G3/5	-35.7	-30.8	-10.0	-6.9	2.7	3.8	8.0
A3/10	-38.1	-33.3	-13.3	-10.3	-3.7	2.6	4.0
A3/12	-40.5	-35.9	-16.7	-13.8	-7.4	-3.8	2.5

Table H17. Outcrop 2, Area A+B+C+D (0.4 m^2) (Pumices)

LITHICS	1/3	1/5	A3/3	A3/5	G3/5	A3/10	A3/12
1/3	1.3	0.0	44.4	44.4	44.4	44.4	44.4
1/5	0.0	1.3	44.4	44.4	44.4	44.4	44.4
A3/3	-30.8	-30.8	0.9	0.0	0.0	0.0	0.0
A3/5	-30.8	-30.8	0.0	0.9	0.0	0.0	0.0
G3/5	-30.8	-30.8	0.0	0.0	0.9	0.0	0.0
A3/10	-30.8	-30.8	0.0	0.0	0.0	0.9	0.0
A3/12	-30.8	-30.8	0.0	0.0	0.0	0.0	0.9

Table H18. Outcrop 2, Area A+B+C+D (0.4 m^2) (Lithics)

PUMICES	1/3	1/5	A3/3	A3/5	G3/5	A3/10	A3/12
1/3	4.2	5.0	35.5	40.0	50.0	55.6	61.5
1/5	-4.8	4.0	29.0	33.3	42.9	48.1	53.8
A3/3	-26.2	-22.5	3.1	3.3	10.7	14.8	19.2
A3/5	-28.6	-25.0	-3.2	3.0	7.1	11.1	15.4
G3/5	-33.3	-30.0	-9.7	-6.7	2.8	3.7	7.7
A3/10	-35.7	-32.5	-12.9	-10.0	-3.6	2.7	3.8
A3/12	-38.1	-35.0	-16.1	-13.3	-7.1	-3.7	2.6

Table H19. Outcrop 2, Area A+B+C+D+E (0.5 m^2) (Pumices)

LITHICS	1/3	1/5	A3/3	A3/5	G3/5	A3/10	A3/12
1/3	1.3	0.0	30.0	30.0	30.0	44.4	44.4
1/5	0.0	1.3	30.0	30.0	30.0	44.4	44.4
A3/3	-23.1	-23.1	1.0	0.0	0.0	11.1	11.1
A3/5	-23.1	-23.1	0.0	1.0	0.0	11.1	11.1
G3/5	-23.1	-23.1	0.0	0.0	1.0	11.1	11.1
A3/10	-30.8	-30.8	-10.0	-10.0	-10.0	0.9	0.0
A3/12	-30.8	-30.8	-10.0	-10.0	-10.0	0.0	0.9

Table H20. Outcrop 2, Area A+B+C+D+E (0.5 m^2) (Lithics)

APPENDIX I

Percentage difference amongst different averaging techniques (plots)

OUTCROP 1

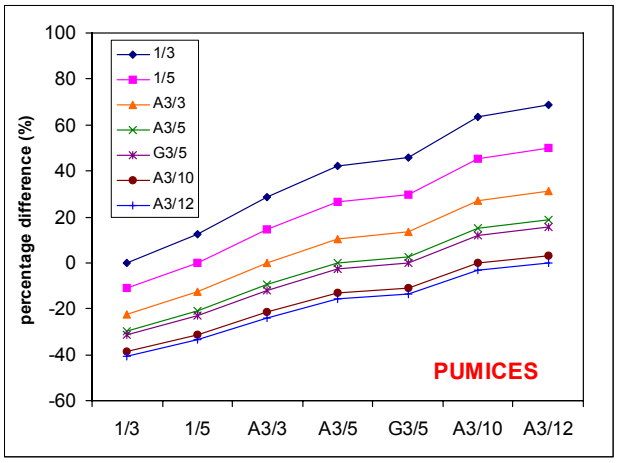

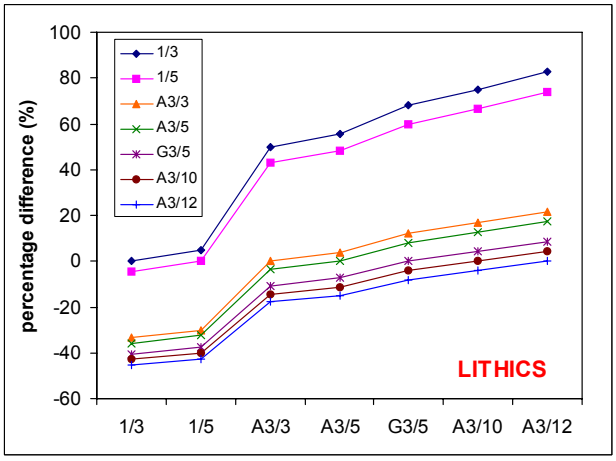

Fig. I1 Percentage difference. Outcrop 1, Area A (0.1 m^2)

OUTCROP 1

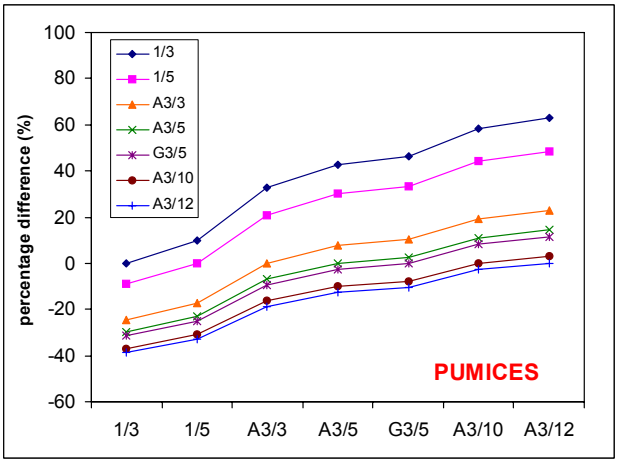

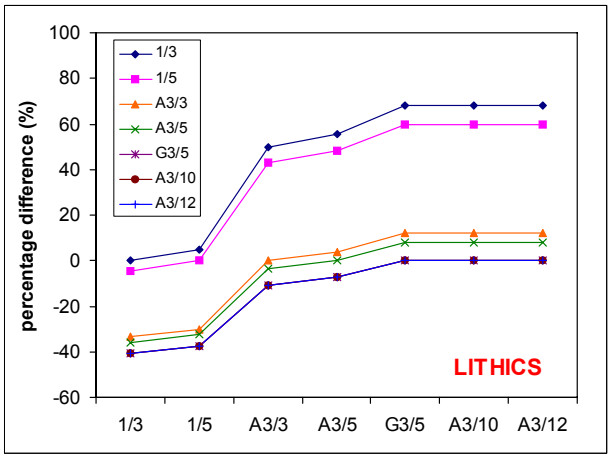

Fig. I2 Percentage difference. Outcrop 1, Area A+B (0.2 m^2)

OUTCROP 1

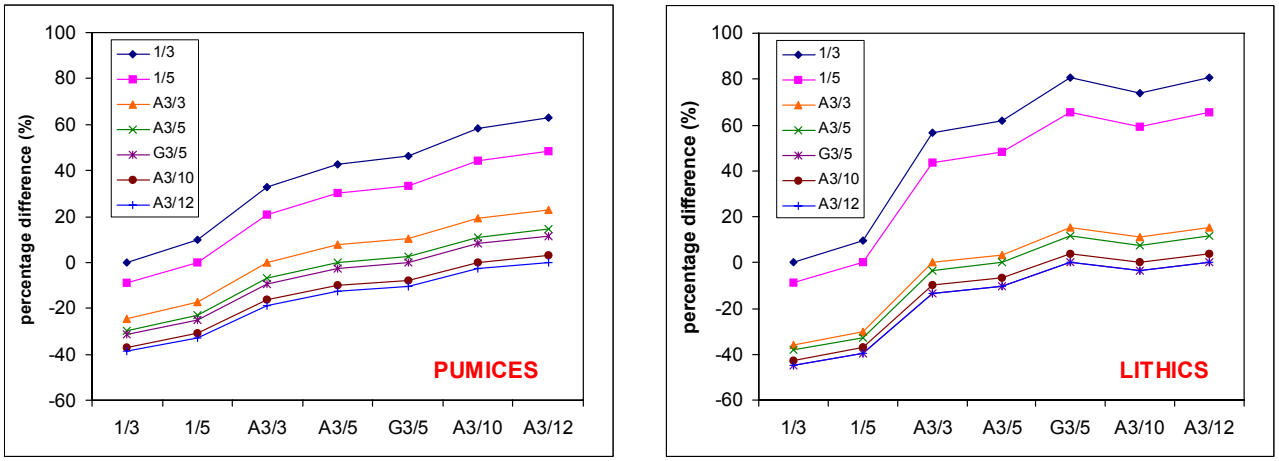

Fig. I3 Percentage difference. Outcrop 1, Area A+B+C (0.3 m^2)

OUTCROP 1

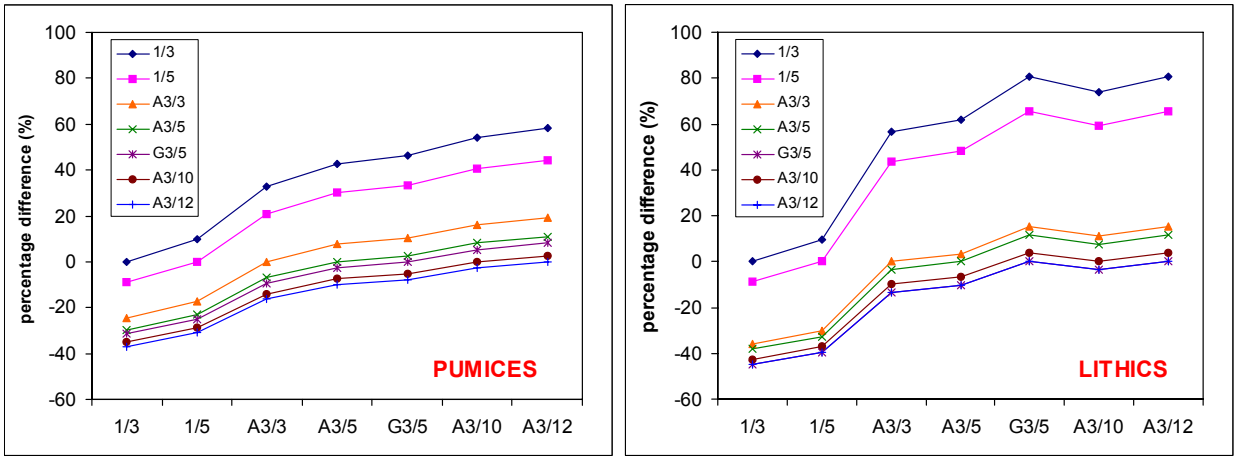

Fig. I4 Percentage difference. Outcrop 1, Area A+B+C+D (0.4 m^2)

OUTCROP 1

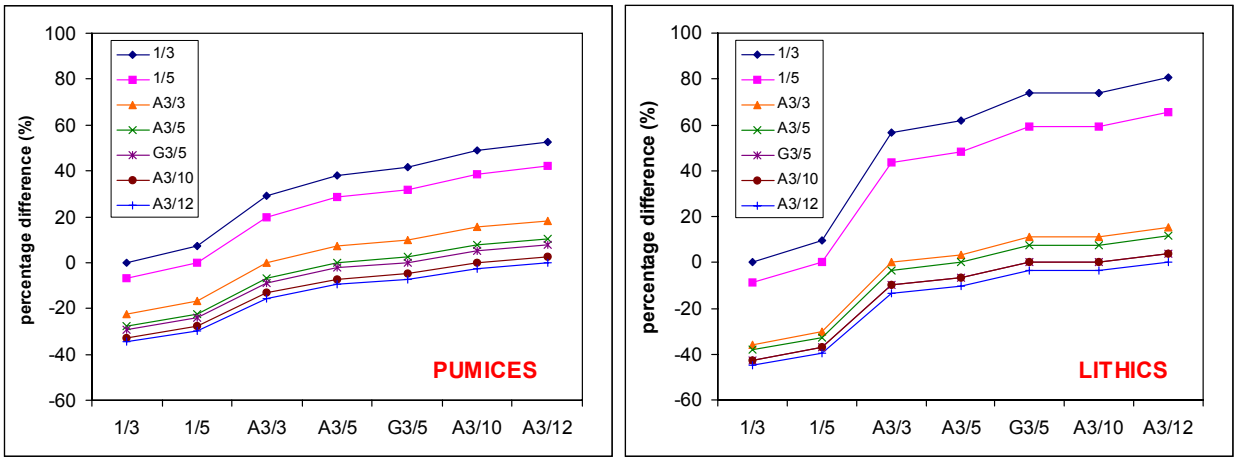

Fig. I5 Percentage difference. Outcrop 1, Area A+B+C+D+E (0.5 m^2)

OUTCROP 2

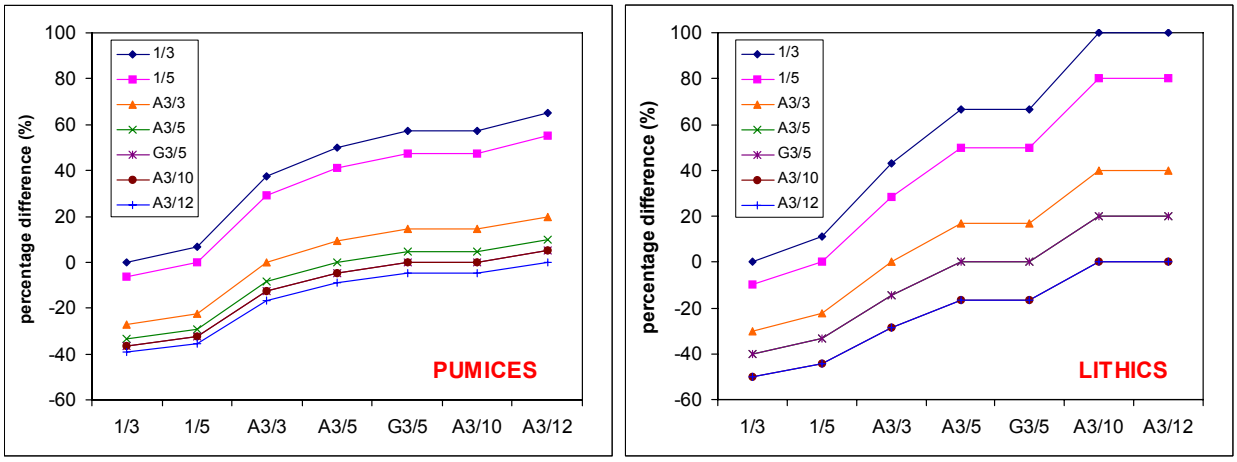

Fig. I6 Percentage difference. Outcrop 2, Area A (0.1 m^2)

OUTCROP 2

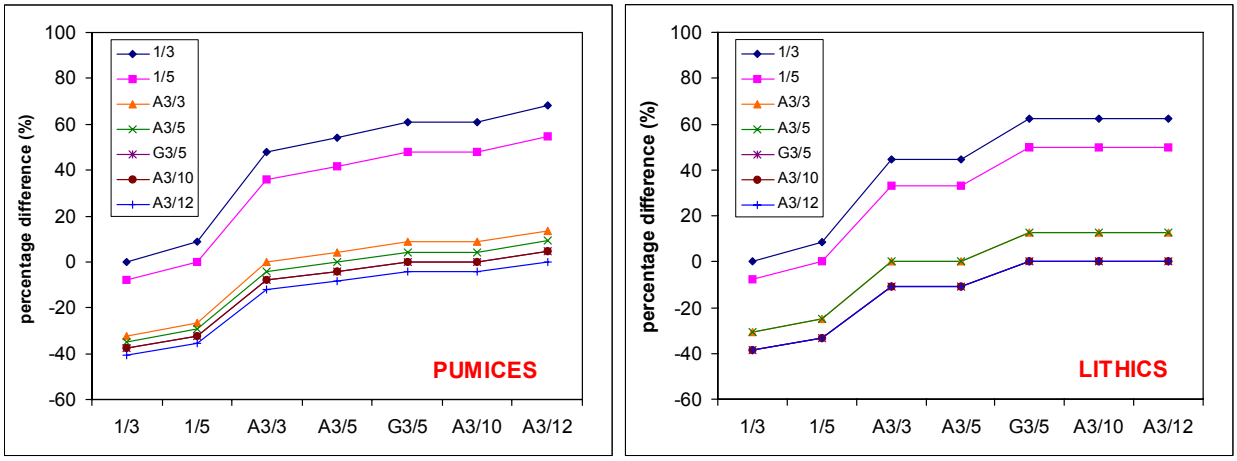

Fig. I7 Percentage difference. Outcrop 2, Area A+B (0.2 m^2)

OUTCROP 2

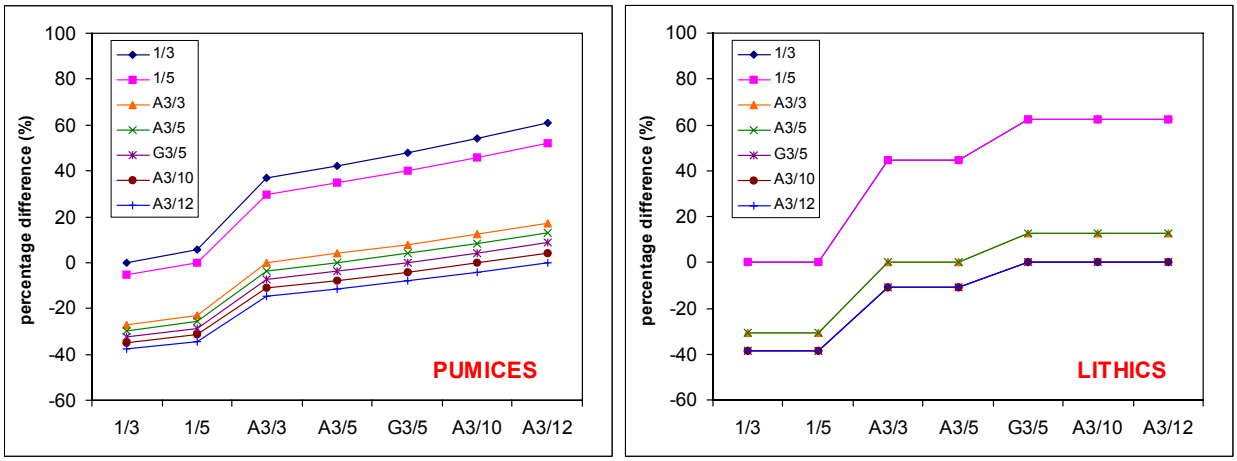

Fig. I8 Percentage difference. Outcrop 2, Area A+B+C (0.3 m^2)

OUTCROP 2

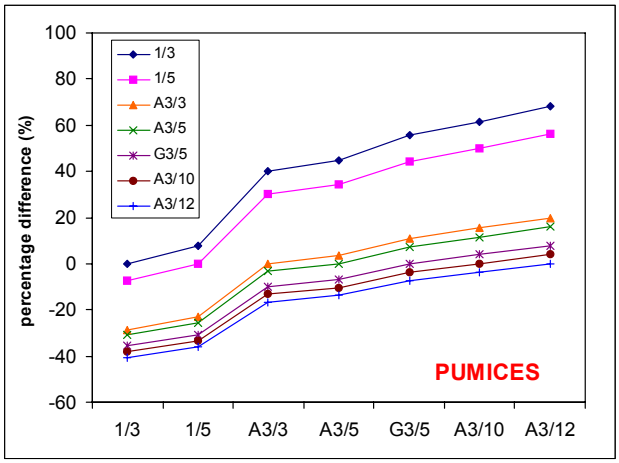

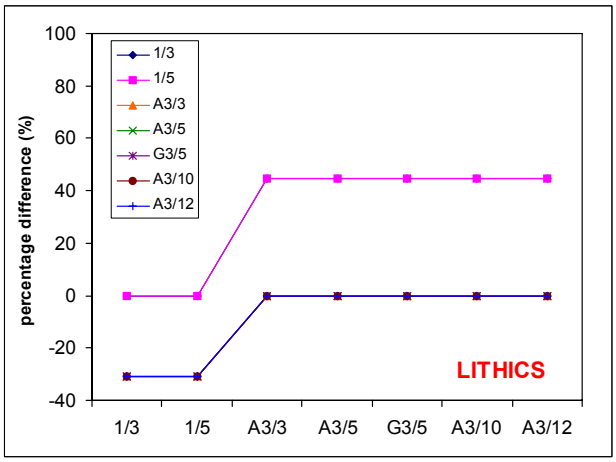

Fig. I9 Percentage difference. Outcrop 2, Area A+B+C+D (0.4 m^2)

OUTCROP 2

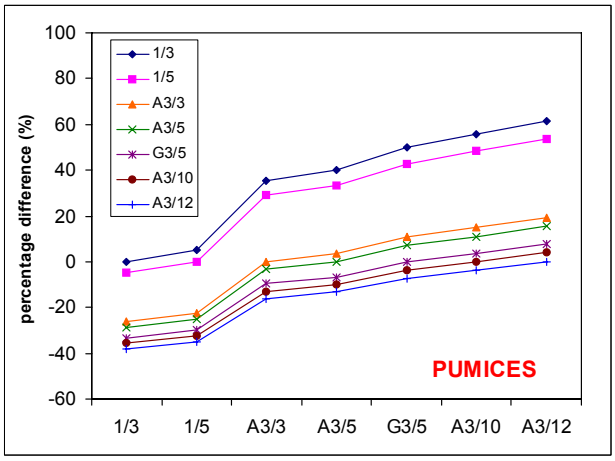

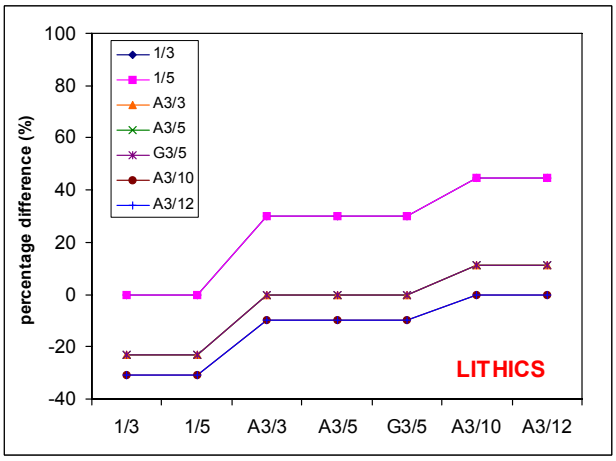

Fig. I10 Percentage difference. Outcrop 2, Area A+B+C+D+E (0.5 m^2)

APPENDIX J

Assessment of the largest clasts

Tables J.1 to J.4 summarize the assessment of the largest pumice and lithic clasts at outcrop 1 and 2. Data show that the average standard deviation at outcrop 2 is lower than outcrop 1 (0.1 vs 0.3) because the clasts are also smaller. In addition, the percentage difference between the values obtained with the largest and the smallest area are around 35% for both pumice and lithics of outcrop 1, and 27% for both pumice and lithics of outcrop 2.

OUTCROP 1 (PUMICES)

	$0.1m^2$ (α to ε)	$0.5m^2$ (A to H)	$1m^2$ (A+B to G+H)	$2m^2$	$4m^2$	unsp. area 4m	unsp. area 16m
1/3	4.8 ± 0.4	5.8 ± 0.4	6.2 ± 0.5	6.6	7	5.1 ± 0.3	5.5
A3/5	3.4 ± 0.3	4.3 ± 0.3	4.5 ± 0.4	4.6	5.4	3.8 ± 0.1	4.2
G3/5	3.2 ± 0.3	4.2 ± 0.4	4.4 ± 0.4	4.5	5.3	3.7 ± 0.1	4.2
A3/12	3.1 ± 0.2	3.9 ± 0.2	4.2 ± 0.2	4.4	4.9	3.4 ± 0.1	3.9

Table J.1. Assessment of the maximum pumice clast at outcrop 1 expressed as arithmetic mean standard deviation (calculated over the available areas). 2 and 4 m^2 do not have a standard deviation only one area of that size was available for the calculation. Values are in cm. Values from the random collection are also shown for comparison (shaded area).

OUTCROP 1 (LITHICS)

	$0.1m^2$ (α to ε)	$0.5m^2$ (A to H)	$1m^2$ (A+B to G+H)	$2m^2$	$4m^2$	unsp. area 4m	unsp. area 16m
1/3	3.5 ± 0.6	3.9 ± 0.3	4.3 ± 0.2	4.6	4.7	3.2 ± 0.4	4.7
A3/5	2.3 ± 0.3	2.7 ± 0.3	3.2 ± 0.2	3.3	3.4	2.2 ± 0.1	2.8
G3/5	2.1 ± 0.2	2.6 ± 0.3	2.9 ± 0.2	3.2	3.2	2.1 ± 0.0	2.6
A3/12	2.0 ± 0.2	2.4 ± 0.2	2.7 ± 0.2	3.0	3.2	1.8 ± 0.0	2.4

Table J.2. Assessment of the maximum lithic clast at outcrop 1 expressed as arithmetic mean standard deviation (calculated over the available areas). 2 and 4 m^2 do not have a standard deviation only one area of that size was available for the calculation. Values are in cm. Values from the random collection are also shown for comparison (shaded area).

OUTCROP 2 (PUMICES)

	$0.1m^2$ (A to J)	$0.2m^2$ (A+B to I+J)	$0.5m^2$	$1m^2$	unsp. area 1m	unsp. area 4m
1/3	3.4 ± 0.3	3.7 ± 0.2	4.2	4.2	2.7 ± 0.3	3.2
A3/5	2.3 ± 0.2	2.6 ± 0.1	3.0	3.1	1.9 ± 0.2	2.4
G3/5	2.2 ± 0.2	2.5 ± 0.1	2.8	3.0	1.9 ± 0.2	2.3
A3/12	2.0 ± 0.2	2.3 ± 0.1	2.6	2.8		2.1

Table J.3. Assessment of the maximum pumice clast at outcrop 1 expressed as arithmetic mean standard deviation (calculated over the available areas). 0.5 and 1 m^2 do not have a standard deviation only one area of that size was available for the calculation. Values are in cm. Values from the random collection are also shown for comparison (shaded area). Missing values are due to the fact that no enough clasts were available for a specific technique (i.e. 3/12).

OUTCROP 2 (LITHICS)

	$0.1m^2$ (A to J)	$0.2m^2$ (A+B to I+J)	$0.5m^2$	$1m^2$	unsp. area 1m	unsp. area 4m
1/3	1.2 ± 0.1	1.3 ± 0.1	1.3	1.6	1 ± 0.4	1.4
A3/5	0.8 ± 0.1	0.9 ± 0.1	1.0	1.1		0.8
G3/5	0.8 ± 0.1	0.9 ± 0.1	1.0	1.1		0.8
A3/12	0.7 ± 0.1	0.8 ± 0.1	0.9	1.0		0.6

Table J.4. Assessment of the maximum pumice clast at outcrop 1 expressed as arithmetic mean standard deviation (calculated over the available areas). 0.5 and 1 m^2 do not have a standard deviation only one area of that size was available for the calculation. Values are in cm. Values from the random collection are also shown for comparison (shaded area). Missing values are due to the fact that no enough clasts were available for a specific technique (i.e. 3/5 and 3/12).